AD_____

Award Number: DAMD17-01-1-0411

TITLE: The Role of Nuclear β_{II}-Tubulin in Breast Cancer Cells

PRINCIPAL INVESTIGATOR: Richard F. Luduena, Ph.D.

CONTRACTING ORGANIZATION: The University of Texas Health Science Center at San Antonio
San Antonio, Texas 78229-3900

REPORT DATE: May 2003

TYPE OF REPORT: Annual

PREPARED FOR: U.S. Army Medical Research and Materiel Command
Fort Detrick, Maryland 21702-5012

DISTRIBUTION STATEMENT: Approved for Public Release;
Distribution Unlimited

The views, opinions and/or findings contained in this report are those of the author(s) and should not be construed as an official Department of the Army position, policy or decision unless so designated by other documentation.

REPORT DOCUMENTATION PAGE

Form Approved
OMB No. 074-0188

1. AGENCY USE ONLY (Leave blank)	2. REPORT DATE	3. REPORT TYPE AND DATES COVERED
	May 2003	Annual (1 May 02 - 30 Apr 03)

4. TITLE AND SUBTITLE
The Role of Nuclear β_{II}-Tubulin in Breast Cancer Cells

5. FUNDING NUMBERS
DAMD17-01-1-0411

6. AUTHOR(S)
Richard F. Luduena, Ph.D.

7. PERFORMING ORGANIZATION NAME(S) AND ADDRESS(ES)
The University of Texas Health Science
Center at San Antonio
San Antonio, Texas 78229-3900

E-Mail: luduena@uthscsa.edu

8. PERFORMING ORGANIZATION REPORT NUMBER

9. SPONSORING / MONITORING AGENCY NAME(S) AND ADDRESS(ES)
U.S. Army Medical Research and Materiel Command
Fort Detrick, Maryland 21702-5012

10. SPONSORING / MONITORING AGENCY REPORT NUMBER

11. SUPPLEMENTARY NOTES
Original contains color plates. All DTIC reproductions will be in black and white.

12a. DISTRIBUTION / AVAILABILITY STATEMENT
Approved for Public Release; Distribution Unlimited

12b. DISTRIBUTION CODE

13. ABSTRACT (Maximum 200 Words)

The research is based on our finding that breast cancers contain the β_{II} isotype of tubulin inside their nuclei. Our aim is to identify the functional significance of nuclear β_{II}. We have used various approaches to this question. We have created another monoclonal antibody, this one specific for the β_V isotype. We have found β_V in the microtubules of breast cancer cells, but not in the nuclei. Thus, we have tested the β_I, β_{II}, β_{III}, β_{IVa}, β_{IVb} and β_V isotypes in these cells. None is in the nuclei. We have also examined the effect of rhizoxin on these cells; this drug disorganizes the microtubules and causes apoptosis at very low concentrations. Finally, we have used affinity modeling to predict the structures of the various isotypes. We have found that they differ at their taxol-binding sites. This raises the possibility that isotype-specific drugs could be designed that may be more effective than currently used therapies.

14. SUBJECT TERMS
Breast cancer, Tubulin isotypes, Cell nucleus

15. NUMBER OF PAGES
69

16. PRICE CODE

17. SECURITY CLASSIFICATION OF REPORT	18. SECURITY CLASSIFICATION OF THIS PAGE	19. SECURITY CLASSIFICATION OF ABSTRACT	20. LIMITATION OF ABSTRACT
Unclassified	Unclassified	Unclassified	Unlimited

Table of Contents

INTRODUCTION

This research is based on the observation that the β_{II} isotype of tubulin is located in the nuclei of many breast cancer cells (1,2). In contrast, it is significantly less abundant in the nuclei of normal cells (1). Our aim in this research is to understand the functional significance of the nuclear localization of β_{II} in breast cancer cells. We are exploring this question by testing hypotheses, one of which is that β_{II} has a specific interaction with the kinetochores and facilitates the binding of spindle microtubules to these structures. We are also approaching this issue by comparing the interactions of β_{II} and other tubulin isotypes to anti-tumor drugs as well as examining the effects of anti-tubulin drugs on the nuclei.

BODY

Task 1. Immunohistochemical analysis of tubulin isotypes in the mitotic spindle of breast cancer cells.

We previously reported that MCF-7 breast cancer cells express the β_I, β_{II}, β_{III} and β_{IV} isotypes, but only put β_{II} in their nuclei (2). We had hoped this year to undertake the immunohistochemical analysis of the distribution of the tubulin isotypes in the mitotic spindle using the immunogold method, but we found that the electron microscopy center at this institution is not in a position to do this for us, so we have been searching for a collaborator to undertake the immunogold labeling. We have finally located one and are intending to accomplish this task this year.

We are also attempting to use confocal microscopy to examine isotype distribution in mitotic spindles.

We have now added a new monoclonal antibody to our tool-kit. We have made an antibody to β_V, a mysterious isotype that is highly conserved in evolution (3). We have found that β_V is present in microtubules in breast cancer cells, but does not occur in the nuclei (Figure 8).

Task 2. Development of method of purifying kinetochores from breast cancer and normal cells.

This task was accomplished last year.

Task 3. Immunohistochemical analysis of tubulin associated with kinetochores.

The finding last year that β_{III}, rather than β_{II}, was associated with kinetochores led us to re-cast our original hypothesis, which was that β_{II} had a unique role in the nucleus arising from its binding to kinetochores. We are presently attempting other approaches to identifying the roles of tubulin isotypes in breast cancer cells. These are as follows:

1. *The sulfhydryl groups of β_{III}.* We showed last year that β_{III} may play a role in breast cancer cells in protecting microtubules from free radicals. We believe that the unusual sulfhydryl group distribution in β_{III} may be a key to this. β_{III} has a serine residue at position 239, where most other animal tubulins have a cysteine. We have previously shown that the sulfhydryl group of cys239 is highly susceptible to oxidation and that oxidation of this particular sulfhydryl group inhibits microtubule assembly (4,5). In addition, β_{III} has a cysteine residue at position 124 that is unknown in any other β-tubulin anywhere, except for β_V and β_{VI} (3). This cysteine constitutes a sulfhydryl cluster with the highly conserved cysteines at positions 127 and 129. It is quite reasonable to postulate that removal of cys239 makes β_{III}-tubulin resistant to free radicals and that addition of cys124 makes β_{III} able to absorb free radicals. In order to test this we are preparing forms of β_{III} with C124S and S239C mutations. Our preliminary results suggest that the C124S mutation slows down growth of breast cancer cells.

2. *Testing the effects of drugs on tubulin in breast cancer cells.* We have treated breast cancer cells with rhizoxin, a drug that has not previously been tested with breast cancer cells (6,7). We

have found that rhizoxin has multiple effects on these MCF-7 breast cancer cells. First, using the MTT method (8) inhibits cell growth with an IC50 of 2 nM (Figure 1). Second, at concentrations as low as 0.5 nM, it causes partial depolymerization of microtubules at the periphery of these cells (Figure 1) and also of HeLa cells. Rhizoxin inhibited microtubule assembly *in vitro* with an IC50 of 5 μM. Using the TUNEL assay (9), apoptosis was detected in MCF-7 cells at concentrations of rhizoxin as low as 5 nM (Figure 2). Using caspase-3 activity (8) as a marker for apoptosis, a similar pattern was observed (Figure 3).

3. *Comparison of the three-dimensional structures of the isotypes.* In collaboration with Dr. Jack Tuszynski of the University of Alberta, we have shown that the three-dimensional structures of the isotypes differ. This was done using affinity modeling based on the structure of bovine brain tubulin that was determined by electron crystallography (10,11). We have compared β_{I}, β_{II}, β_{III}, β_{IVa}, β_{IVb}, β_{VI} and β_{VII}. We have specifically focused on comparing the taxol binding sites (Figures 4-7). We hope that a spin-off of this project will be the design of better drugs against breast cancer.

We intend to do the following tasks in the last year of the grant.

Task 4. Measurement of tubulin isotype binding to kinetochores.

Task 5. Measurement of ability of chromosomes to nucleate assembly of tubulin isotypes.

Task 6. Determination of the ability of chromosomes to capture microtubules made of isotypically purified tubulin.

KEY RESEARCH ACCOMPLISHMENTS

- MCF-7 breast cancer cells contain the β_V isotype of tubulin.
- Rhizoxin inhibits peripheral microtubule assembly in breast cancer cells.
- Rhizoxin induces apoptosis in breast cancer cells.
- The three-dimensional structures of the taxol binding site on β-tubulin are different for the β_I, β_{II}, β_{III}, β_{IVa}, β_{IVb}, β_{VI} and β_{VII} isotypes.

REPORTABLE OUTCOMES

1. Manuscripts, abstracts, presentations, degrees obtained:

Manuscripts:

Walss-Bass, C., Xu, K., David, S., Fellous, A. and Ludueña, R.F. (2002) Occurrence of nuclear β_{II}-tubulin in cultured cells. *Cell and Tissue Research* **308**, 215-223. **(Appendix 1)**[a].

Xu, K. and Ludueña, R.F. (2002) Characterization of nuclear β_{II}-tubulin in tumor cells: a possible novel target for taxol. *Cell Motility and the Cytoskeleton* **53**, 39-52. **(Appendix 2)**[a].

Woo, K., Jensen-Smith, H.C., Ludueña, R.F. and Hallworth, R. (2002) Differential expression of β tubulin isotypes in gerbil nasal epithelia. *Cell and Tissue Research* **309**, 331-335 **(Appendix 3)**[a].

Dumontet C, Isaac S, Souquet PJ, Bejui-Thivolet F, Pacheco Y, Peloux N, Frankfurter A, Ludueña R & Perol M (2002) Expression of class III β tubulin in non-small cell lung cancer is correlated with resistance to taxane chemotherapy. *Elect. J. Oncol.* **1**, 58-64.

Khan, I.A. and Ludueña, R.F. (2003) Different effects of vinblastine on the polymerization of isotypically purified tubulins from bovine brain. *Investigational New Drugs* **21**, 3-13 **(Appendix 4)**[b].

Walss-Bass, C., Kreisberg, J.I. and Ludueña, R.F. (2003) Effect of the anti-tumor drug vinblastine on nuclear β_{II}-tubulin in cultured rat kidney mesangial cells. *Investigational New Drugs*, **21**, 15-20 **(Appendix 5)**[b].

Perry, B., Jensen-Smith, H.C., Ludueña, R.F. and Hallworth, R. (2003) Differential expression of β tubulin isotypes in gerbil vestibular end organs. *Journal of the Association for Research in Otorhinolaryngology (JARO)*, in press[b].

Jensen-Smith, H.C., Ludueña, R.F. and Hallworth, R (2003) Requirement for the βI and βIV tubulin isotypes in mammalian cilia. *Cell Motil. Cytoskeleton* **55**, in press.

Yeh, I.-T. and Ludueña, R.F. The β_{II} isotype of tubulin is present in the cell nuclei of a variety of cancers. *Cell Motility and the Cytoskeleton*, submitted for publication[c].

Khan, I.A., Mittal, A., Prasad, V., Moore, M.J.B., Sprague, E. and Ludueña, R.F. The interaction of combretastatin A-4-phosphate with tubulin isotypes. *Cell Motility and the Cytoskeleton*, submitted for publication

Jensen-Smith, H.C., Eley, J., Steyger, P.S., Ludueña, R.F. and Hallworth, R. Cell type-specific reduction of β tubulin isotypes synthesized in the developing gerbil organ of Corti. *Cell Motility and the Cytoskeleton*, submitted for publication

[a]Listed in last year's progress report as "in press".
[b]Listed in last year's progress report as "submitted for publication".
[c]Listed in last year's progress report as "to be submitted".

Abstracts: (Appendix 6)

Banerjee, A., Joe, P., Lazzell, A., Prasad, V. and Ludueña, R.F. (2002) Generation of a monoclonal antibody to the βV isotype of tubulin. Mol. Biol. Cell **13**, 463a.

Banerjee, A., Mukherjee, S., Ludueña, R.F. and Choudhury, G.G. (2002) Generation of beta tubulin cDNA constructs for mammalian expression: overexpression of beta III increases resistance to colchicine and paclitaxel. Mol. Biol. Cell **13**, 464a.

Presentations:

Banerjee, A., Joe, P., Lazzell, A., Prasad, V. & Ludueña, R.F. (2002) Generation of a monoclonal antibody to the βV isotype of tubulin. *American Society for Cell Biology*, San Francisco, CA, December 12-16, 2002 (poster).

Banerjee, A., Mukherjee, S., Ludueña, R.F. and Choudhury, G.G. (2002) Generation of beta tubulin cDNA constructs for mammalian expression: overexpression of beta III increases resistance to colchicine and paclitaxel. *American Society for Cell Biology*, San Francisco, CA, December 12-16, 2002 (poster).

Ludueña, R.F. Functional significance of tubulin isotypes. University of Illinois Medical Center, Chicago, IL, March 5, 2003 (seminar).

Ludueña, R.F. Functional significance of tubulin isotypes. Northwestern University, Chicago, IL, March 6, 2003 (seminar).

Ludueña, R.F. Tubulin isotypes in normal and cancerous cells. Creighton University, Omaha, NE, May 7, 2003 (distinguished seminar).

Yeh, I.-T. and Ludueña, R.F. The β_{II} isotype of tubulin is present in the cell nuclei of a variety of cancers. Center for Biomedical Neuroscience Retreat, San Antonio, TX, May 20, 2003 (poster).

2. Funding Applied for Based on Work Supported by this Award

Applied for and Funded:

Title: Blood βII-Tubulin as a Biomarker for Prostate Cancer
Funding Agency: National Institutes of Health: EDRN Program
PI: Richard F. Ludueña
Dates: May 1, 2003-April 30, 2004 **Amount of Funding**: $75,000

Title: Mechanism of Action of ILX651

Funding Agency: Ilex Oncology
PI: Richard F. Ludueña
Dates: June 1, 2003-January 31, 2004 **Amount of Funding**: $ 37,591

Applied for and Not Funded:

Title: Development of a Novel Drug for Breast Cancer
Funding Agency: Susan B. Komen Breast Cancer Research Foundation
PI: Richard F. Ludueña
Dates: May 1, 2003-April 30, 2004 **Amount of Funding**: $ 75,000

Pending:

Title: Development of a Novel Drug for Prostate Cancer
Funding Agency: US Army Prostate Cancer Research Program
PI: Richard F. Ludueña
Dates: November 1, 2003-April 30, 2005 **Amount of Funding**: $ 74,998

Letter of Intent (LOI) Sent:

Title: Development of Novel Anti-malarial Drugs Targeting *Plasmodium* Tubulin
Funding Agency: Ellison Medical Foundation
PI: Richard F. Ludueña
Dates: Pending approval of LOI **Amount of Funding**: Pending approval of LOI

3. Personnel Receiving Salary from this Grant:

Richard F. Ludueña, Ph.D., Professor, Principal Investigator
Veena Prasad, Senior Research Associate
Phyllis Trcka Smith, Senior Research Assistant

CONCLUSIONS

Since our original hypothesis was put into question by our results, we decided to attempt some different approaches to the function of the β_{II} isotype in breast cancer cells. We were able to make an antibody to the β_V isotype and found that it forms microtubules in breast cancer cells but does not locate to the nucleus. We also found that rhizoxin causes microtubule disassembly and apoptosis in these cells. Using affinity modeling we learned that the binding sites for taxol differ among the isotypes. The binding site on β_{III} is significantly different from the site on the other isotypes.

This last finding is potentially of great interest since β_{III} is common to a large variety of cancers including breast cancer and since β_{III} normally has a highly restricted distribution. It is likely that a drug specific for β_{III} would be useful therapeutically since it may have fewer side effects than currently used drugs. By affinity modeling we could design a drug specific for β_{III}. So far we have only examined the taxol-binding site. However, it is quite reasonable to expect that other drug-binding sites would also differ among the isotypes and allow for isotype-specific drug design.

REFERENCES

1. Walss-Bass C, Xu K, David S, Fellous A & Ludueña RF (2002) Occurrence of nuclear β_{II}-tubulin in cultured cells. *Cell and Tissue Research* **308**, 215-223.
2. Xu K & Ludueña RF (2002) Characterization of nuclear β_{II}-tubulin in tumor cells: a possible novel target for taxol. *Cell Motility and the Cytoskeleton* **53**, 39-52.
3. Ludueña RF (1998) The multiple forms of tubulin: different gene products and covalent modifications. *Int. Rev.* Cytol. **178**, 207-275.
4. Ludueña RF, Roach MC, Trcka PP, Little M, Palanivelu P, Binkley P & Prasad V (1982) β_2-tubulin, a form of chordate brain tubulin with lesser reactivity toward an assembly-inhibiting sulfhydryl-directed cross-linking reagent. *Biochemistry* **21**, 4787-4794.
5. Little M & Ludueña RF (1985) Structural differences between β_1- and β_2-tubulins: implications for microtubule assembly and colchicine binding. *EMBO J.* **4**, 51-56.
6. Takahashi M, Iwasaki S, Kobayashi H & Okuda S (1987) Studies on macrocyclin lactone antibiotics. XI. Anti-mitotic and anti-tubulin activity of new antitumor antibiotics, Rhizoxin and its homologues, *J. Antibiotics* **40**, 66-72.
7. Sullivan AS, Prasad V, Roach MC, Takahashi M, Iwasaki S & Luduena RF (1990) Interaction of rhizoxin with bovine brain tubulin, *Cancer Research* **50**, 4277-4280.
8. Leoni LM, Hamel E, Genini D, Shih H, Carrera CJ, Cottam HB & Carson DA. (2000) Indanocine, a microtubule-binding indanone and a selective inducer of apoptosis in multidrug-resistant cancer cells. *J. Nat. Cancer Inst.* **92**, 217-224,
9. Oberhaus SM (2003) TUNEL and immunofluorescence double-labeling assay for apoptotic cells with specific antigen(s). *Meth.Mol. Biol.* **218**, 85-96.
10. Nogales E, Wolf SG, Khan IA, Luduena RF & Downing KH (1995) Structure of tubulin at 6.5 Å and location of the taxol-binding site. *Nature* **375**, 424-427.
11. Nogales E, Wolf SG & Downing KH (1998) Structure of the $\alpha\beta$ tubulin dimer by electron crystallography. *Nature* **391**, 199-203.

APPENDICES

Appendix 7, Figures 1-8

Figure 1. Effect of rhizoxin on cellular microtubules. MCF-7 breast cancer cells were treated with (bottom panels) and without (top panels) 50 nM rhizoxin. Cells were then treated with an antibody to β_{IVb}-tubulin (left) or with DAPI to indicate the DNA (right). Note that microtubules are missing from the periphery of these cells.

Figure 2. Effect of rhizoxin on apoptosis as assayed by the TUNEL method. MCF-7 breast cancer cells were treated with the indicated concentrations of rhizoxin and then with either DAPI (blue) or with the TUNEL reagent (green). TUNEL is a system that detects DNA ends and hence should detect apoptosis, which is characterized by DNA fragmentation. Note that even at 5 nM concentration, rhizoxin is causing apoptosis.

Figure 3. Effect of rhizoxin on apoptosis as assayed by caspase-3 release. MCF-7 breast cancer cells were treated with the indicated concentrations of rhizoxin and then with either DAPI (blue) or with an a test for caspase (red). Caspase-3 is a proteolytic enzyme activated during apoptosis. Note that even at 5 nM concentration, rhizoxin is causing apoptosis.

Figure 4. Taxol binding site on bovine brain tubulin. *Left:* Structure of the taxol-binding site on bovine brain tubulin as determined by electron crystallography (11). *Right:* Bovine brain tubulin with taxol binding to the taxol-binding site. Note that the structure changes with the presence of taxol. Acidic residues (red); basic residues (blue); taxol (green).

Figure 5. Comparison of the structures of the taxol-binding sites of the β_I and β_{III} isotypes of tubulin. *Left:* β_I. *Right:* β_{III}. Acidic residues (red); basic residues (blue).

Figure 6. Comparison of the structures of the taxol-binding sites of the β_{IVb} and β_{III} isotypes of tubulin. *Left:* β_{IVb}. *Right:* β_{III}. Acidic residues (red); basic residues (blue).

Figure 7. Comparison of the structures of the taxol-binding sites of the β_{VII} and β_{III} isotypes of tubulin. *Left*: β_{VII}. *Right*: β_{III}. Acidic residues (red); basic residues (blue).

Figure 8. β_V in MCF-7 breast cancer cells. MCF-7 cells were treated with a monoclonal antibody to β_V. Immunofluorescence microscopy was then performed. Note incorporation of β_V into microtubules.

Appendix 1

Cell Tissue Res (2002) 308:215–223
DOI 10.1007/s00441-002-0539-6

REGULAR ARTICLE

Consuelo Walss-Bass · Keliang Xu · Sebastien David
Arlette Fellous · Richard F. Ludueña

Occurrence of nuclear β_{II}-tubulin in cultured cells

Received: 2 July 2001 / Accepted: 1 February 2002 / Published online: 5 April 2002

Abstract Microtubules are cylindrical organelles that play critical roles in cell division. Their subunit protein, tubulin, is a target for various antitumor drugs. Tubulin exists as various forms, known as isotypes. In most normal cells, tubulin occurs only in the cytosol and not in the nucleus. However, we have recently reported the finding of the β_{II} isotype of tubulin in the nuclei of cultured rat kidney mesangial cells. Mesangial cells, unlike most normal cell lines, have the ability to proliferate rapidly in culture. In efforts to determine whether nuclear β_{II}-tubulin occurred in other cell lines, we examined the distribution of the β_I, β_{II}, and β_{IV} mammalian tubulin isotypes in a variety of normal and cancer human cell lines by immunofluorescence microscopy. We have found that, in the normal cell lines, all three isotypes are present only in the cytoplasm. However, the β_{II} isotype of tubulin is located not only in the cytoplasm, but also in the nuclei of the following cell lines: LNCaP prostate carcinoma, MCF-7, MDA-MB-231, MDA-MB-435, and Calc18 breast carcinoma, C6 and T98G glioma, and HeLa cells. In contrast, the β_I and β_{IV} isotypes, which are also synthesized in cancer cells, are not localized to the nucleus but are restricted to the cytoplasm. We have also seen β_{II} in breast cancer excisions. In most of these cells, β_{II} appears to be concentrated in the nucleoli. These results suggest that transformation may lead to localization of β_{II}-tubulin in cell nuclei, serving an as yet unknown function, and that nuclear β_{II} may be a useful marker for detection of tumor cells.

Keywords Tubulin · Nuclear tubulin · Tubulin isotypes · Cell proliferation · Immunofluorescence · Human

Abbreviations *PBS:* Phosphate-buffered NaCl solution · *DAPI:* 4′,6-diamidino-2-phenylindole dihydrochloride · *LNCaP:* lymph node carcinoma of the prostate · *EGTA:* ethyleneglycol-*bis*-(β-aminoethylether) · *N, N, N, N′*-tetraacetic acid · *PIPES:* piperazine-*N, N′-bis*-(2-ethanesulfonic acid) · *PMSF:* phenylmethyl sulfonyl fluoride · *PDGF:* platelet-derived growth factor · *IL-1:* interleukin-1

Introduction

A fundamental fact about cancer is that cancer cells are our own cells misbehaving. They are not really alien cells. Most anticancer drugs target cell division, a process that is faster in cancer cells than in most normal cells. The problem, however, is that certain normal cells, such as those of the bone marrow, also divide fairly rapidly. Hence, the agents of chemotherapy have serious side effects, which limit their use. Therefore, the challenge for cancer chemotherapy is to find a drug that attacks cancer cells but not normal cells.

Microtubules, made of the protein tubulin, are organelles that play a critical role in mitosis; they attach to chromosomes as they line up in metaphase and help move them into the daughter cells (Hyams and Lloyd 1994). For this reason, the protein tubulin is a major target for antitumor drugs such as vinblastine and taxol (Wilson and Jordan 1994). Nevertheless, these drugs do not discriminate between normal and cancer cells, both of which contain tubulin, and therefore have serious side effects and limitations.

The tubulin protein is made of two subunits, α and β (Hyams and Lloyd 1994). These subunits exist as numerous isotypes, which differ in their tissue and subcellular

This research has been supported by grants CA26376 from the National Institutes of Health, AQ-0726 from the Welch Foundation, and DAMD17-98-1-8246 from the US Army Breast Cancer Research Program to R.F.L., as well as by grant P30 CA54174 from the National Cancer Institute to the San Antonio Cancer Institute

C. Walss-Bass · K. Xu · R.F. Ludueña (✉)
Department of Biochemistry,
University of Texas Health Science Center,
San Antonio, TX 78284-7760, USA
e-mail: luduena@uthscsa.edu
Tel.: +1-210-5673732, Fax: +1-210-5676595

S. David · A. Fellous
Laboratoire de Pharmacologie Experimentale et Clinique,
27 Rue Juliette Dodu, 75010 Paris, France

localization, as well as in their interaction with antitumor drugs (Ludueña 1998). We have previously found that the β_{II} isotype of tubulin is present in the nuclei of rat kidney mesangial cells (Walss et al. 1999). In order to determine whether this finding was an isolated incident or occurred in other cell types, we have now examined the intracellular distribution of the vertebrate β-tubulin isotypes β_I, β_{II}, and β_{IV} in several cultured human cell lines, both normal and cancerous. We have found that the β_{II} isotype of tubulin is present in the nuclei of all the cancer cells investigated, but is absent from the nuclei of most of the normal cells. In the nuclei, β_{II} is particularly concentrated in the nucleoli. These results suggest that transformation may lead to localization of β_{II} in cell nuclei, serving an as yet unknown function. Furthermore, nuclear β_{II} may be a useful marker for detection of tumor cells and may serve as a target for antitumor drugs such as taxol and vinblastine, to selectively attack cancer cells. Despite the fact that microtubules are generally considered to be purely cytoplasmic organelles, there have been a few previous reports of tubulin in the nucleus (Menko and Tan 1980; Armbruster et al. 1983; Ranganathan et al. 1997), although no function has been proposed for such tubulin. Our results raise the possibility that nuclear tubulin may lend itself to proliferation or transformation.

Materials and methods

Source of cells and antibodies

The human dermal fibroblasts (HDF) were a kind gift from Dr. Eugene Sprague [University of Texas Health Science Center at San Antonio (UTHSCSA), San Antonio, Tex.]. The 506 smooth muscle cells from human colon and the HSK fibroblasts from baby foreskin were a kind gift from Dr. Mary Pat Moyer. (UTHSCSA). The osteoblasts were a kind gift from Dr. John Lee (UTHSCSA). The MCF-10F breast epithelial cells, the LNCaP prostate carcinoma cells, as well as the MCF-7 and MDA-MB-231 breast carcinoma cells were a kind gift from Dr. Nandini Chaudhuri (UTHSCSA). The Calc 18 breast carcinoma cell line was a kind gift from Dr. Jean-François Riou, Rhône-Poulenc, Paris, France. MDA-MB-435 cells used in confocal microscopy experiments were a kind gift from Dr. Susan Mooberry, Southwest Foundation for Biomedical Research, who also gave us the HeLa cells. C6 and T98G glioma cells were kindly provided by Dr. Martin Adamo of the Department of Biochemistry, University of Texas Health Science Center, San Antonio, Tex.. Fluorescein-colchicine, fluorescein, and acridine orange were from Molecular Probes, Eugene, Ore.

Excisions of mammary adenocarcinomas were provided by the Department of Anapathology, Hôpital St. Louis, Paris, France. The monoclonal antibodies SAP.4G5, JDR.3B8, and ONS.1A6, specific for the β_I, β_{II}, and β_{IV} isotypes of tubulin, respectively, were prepared as previously described (Banerjee et al. 1988, 1992; Roach et al. 1998).

Immunofluorescence microscopy

All cells were grown to near confluency on glass coverslips at 37°C and 5% CO_2. Cells were then washed twice with PBS (0.15 M NaCl, 0.0027 M KCl, 0.00147 M KH_2PO_4, 0.01 M $NaHPO_4$; pH 7.2), fixed for 15 min with 3.7% paraformaldehyde at room temperature, and permeabilized for 1 min with 0.5% Triton X-100 in PBS. Cells were then incubated at 4°C overnight with the respective isotype-specific monoclonal IgG mouse antibody (anti-β_I, 0.05 mg/ml; anti-β_{II}, 0.03 mg/ml; anti-β_{IV}, 0.08) diluted in PBS containing 10% normal goat serum (Jackson Immunoresearch, West Grove, Pa.). Cells were rinsed in PBS and labeled with Cy3-conjugated goat anti-mouse antibody (1:100; Jackson Immunoresearch) for 1 h at room temperature. Cells were then rinsed three times with PBS. For DNA detection, cells were stained with DAPI (Molecular Probes, Eugene, Ore.; 2 µl/ml in PBS) during the last wash with PBS after incubation with the secondary antibody. Coverslips were mounted on glass slides and examined with a Zeiss epifluorescence photomicroscope using a Plan-Neufluar ×63 oil objective. In experiments involving fluorescein-colchicine or fluorescein, cells were incubated in the dark with the reagent for 2 h, then mounted on glass slides and examined. If colocalization with RNA was to be examined, the cells were incubated immediately after fluorescein-colchicine treatment with acridine orange (10 mg/ml) in PBS at room temperature for 5 min. Cells were then washed with PBS and mounted on a glass slide for examination. Immunofluorescence microscopy was performed either on an Olympus Fluoview laser scanning confocal microscope or on a Zeiss epifluorescence photomicroscope.

Immunoperoxidase staining

Tumors (ductal breast adenocarcinoma) were fixed in formol and embedded in paraffin. Sections (6 µm) were obtained, placed on slides, and treated with xylene to remove paraffin, then with ethanol solutions from 100% to 70% to rehydrate the sections. The epitopes were restored in a microwave oven set at 680 W by the method of Cattoretti et al. (1993; 3×5 min in 10 mM Na citrate, pH 6.8. Endogenous peroxidases were inhibited by treatment with 3% H_2O_2 for 30 min. Phosphate-buffered saline containing 10% fetal calf serum was used as both the blocking buffer and the antibody dilution buffer. Slides were incubated with anti-β_{II} (1:2000) overnight at 4°C followed by incubation with biotinylated secondary antibody for 40 min at room temperature. Signal amplification was provided by treatment with streptavidin-peroxidase complex (Strept ABC kit; Dako, Trappes, France). The signal was detected by a colorimetric method using aminoethylcarbazol (Sigma Aldrich, St. Quentin Falavier, France). Samples were photographed with a tri-CCD camera (LH750 RC3; Lhesa Electronic Systems).

In situ cell fractionation

LNCaP cells, grown on glass coverslips, were washed twice with ice-cold PBS and incubated on ice for 5 min with cold cytoskeleton buffer (10 mM PIPES, pH 6.8, 300 mM sucrose, 100 mM NaCl, 3 mM $MgCl_2$, 1 mM EGTA, 1% Triton X-100, 1.2 mM PMSF, 0.1% aprotinin, 0.1% pepstatin A, 1% vanadyl ribonucleoside complex). This procedure removes all soluble cytoplasmic and nucleoplasmic proteins. This was followed by a 5-min incubation on ice with double detergent buffer (10 mM TRIS-HCl, pH 7.4, 10 mM NaCl, 3 mM $MgCl_2$, 0.5% deoxycholate, 1% Tween-40, 1.2 mM PMSF, 0.1% aprotinin, 0.1% pepstatin A, 1% vanadyl ribonucleoside complex), which removes all cytoskeletal proteins, except the intermediate filaments that remain tightly associated with the nucleus. Cells prepared this way are the cytosol-extracted cells. For nuclear matrix preparations, these cells were further incubated at room temperature for 1 h in cytoskeleton-50 buffer (same as above except with 50 mM NaCl instead of 100 mM) containing 100 µg/ml of DNAse I (Sigma Chemical, St. Louis, Mo.). The chromatin was then removed by adding 2 M $(NH_4)_2SO_4$ dropwise to a final concentration of 0.25 M. What is left behind is the nuclear matrix structure and the intermediate filaments (Fey et al. 1984). Cells were then fixed with 3.7% paraformaldehyde in cytoskeleton buffer and treated as in the regular immunofluorescence procedure. For DNA detection, cells were stained with DAPI (2 µl/ml in PBS) during the last wash with PBS after incubation with the secondary antibody. Removal of chroma-

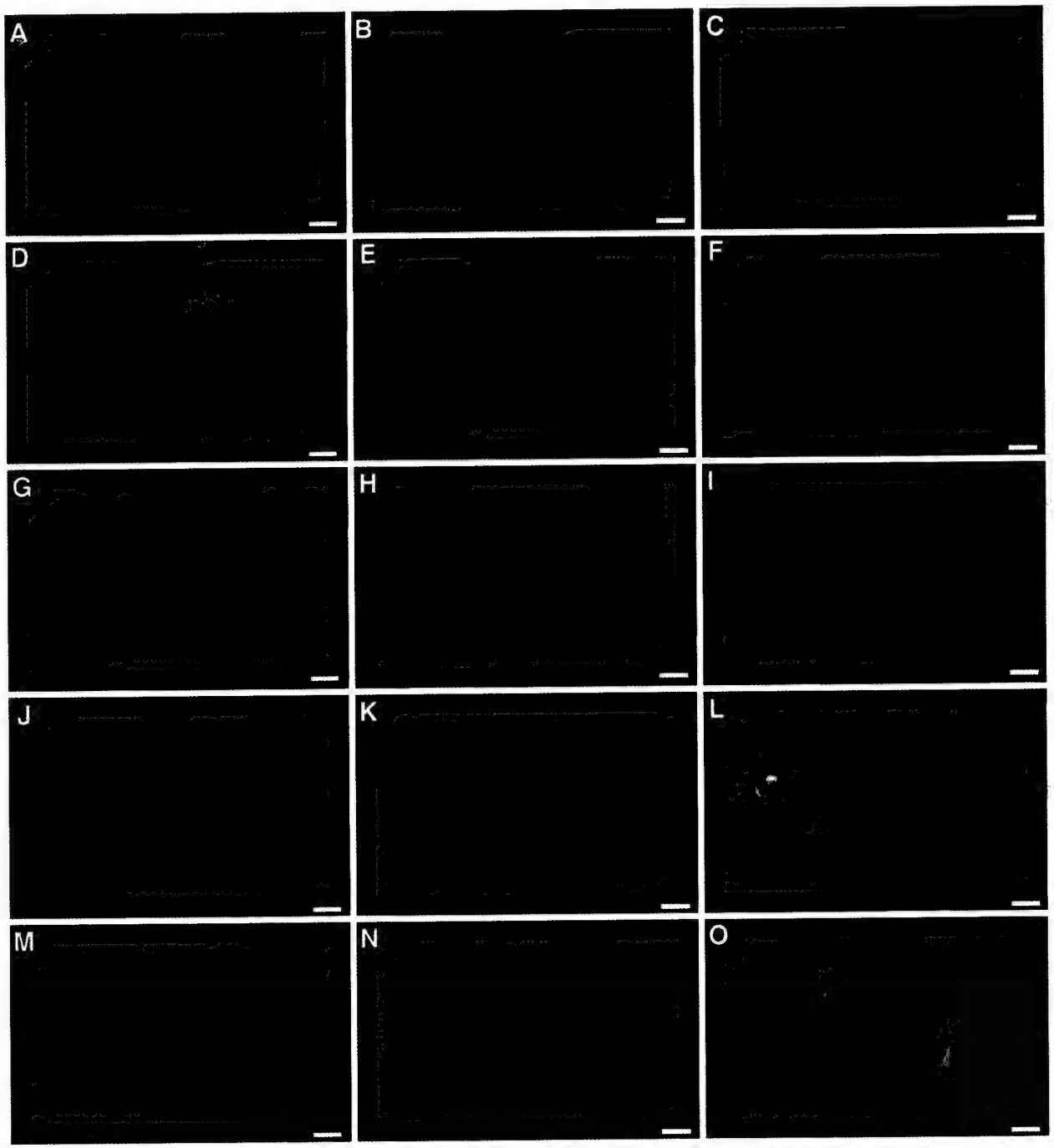

Fig. 1A–O Detection of the tubulin β isotypes, β_I, β_{II}, and β_{IV} in cultured normal human cells. **A, D, G, J, M** Cells treated with anti-β_I by indirect immunfluorescence. **B, E, H, K, N** Cells treated with anti-β_{II} by indirect immunofluorescence. **C, F, I, L, O** Cells treated with anti-β_{IV} by indirect immunfluorescence. **A–C** Human dermal fibroblasts. **D–F** HSK fibroblasts. **G–I** MCF-10F breast endothelial cells. **J–L** Osteoblasts. **M–O** Five hundred and six smooth muscle cells. *Bar* 28 μm. The one cell in panel K where β_{II} appears to be concentrated in the area of the nucleus is actually a mitotic cell in prophase

tin in the nuclear matrix preparations was monitored in this way. For blocking experiments, primary antibodies were incubated with a 200-fold excess of the respective peptide for 30 min at room temperature, prior to incubation with fixed and permeabilized cells.

Results

We have examined the intracellular distribution of the β_I-, β_{II}-, and β_{IV}-tubulin isotypes by indirect immunofluorescence on five different cultured normal human cell lines: HDF human dermal fibroblasts, HSK fibroblasts from baby foreskin, MCF-10F breast endothelial cells, osteoblasts, and 506 smooth muscle cells. In each case, the β_I- and β_{IV}-tubulin isotypes were found in the cytosol, as part of the microtubule network (Fig. 1A, D, G, J, M for β_I and C, F, I, L, O for β_{IV}). The same was seen for β_{II}-tubulin in these cell lines (Fig. 1B, E, H, K, N). In addition, in the smooth muscle cells, β_{II}-tubulin appeared to

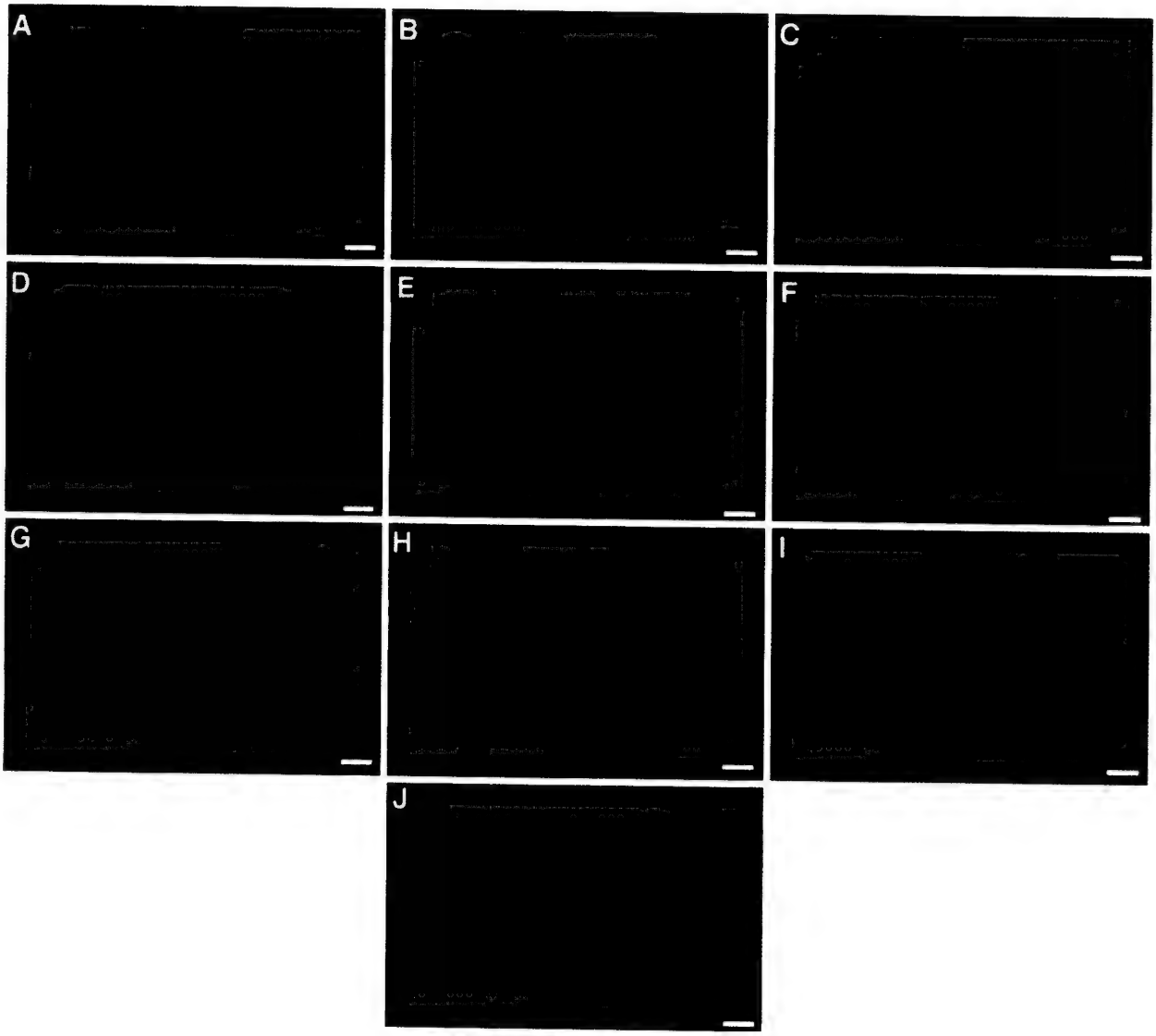

Fig. 2A–J Occurrence of β_{II}-tubulin in the nuclei of cultured human cancer cells. **A, D, G** Cells treated with anti-β_I by indirect immunfluorescence. **B, E, H, J** Cells treated with anti-β_{II} by indirect immunofluorescence. **C, F, I** Cells treated with anti-β_{IV} by indirect immunofluorescence. **A–C** LNCaP prostate carcinoma cells. **D–F** MCF-7 breast carcinoma cells. **G–I** MDA-MB-231 breast carcinoma cells. **J** Calc 18 breast carcinoma cells. *Bar* 28 μm

be present in the centrosomes (Fig. 1N). In no case were any of the isotypes, including β_{II}, found in the nuclei, as no nuclear fluorescence was observed in any of the cell lines investigated.

The presence of β_{II}-tubulin in the nuclei was detected by labeling with anti-β_{II} in all the cancer cell lines investigated. These include LNCaP prostate carcinoma and three types of breast carcinoma: MCF-7, MDA, and Calc 18 cell lines (Fig. 2B, E, H, J). In the LNCaP, MCF-7, and MDA-MB-231 cells, the nucleus was almost indistinguishable from the cytosol; the whole cell appeared to be stained equally with anti-β_{II} (Fig. 2B, E, H). Comparison of the nuclear staining by anti-β_{II} in these cells with that of DAPI, which shows the position of the nuclei, reveals that anti-β_{II} does in fact stain the nucleus in LNCaP, MCF-7, and MDA-MB-231 cells (not shown). In contrast, in the Calc 18 cells, the cytosol was labeled only weakly by anti-β_{II}, while the nuclear labeling was very strong (Fig. 2J). The intranuclear distribution of β_{II}-tubulin appeared to be the same in all the cancer cells. The pattern of nuclear fluorescence was homogenous within the nucleus, except for the Calc 18 cells, in which there appeared to be no β_{II} staining in the nucleoli (Fig. 2J). Some of the MCF-7 cells may also have had less staining in the nucleoli than in the rest of the nuclei (Fig. 2E). The β_I and β_{IV} isotypes were found only in the cytosol, as part of the interphase microtubule network, of each of the cancer cells investigated (Fig. 2A, D, G for β_I and C, F, I for β_{IV}).

To determine the subnuclear localization of β_{II}-tubulin, in situ cell fractionation was performed in LNCaP cells. Removal of the soluble cytoplasmic and nucleoplasmic proteins by detergent extraction did not cause the nuclear fluorescence, obtained by staining with anti-β_{II}, to disappear (Fig. 3A). Furthermore, nuclear fluorescence was still detected after chromatin and chromatin-

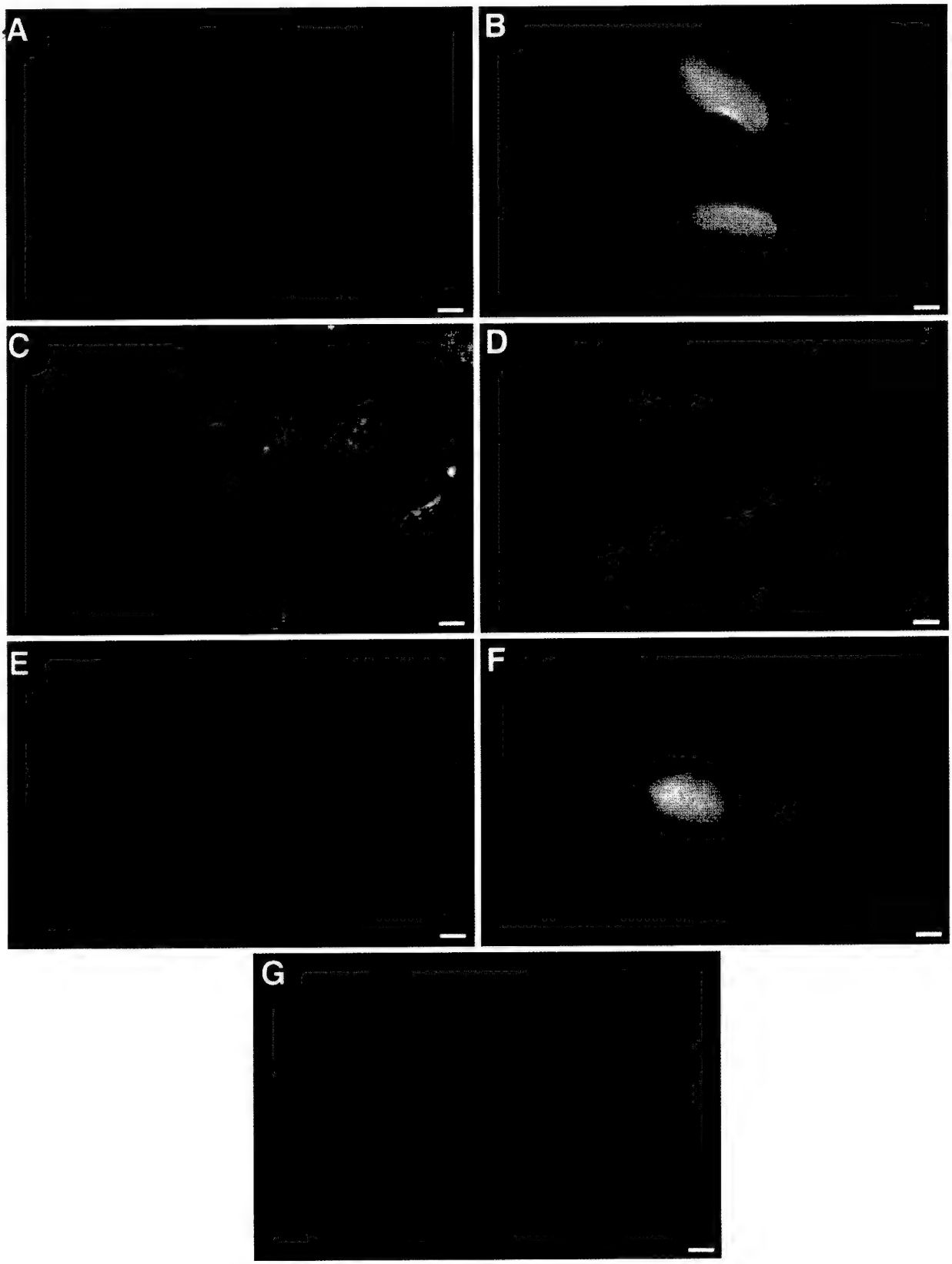

Fig. 3A–G Subcellular localization of β_{II}-tubulin in LNCaP cells. **A** Cytosol-extracted cells treated with anti-β_{II}. **B** Same cells as in **A**, stained with DAPI. **C** Cytosol- and chromatin-extracted cells treated with anti-β_{II}. **D** Same cells as in C, stained with DAPI. The almost complete absence of fluorescence indicates that most of the chromatin was successfully removed. **E** Cytosol-extracted cells treated with anti-β_{II} that had been blocked with its peptide epitope. **F** Same cells as in **E**, stained with DAPI to show position of nuclei. **G** Cytosol- and chromatin-extracted cells treated with anti-β_{II} that had been previously blocked with its peptide epitope. Note the absence of fluorescence. *Bar* 28 μm

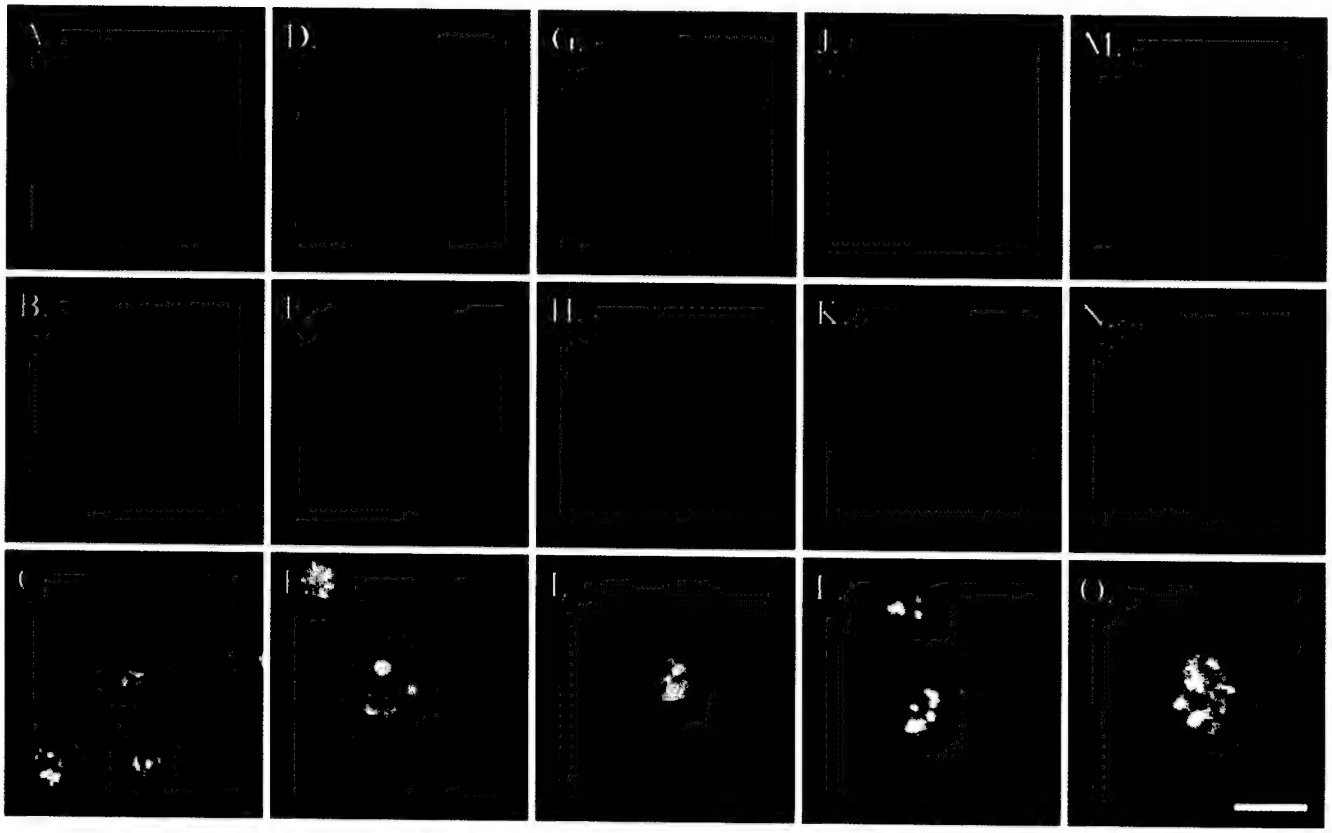

Fig. 4A–O Colocalization of β_{II}-tubulin and RNA in the nucleoli of several carcinoma cells. Cells were treated to extract the chromatin as in Fig. 3. Cells were then treated with anti-β_{II} and acridine orange. β_{II} staining is shown in **A, D, G, J**, and **M**. Acridine orange staining of the corresponding cells is shown in **B, E, H, K**, and **N**. The superimposed images of β_{II} and acridine orange staining are shown in **C, F, I, L**, and **O**. Cells are as follows: C6 glioma (**A–C**); T98G glioma (**D–F**); MCF-7 breast cancer (**G–I**); MDA-MB-435 breast cancer (**J–L**); HeLa cells (**M–O**). Note colocalization of RNA and β_{II}-tubulin. *Bar* 20 μm

associated proteins were removed by DNAse digestion (Fig. 3C). In these cells, β_{II} appeared to accumulate in the nucleolar remnants. These results suggest that β_{II}-tubulin is part of the nuclear matrix in LNCaP cells. Preincubation of anti-β_{II} with its peptide epitope inhibited the nuclear fluorescence in both the cytosol-extracted and the nuclear matrix preparations, indicating that nuclear fluorescence obtained in these cells was due to specific binding of the antibody to β_{II}-tubulin (Fig. 3E, G).

The results obtained with LNCaP cells suggested that β_{II}-tubulin is concentrated in their nucleoli. Although the morphology of the β_{II}-containing structures suggested that they were nucleoli, independent evidence for this was desirable. Since nucleoli are rich in RNA, we used acridine orange, a stain for RNA, to see if the β_{II}-tubulin colocalized with RNA in a variety of cancer cells (Fig. 4). These included C6 glioma (Fig. 4A–C), T98G glioma (Fig. 4D–F), MCF-7 breast cancer (Fig. 4G–I), MDA-MB-435 breast cancer (Fig. 4J–L), and HeLa cells (Fig. 4M–O). We used confocal microscopy to have a clearer picture of the putative nucleoli. The results indicate that β_{II}-tubulin colocalizes almost perfectly with the RNA clusters in the nucleoli.

The above results imply that β_{II}-tubulin is located in the nucleoli of a variety of cultured cancer cells, but they do not address the question of whether β_{II} is in a functional state. One way to address this possibility, as was previously done with β_{II}-tubulin in cultured rat kidney mesangial cells (Walss et al. 1999), is to see whether it binds to colchicine. Accordingly, the same panel of cancer cells used in Fig. 4 was incubated with fluorescein-colchicine and then stained with acridine orange to identify the RNA. As seen in Fig. 5, the fluorescein-colchicine and acridine orange consistently colocalize. In order to eliminate the possibility that fluorescein-colchicine somehow has a particular affinity for nuclei and/or nucleoli, fetal rat calvaria cells, known to lack β_{II}-tubulin, were incubated with fluorescein-colchicine; no nuclear accumulation of fluorescence was seen (not shown). The results in Fig. 5 indicate that the nucleolar β_{II}-tubulin is in its native state, capable of binding colchicine, and is presumably in the form of an $\alpha\beta_{II}$ dimer.

In this study we have examined a variety of cultured cells, some transformed and some not. The transformed cells we have examined contain nuclear β_{II}, whereas few of the nontransformed do. Although based on a small sample, our results raise the possibility that cancer cells are more likely to contain nuclear β_{II}. It is possible, however, that nuclear β_{II} is some kind of artifact arising from growing cells in culture, an artifact conceivably more likely to occur with transformed cells. In order to see whether β_{II}-tubulin can occur in the nuclei of cancer

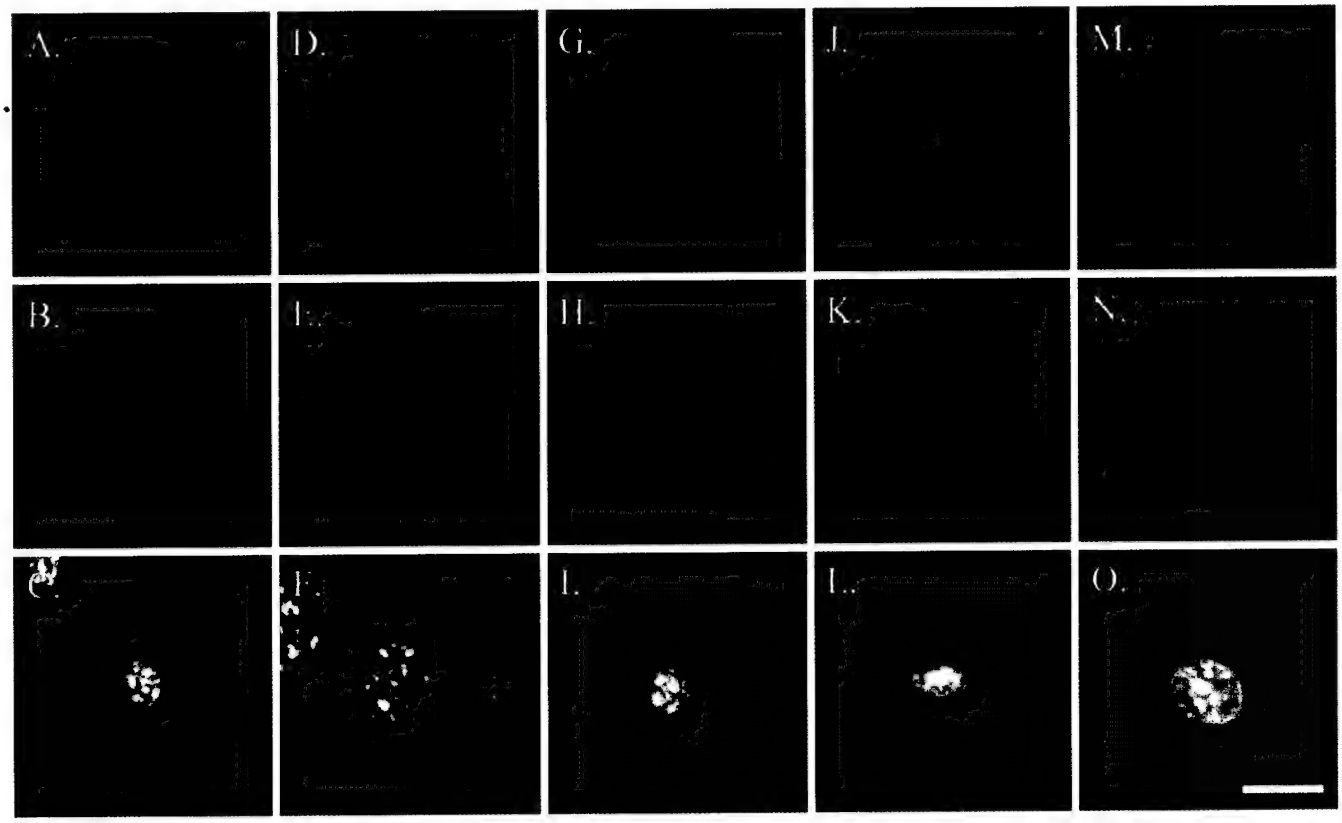

Fig. 5A–O Presence of functional tubulin in the nucleoli of several carcinoma cells. Cells were treated to extract the chromatin as in Fig. 3. Cells were then treated with fluorescein-colchicine and acridine orange. Fluorescein-colchicine staining is shown in **A, D, G, J**, and **M**. Acridine orange staining of the corresponding cells is shown in **B, E, H, K**, and **N**. The superimposed images of fluorescein-colchicine and acridine orange staining are shown in **C, F, I, L**, and **O**. Cells are as follows: C6 glioma (**A–C**); T98G glioma (**D–F**); MCF-7 breast cancer (**G–I**); MDA-MB-435 breast cancer (**J–L**); HeLa cells (**M–O**). Acridine orange stains RNA; note colocalization of RNA and colchicine. *Bar* 20 μm

cells in situ, we examined mammary adenocarcinomas from two patients with breast cancer (Fig. 6). Immunoperoxidase staining reveals that β_{II} occurs in the nuclei of the cancer cells, although not all cancer cell nuclei stain with equal intensity (Fig. 6A); higher magnification shows that β_{II} appears to be concentrated in small intranuclear bodies that may be nucleoli (Fig. 6B).

Discussion

In the work described here, we examined a total of eight cancer cell lines, all of which appear to contain the β_{II} isotype of tubulin in their nuclei. We also see β_{II} in the nuclei of adenocarcinoma cells in breast cancer excisions. We examined five nontransformed cell lines and found that none of them contain nuclear β_{II}. In previous work, however, we have found that the nontransformed rat kidney mesangial cells contain nuclear β_{II} (Walss et al. 1999), as do Rat-1 fibroblasts (Prasad and R.F. Ludueña, unpublished results) but not MDCK epithelial cells (Modig and R.F. Ludueña, unpublished results). Similarly, Ranganathan et al. (1997) have found β_{II}-tubulin in the nuclei of prostate carcinoma as well as in adjacent areas of benign prostate hypertrophy. There have also been some early reports of nuclear tubulin that were not followed up. Menko and Tan (1980) have purified tubulin from the nuclei of 3T3 cells and shown that it bound to colchicine, while Armbruster et al. (1983) have demonstrated its presence in the nuclei of Chinese hamster ovary cells by immunogold staining. In brief, the results presented here, as well as those of Ranganathan et al. (1997), raise the possibility that localization of tubulin in the nucleus may be a phenomenon that is more likely to occur in cancer cells.

Our initial discovery of nuclear β_{II}-tubulin was in rat kidney mesangial cells, obtained from a nontransformed primary cell line. Although these cells are not cancerous, they grow very quickly in culture. Mesangial cells are known to maintain a basal proliferation rate in vitro, even in the absence of exogenous mitogens (Floege et al. 1990). This is most likely due to the fact that these cells self-produce growth factors such as platelet-derived growth factor (PDGF; Abboud et al. 1987), and interleukin-1 (IL-1; Mene et al. 1989), and in this way undergo autocrine-mediated proliferation in vitro (Floege et al. 1991a). Furthermore, cultured mesangial cells are commonly maintained in the presence of 20% fetal calf serum, of which PDGF is the principal mitogen (Floege et al. 1991b). PDGF is known to be the most potent mitogen for cultured mesangial cells, as it has been shown to

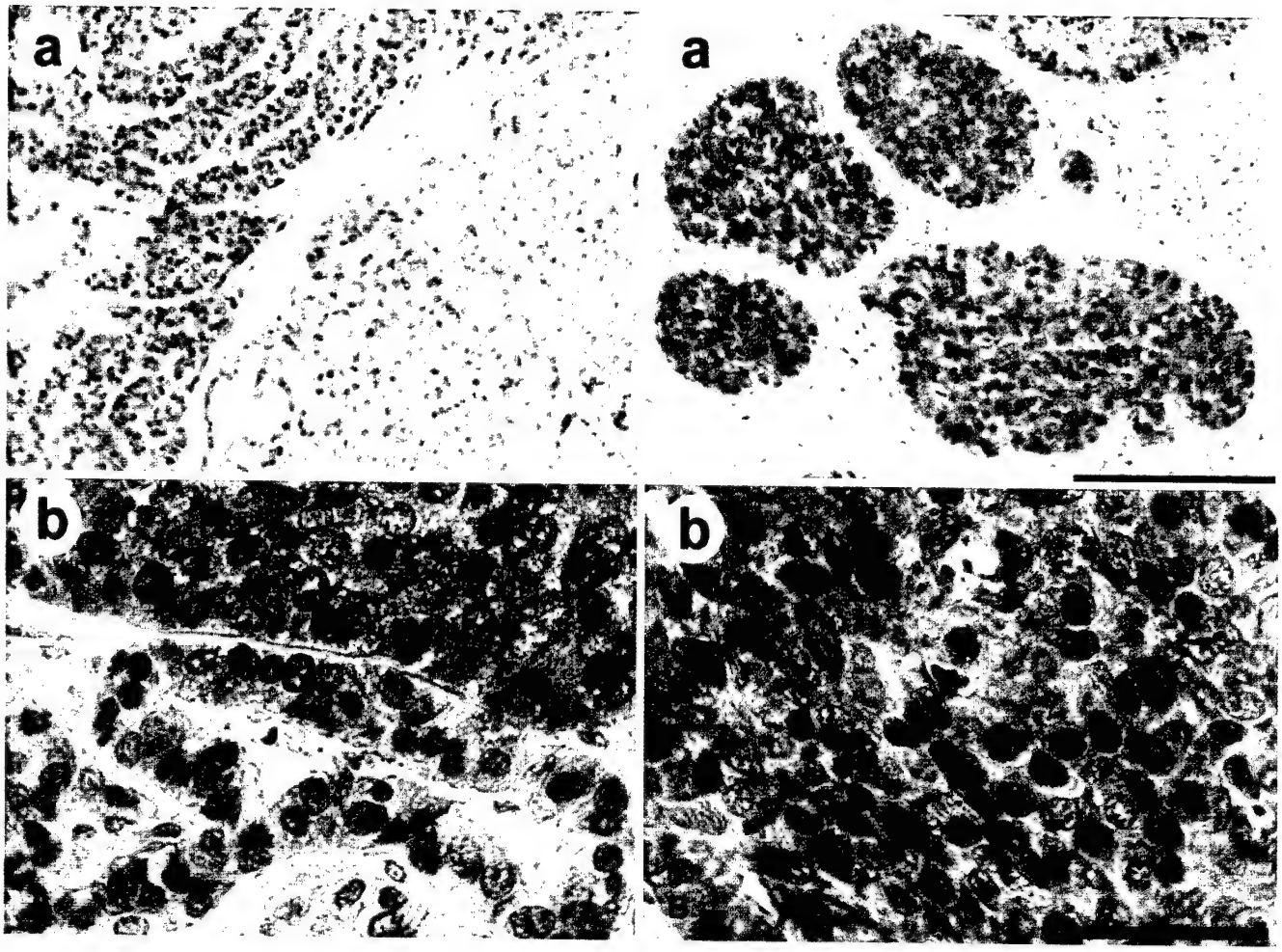

Fig. 6A, B Presence of β_{II}-tubulin in nuclei of human breast cancer tissue. Immunoperoxidase staining of two different breast tumors (*a* and *b*) was performed as described in Materials and methods. Note widespread presence of β_{II} in the nuclei and slightly more intense staining in what appear to be nucleoli. Tumors are shown at two different magnifications. *Bars a* 200 μm; *b* 50 μm

increase the thymidine incorporation rate in these cells by 10- to 15-fold (Floege et al. 1991b). This explains the rapid proliferation of mesangial cells in vitro, in contrast to normal mesangial cells in vivo, which are almost nonproliferative (Pabst and Sterzel 1983) and have been shown to proliferate rapidly only in cases of renal glomerular injury or disease (Schocklmann et al. 1999). Considering these facts, together with our present finding of β_{II}-tubulin in the nuclei of cultured cancer cells, we hypothesize that nuclear β_{II}-tubulin may play a role in assisting rapid cell proliferation. This would explain the finding of β_{II} inside the nuclei of cancer cells but not normal cells. It is possible that other normal cells that proliferate rapidly may also contain β_{II} in their nuclei.

The β_{II} isotype of tubulin has been found to be part of the nuclear matrix in mesangial cells and also has been shown to accumulate in the nucleolus. We now show that this is also the case for β_{II}-tubulin in various cancer cells; nuclear fluorescence due to anti-β_{II} staining was detected in the nuclear matrix and the nucleolar remnants after chromatin digestion. The fact that tubulin has been reported to interact with chromatin in vitro (Mithieux et al. 1984, 1986) could be related to the functions of β_{II} in the nucleolus and the nuclear matrix. In the former case, β_{II} could be binding to the DNA regions, which contain the ribosomal RNA genes, whereas in the latter situation it could be functioning as a chromosomal scaffold. Interestingly, it is known that the antitubulin drug vinblastine affects biochemical processes that are seemingly unrelated to tubulin, such as DNA and RNA synthesis (Creasey 1968; Bernstam et al. 1980). It is possible that its effects on these processes could occur through an interaction with nuclear β_{II}-tubulin.

We have shown that β_{II}-tubulin accumulates preferentially in the nuclei of cancer cells. Perhaps its role in the nucleus is to accelerate DNA and RNA synthesis and therefore facilitate proliferation. Alternatively, nuclear β_{II} may have no specific nuclear function, but rather a unique and as yet unknown function in the mitotic spindle; its location in the nucleus, therefore, may allow it to act quickly when mitosis begins. If either hypothesis were correct, it makes sense that nuclear β_{II} would be needed more in cancer cells, to assist rapid cell proliferation. In conclusion, one may speculate that nuclear β_{II} may become an interesting and novel target for cancer

chemotherapy. A tubulin-specific drug whose major effects are on cancer cells would be very exciting.

Although our results suggest that there is a correlation between transformation and the presence of nuclear β_{II}, there is another correlation that needs to be considered. Of the eight cancer cell lines used in this study, five were from tumors of epithelial origin. Of the nontransformed cell lines we have used here, as well as those used by Menko and Tan (1980), Armbruster et al. (1983), and Walss et al. (1999), seven were of epithelial origin. Grouping the results according to epithelial origin, we find that eight out of nine cell lines of epithelial origin have nuclear β_{II}, whereas that is true for only four out of nine cell lines of nonepithelial origin. This is comparable to the presence of nuclear β_{II} in eight out of eight transformed cell lines and four out of ten nontransformed cell lines. It is quite possible that nuclear localization of β_{II} is more likely to occur in transformed cells, particularly if they are of epithelial origin. Further investigation may clarify these relationships.

Acknowledgements We thank: Dr. Eugene Sprague for providing the human dermal fibroblasts, Dr. Mary Pat Moyer for providing the 506 smooth muscle cells and the HSK fibroblasts, Dr. John Lee for providing the osteoblasts, Dr. Nandini Chaudhuri for providing the LNCaP, MCF-7, and MDA-MB-231 cells, Dr. Jean-François Riou for providing the Calc 18 cells, Dr. Susan Mooberry for the gift of MDA-MB-435 and HeLa cells, and Dr. Martin Adamo for the C6 and T98G glioma. We also thank Phyllis Smith for preparation of the monoclonal antibodies used in these experiments and Dr. Victoria Centonze for invaluable assistance with confocal microscopy.

References

Abboud HE, Poptic E, Dicorleto PE (1987) Production of platelet–derived growth factor-like protein by rat mesangial cells in culture. J Clin Invest 80:675–683

Armbruster BL, Wunderli H, Turner BM, Raska I, Kellenberger E (1983) Immunocytochemical localization of cytoskeletal proteins and histone 2B in isolated membrane-depleted nuclei, metaphase chromatin, and whole Chinese hamster ovary cells. J Histochem Cytochem 31:1385–1393

Banerjee A, Roach MC, Wall KA, Lopata MA, Cleveland DW, Ludueña RF (1988) A monoclonal antibody against the type II isotype of β-tubulin. Preparation of isotypically altered tubulin. J Biol Chem 263:3019–3034

Banerjee A, Roach MC, Trcka P, Ludueña RF (1992) Preparation of a monoclonal antibody specific for the class IV isotype of β-tubulin. Purification and assembly of $\alpha\beta_{II}$, $\alpha\beta_{III}$, and $\alpha\beta_{IV}$ tubulin dimers from bovine brain. J Biol Chem 267:5625–5630

Bernstam VA, Gray RH, Bernstein IA (1980) Effect of microtubule-disrupting drugs on protein and RNA synthesis in *Physarum polycephalum* amoebae. Arch Microbiol 128:34–40

Cattoretti G, Pileri S, Parravicini C, Becker MH, Poggi S, Bifulco C, Key G, D'Amato L, Sabattini E, Feudale E (1993) Antigen unmasking on formalin-fixed, paraffin-embedded tissue sections. J Pathol 171:83–98

Creasey WA (1968) Modifications in biochemical pathways produced by the *Vinca* alkaloids. Cancer Chemother Res 52:501–507

Fey EG, Wan KM, Penman S (1984) Epithelial cytoskeletal framework and nuclear matrix-intermediate filament scaffold: three-dimensional organization and protein composition. J Cell Biol 98:1973–1984

Floege J, Topley N, Wessel K, Kaever V, Radeke HH, Hoppe J, Kishimoto T, Resch K (1990) Monokines and platelet-derived growth factor modulate prostanoid production in growth arrested human mesangial cells. Kidney Int 37:859–869

Floege J, Topley N, Resch K (1991a) Regulation of mesangial cell proliferation. Am J Kidney Dis 17:673–676

Floege J, Topley N, Hoppe J, Barrett TB, Resch K (1991b) Mitogenic effect of platelet-derived growth factor in human glomerular mesangial cells: modulation and/or suppression by inflammatory cytokines. Clin Exp Immunol 86:334–341

Hyams JS, Lloyd CW (eds) (1994) Microtubules. Wiley-Liss, New York

Ludueña RF (1998) Multiple forms of tubulin: different gene products and covalent modifications. Int Rev Cytol 178:207–275

Mene P, Simonson MS, Dunn MJ (1989) Physiology of the mesangial cell. Physiol Rev 69:1347–1424

Menko AS, Tan KB (1980) Nuclear tubulin of tissue cultured cells. Biochim Biophys Acta 629:359–370

Mithieux G, Alquier C, Roux B, Rousset B (1984) Interaction of tubulin with chromatin proteins. H1 and core histones. J Biol Chem 259:15523–15531

Mithieux G, Roux B, Rousset B (1986) Tubulin-chromatin interactions: evidence for tubulin-binding sites on chromatin and isolated oligonucleosomes. Biochim Biophys Acta 888:49–61

Pabst R, Sterzel RB (1983) Cell renewal of glomerular cell types in normal rats. An autoradiographic study. Kidney Int 24:626–631

Ranganathan S, Salazar H, Benetatos CA, Hudes GR (1997) Immunohistochemical analysis of β-tubulin isotypes in human prostate carcinoma and benign prostate hypertrophy. Prostate 30:263–268

Roach MC, Boucher VL, Walss C, Ravdin P, Ludueña RF (1998) Preparation of a monoclonal antibody specific for the class I isotype of β-tubulin: the β isotypes of tubulin differ in their cellular distributions within human tissues. Cell Motil Cytoskel 39:273–285

Schocklmann HO, Lang S, Sterzel RB (1999) Regulation of mesangial cell proliferation. Kidney Int 56:1199–1207

Walss C, Kreisberg JI, Ludueña RF (1999) Presence of the β_{II} isotype of tubulin in the nuclei of cultured mesangial cells from rat kidney. Cell Motil Cytoskel 42:274–284

Wilson L, Jordan MA (1994) Pharmacological probes of microtubule function. In: Hyams JS, Lloyd CW (eds) Microtubules. Wiley-Liss, New York, pp 59–83

Appendix 2

Cell Motility and the Cytoskeleton 53:39–52 (2002)

Characterization of Nuclear β_{II}-Tubulin in Tumor Cells: A Possible Novel Target for Taxol

Keliang Xu and Richard F. Ludueña*

Department of Biochemistry, The University of Texas Health Science Center at San Antonio

As the subunits of microtubules, α- and β-tubulins have been thought to only exist in the cytoplasm where they are incorporated into microtubules. However, the β_{II} isotype of tubulin has recently been observed in the nuclei of rat kidney mesangial cells [Walss et al., 1999: *Cell Motil. Cytoskeleton* 42:274–284]. In this study, we detected nuclear β_{II}-tubulin in rat C6 glioma cells, human T98G glioma cells, human MCF-7 breast carcinoma cells, human MDA-MB-435 breast carcinoma cells, and human Hela cervix carcinoma cells. In addition, nuclear β_{II}-tubulin in these cells was found to exist as $\alpha\beta_{II}$ dimers instead of assembled microtubules and appeared to be particularly concentrated in the nucleoli. Several anti-tubulin drugs were used to treat C6 cells to determine their influence on nuclear β_{II}-tubulin. Taxol, a tubulin drug with higher specificity for β_{II}-tubulin than for other β-tubulin isotypes, irreversibly decreased nuclear β_{II} content in a concentration-dependent manner in C6 cells. Meanwhile, cells were found to be apoptotic as was suggested by the presence of multiple micronuclei and DNA fragmentation. On the other hand, no depletion of nuclear β_{II}-tubulin was observed when C6 cells were incubated with colchicine or nocodazole, two anti-tubulin drugs with higher specificity for the $\alpha\beta_{IV}$ isotype, supporting the hypothesis that drugs with higher specificity for β_{II}-tubulin deplete nuclear β_{II}-tubulin. Cell Motil. Cytoskeleton 53: 39–52, 2002.

Key words: nuclear structure; tubulin; apoptosis; taxol; isotypes

INTRODUCTION

The structural subunit of microtubules, the 100-kDa protein tubulin, is a heterodimer of two polypeptide chains designated α and β [Bryan and Wilson, 1971; Ludueña et al., 1977]. Both α- and β-tubulin exist as numerous isotypes encoded by different genes, among which β isotypes exhibit more complex and variable tissue distributions than do the α isotypes [Ludueña, 1998]. It has been previously reported that the β_{II} isotype of tubulin, which was thought to be normally present only in the cytoplasm where it participates in microtubule formation, is present in the nuclei of a prostate tumor [Ranganathan et al., 1997] and a breast tumor [Walss et al., 2000] as well as cultured rat kidney mesangial cells, a non-transformed cell line [Walss et al., 1999]. In contrast, biopsy samples of several normal human tissues using immunoperoxidase staining, did not show any evidence for the existence of nuclear β_{II}-tubulin [Roach et al., 1998]. These results raise the possibility that nuclear β_{II}-tubulin may be correlated with the cancerous state. In this study, we searched for

Contract grant sponsor: NIH; Contract grant numbers: CA26376, P30 CA54174; Contract grant sponsor: US Army BCRP; Contract grant number: DAMD 17-98-1-8246 and DAMD 1701-1-0411; Contract grant sponsor: Welch Foundation; Contract grant number: AQ-0726.

*Correspondence to: Dr. Richard F. Ludueña, Department of Biochemistry, Mail Code 7760, The University of Texas Health Science Center at San Antonio, 7703 Floyd Curl Drive, San Antonio, TX 78229-3900. E-mail: luduena@uthscsa.edu

Received 16 January 2002; Accepted 16 April 2002

Published online 22 July 2002 in Wiley InterScience (www.interscience.wiley.com). DOI: 10.1002/cm.10060

β_{II}-tubulin in the nuclei of several cancer cells. We found that nuclear β_{II}-tubulin exists in the nuclear matrix and is often concentrated in the nucleolus. In addition, the depletion of nuclear β_{II}-tubulin after taxol treatment was observed as well as cell apoptosis in rat C6 glioma cells. As a successful anti-tumor drug with higher specificity for β_{II}-tubulin than for other β-tubulin isotypes [Derry et al., 1997], taxol has been known to target polymerized microtubules, presumably in the cytoplasm of cells [Schiff and Horwitz, 1981; Parness and Horwitz, 1981; Wilson and Jordan, 1994]. Our results suggest the possibility that nuclear β_{II}-tubulin in cancer cells may constitute a novel target for taxol.

MATERIALS AND METHODS

Cell Culture

Rat C6 glioma cells, human T98G glioma cells (kind gifts from Dr. Martin Adamo, Department of Biochemistry, University of Texas Health Science Center at San Antonio; UTHSCSA), human MCF-7 breast carcinoma cells (a kind gift from Dr. Robert Klebe, Department of Cellular and Structural Biology, UTHSCSA), human MDA-MB-435 breast carcinoma cells, and Hela cells (kind gifts from Dr. Susan Mooberry, Southwest Foundation for Biomedical Research) were cultured in Ham's F-12 (Gibco/BRL, Rockville, MD) with 1 mM glutamine, Minimum Essential Medium (Gibco/BRL) with Earle's salts and L-glutamine, HyQ DME/F-12 (Hyclone, Logan, UT) with 2.5 mM L-glutamine, Improved MEM Zinc Option (Gibco/BRL) with 2 mg/L L-glutamine, L-proline, and 50 μg/ml gentamicin sulfate, and Basal Medium Eagle (Gibco/BRL) with Earle's salts and L-glutamine, respectively. All media contained 100 IU/ml penicillin, 100 μg/ml streptomycin, and 10% fetal bovine serum (FBS) (Gibco/BRL). For each cell line, an equivalent number of cells were plated onto each coverslip in six-well plates or 100-mm tissue culture dishes and incubated for 24–48 h at 37°C in 5% CO_2. For drug treatment, cells were incubated in appropriate medium with either taxol (provided by the National Cancer Institute), colchicine (Sigma Chemical Corp., St Louis, MO), or nocodazole (Sigma Chemical Corp.) at the indicated concentrations and for the indicated times as described below. Cells were used between the 4th and 30th passages in this study.

Antibodies and Peptides

The monoclonal antibodies SAP.4G5, JDR.3B8, SDL.3D10, and ONS.1A6 specific, respectively, for the β_I, β_{II}, β_{III}, and β_{IV} isotypes of tubulin were prepared as previously described [Banerjee et al., 1988, 1990, 1992; Roach et al., 1998]. The sequences of the peptides (BioSearch Corp., San Rafael, CA) used as immunogens to raise these antibodies were CEEAEEEA, CEGEEDEA, CESESQGPK, and CEAEEEVA, respectively. Each sequence is identical to the C-terminal sequence of the corresponding isotype of tubulin except for the N-terminal cysteine. The monoclonal primary nucleolin antibody (C23) was obtained from Santa Cruz Biotechnology (Santa Cruz, CA). The monoclonal antibody AYN.6D10, specific for the tyrosinated forms of the Mα1, Mα3, and Mα4 mammalian α-tubulin isotypes was a kind gift from Dr. Asok Banerjee (Department of Biochemistry, UTHSCSA). The rhodamine-labeled anti-β_{II} was generated as described [Walss et al., 1999]. Cy3-conjugated goat anti-mouse IgG and fluorescein-conjugated goat anti-mouse IgG were both obtained from Jackson Immunoresearch (West Grove, PA).

Immunofluorescence Microscopy

Cultured cells on coverslips were rinsed twice with phosphate-buffered saline (PBS), fixed with 3.7% paraformaldehyde at room temperature for 15 min, and permeabilized with 0.5% Triton X-100 in PBS for 1 min. Cells were then incubated overnight with the respective isotype-specific monoclonal IgG mouse antibody (anti-β_I, 0.17 mg/ml; anti-β_{II}, 0.03 mg/ml; anti-β_{III}, 0.08 mg/ml; anti-β_{IV}, 0.17 mg/ml; anti-α, 0.02–0.03 mg/ml) diluted in PBS containing 10% normal goat serum (Jackson Immunoresearch). Cells were rinsed with PBS and incubated with Cy3-conjugated goat anti-mouse IgG (1:50) for 1 h at room temperature. Cells were then stained with 4′, 6-diamidino-2-phenylindole, dihydrochloride (DAPI) (Molecular Probes, Eugene, OR) to visualize the nucleus. Coverslips were mounted on glass slides and examined with a Zeiss epifluorescence photomicroscope using a Plan-Neufluar 60× oil objective or an Olympus Fluoview laser scanning confocal microscope. For blocking experiments, primary antibodies were incubated with a 200-fold excess of the respective peptide for 30 min at room temperature prior to incubation with cells. In the experiments using fluorescein-colchicine (Molecular Probes), fixed and permeabilized cells were incubated with fluorescein-colchicine (0.1 mg/ml) or fluorescein in the dark at room temperature for 2 h. Coverslips were then mounted on glass slides for visualization.

For the double immunofluorescence experiments, cytosol- and chromatin-extracted cells were incubated with anti-α (0.02-0.03 mg/ml) or anti-nucleolin (0.01 mg/ml) at 4°C overnight, rinsed with PBS and incubated with fluorescein-conjugated goat anti-mouse IgG (1:50). Cells were rinsed and further incubated with rhodamine-labeled anti-β_{II} (0.1 mg/ml) at 4°C overnight.

In Situ Cell Fractionation

Cells grown to 50% confluence on glass coverslips were washed twice with ice-cold PBS and incubated on ice for 5 min with cold CSK-100 buffer (10 mM Pipes, PH 6.8, 300 mM sucrose, 100 mM NaCl, 3 mM $MgCl_2$, 1 mM EGTA, 1% Triton X-100, 1.2 mM PMSF, 0.1% aprotinin, 0.1% pepstatin A, and 1% vanadyl ribonucleoside complex) to remove all soluble cytoplasmic and nucleoplasmic proteins. These cells were further incubated at room temperature for 1 h in CSK-50 buffer (same as CSK-100 except with 50 mM NaCl instead of 100 mM) containing 100 μg/ml of DNase I (Sigma Chemical Corp.). The chromatin was then removed by addition of 2 M $(NH_4)_2SO_4$ dropwise to a final concentration of 0.25 M. What was left behind consisted of the nuclear matrix and the intermediate filaments [Fey et al., 1984]. Cells were then fixed with 3.7% paraformaldehyde in CSK-100 buffer and stained using the regular immunofluorescence procedure.

DNA Fragmentation

C6 cells were grown on 100-mm tissue culture dishes to confluence and treated with taxol or vehicle (DMSO) at 37°C for 72 h. Cells in each dish were then harvested by trypsinization and spun down at 1,000*g* for 5 min. The cell pellet was then lysed in 300 μl of 0.5% Triton X-100 TE buffer (pH 8.0) at room temperature for 15 min, followed by two extractions with phenol/chloroform. Genomic DNA was then precipitated in ethanol at −20°C overnight. DNA was then collected and treated with 50 μg/ml RNase A (Sigma) in 20 μl TE (pH 8.0) at 37°C for 1 h. Ten percent glycerol was added to the sample, and DNA fragments were separated on a 1.8% agarose gel and visualized under an ultra-violet light [Sabbatini and McCormick, 1999].

RESULTS

Subcellular Localization of Tubulin Isotypes in Tumor Cells

The subcellular localization of the tubulin isotypes β_I, β_{II}, β_{III}, and β_{IV} in rat C6 glioma cells, human T98G glioma cells, human MCF-7 breast carcinoma cells, human MDA-MB-435 breast carcinoma cells, and human Hela cervix carcinoma cells was determined by indirect immunofluorescence microscopy using mouse monoclonal antibodies specific for each isotype. As shown in the confocal micrographs, all of these tumor cells express the four β-tubulin isotypes (Fig. 1). β_I, β_{III}, and β_{IV} only appeared in the cytoplasm (Fig. 1), while β_{II} was localized in both the nucleus and the cytoplasm. Compared to the cytoplasmic microtubule network, nuclear β_{II} was more evenly distributed, suggesting that it is probably not in microtubule form. Pre-incubation of the β_{II} antibody with a 200-fold excess of β_{II} peptide blocked the fluorescence (data not shown), while pre-incubation of the β_{II} antibody with a 200-fold excess of the β_I, β_{III}, or β_{IV} peptides did not affect the fluorescence, demonstrating that the β_{II} antibody is specific for β_{II}-tubulin.

Nuclear β_{II}-Tubulin Exists as $\alpha\beta_{II}$ Dimers

The fact that tubulin molecules usually exist in the αβ heterodimer form raises the possibility that α-tubulin is associated with nuclear β_{II}-tubulin. Hence, we determined whether α-tubulin occurs in the nuclei of these cells; indirect immunofluorescence was performed using a monoclonal antibody specific for tyrosinated α-tubulin. While the cytoplasmic microtubule networks were stained by the antibody, the nuclei did not appear to be fluorescent (data not shown). It is possible that the α-tubulin epitope was masked by chromatin and therefore could only be observed after chromatin was removed. Indeed, after the cytosol and the chromatin were removed, leaving only the nuclear matrix, small fluorescent bodies were observed (not shown). These results suggest that α-tubulin also localizes to the nuclear matrix. In order to confirm the colocalization of α- and β_{II}-tubulin, double immunofluorescence microscopy was performed after in situ cell fractionation. The fluorescent patterns of α-tubulin were indeed same as those of β_{II}-tubulin in the same cells (not shown). These results suggest that α-tubulin associates with β_{II}-tubulin in the nuclei of C6, T98G, MCF-7, MDA, and Hela cells.

To determine whether nuclear β_{II}-tubulin exists in the form of tubulin dimers in their native state rather than assembled microtubules or denatured tubulin, fluorescein-colchicine was used as a fluorescent probe since colchicine is known to only bind to soluble native tubulin dimers, but not the tubulin in microtubules [Banerjee and Ludueña, 1992]. The nuclei of all these tumor cells were stained extensively by fluorescein-colchicine as shown in Figure 2, suggesting that nuclear β_{II}-tubulin exists in the form of soluble dimers rather than microtubules and that these dimers are functional. No nuclear fluorescence was observed in control experiments in which cells were treated with fluorescein rather than fluorescein-colchicine (data not shown), demonstrating that the nuclear fluorescence obtained with fluorescein-colchicine was due to the binding of colchicine rather than that of the fluorescein moiety.

Nuclear β_{II}-Tubulin Concentrates in the Nucleolus

In order to determine the subnuclear localization of β_{II}-tubulin, in situ cell fractionation was performed. We removed the cytosol and the chromatin from these five tumor cells while the nuclear matrix was kept intact. As shown in Figure 3, nuclear matrix was stained by fluo-

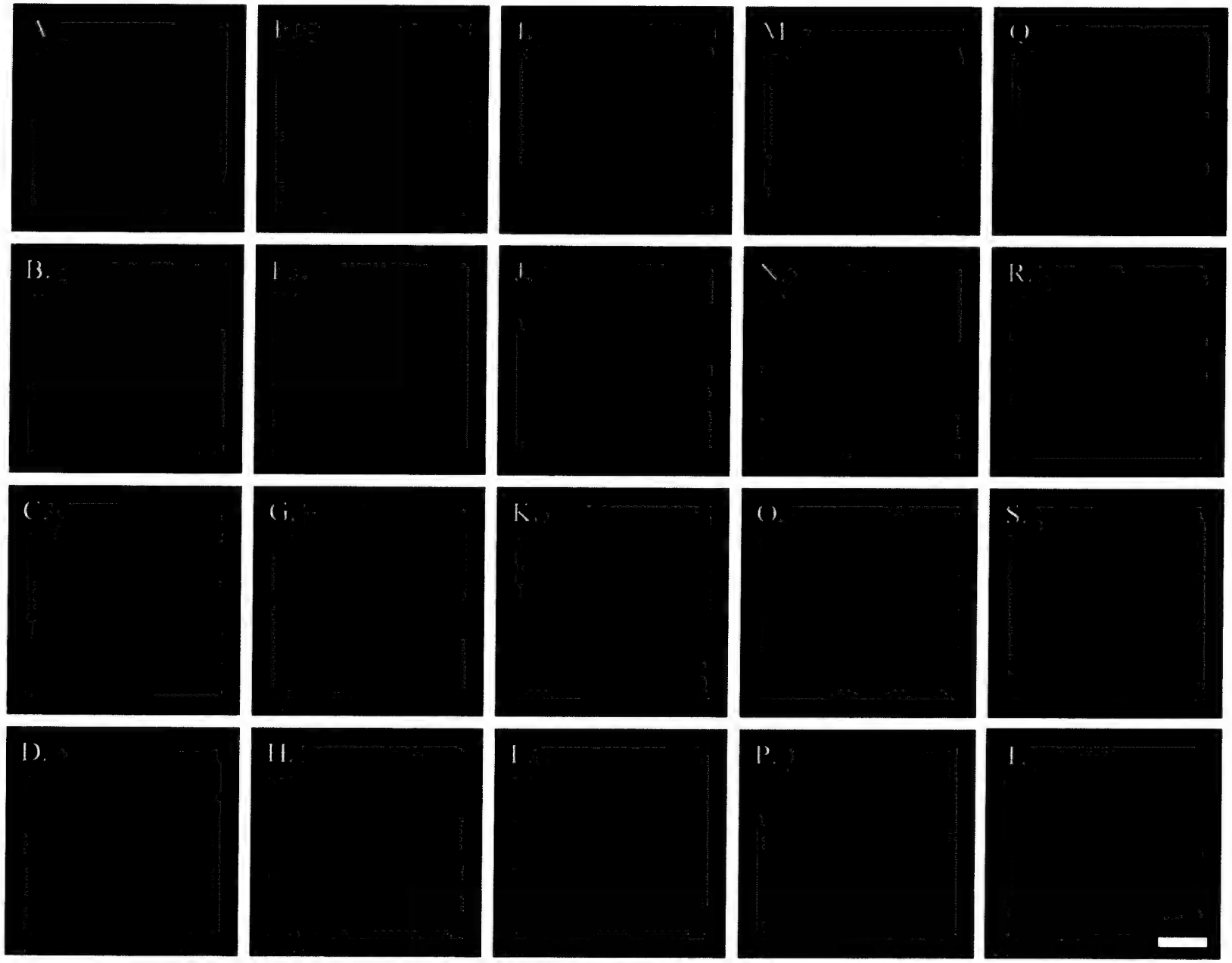

Figure 1.

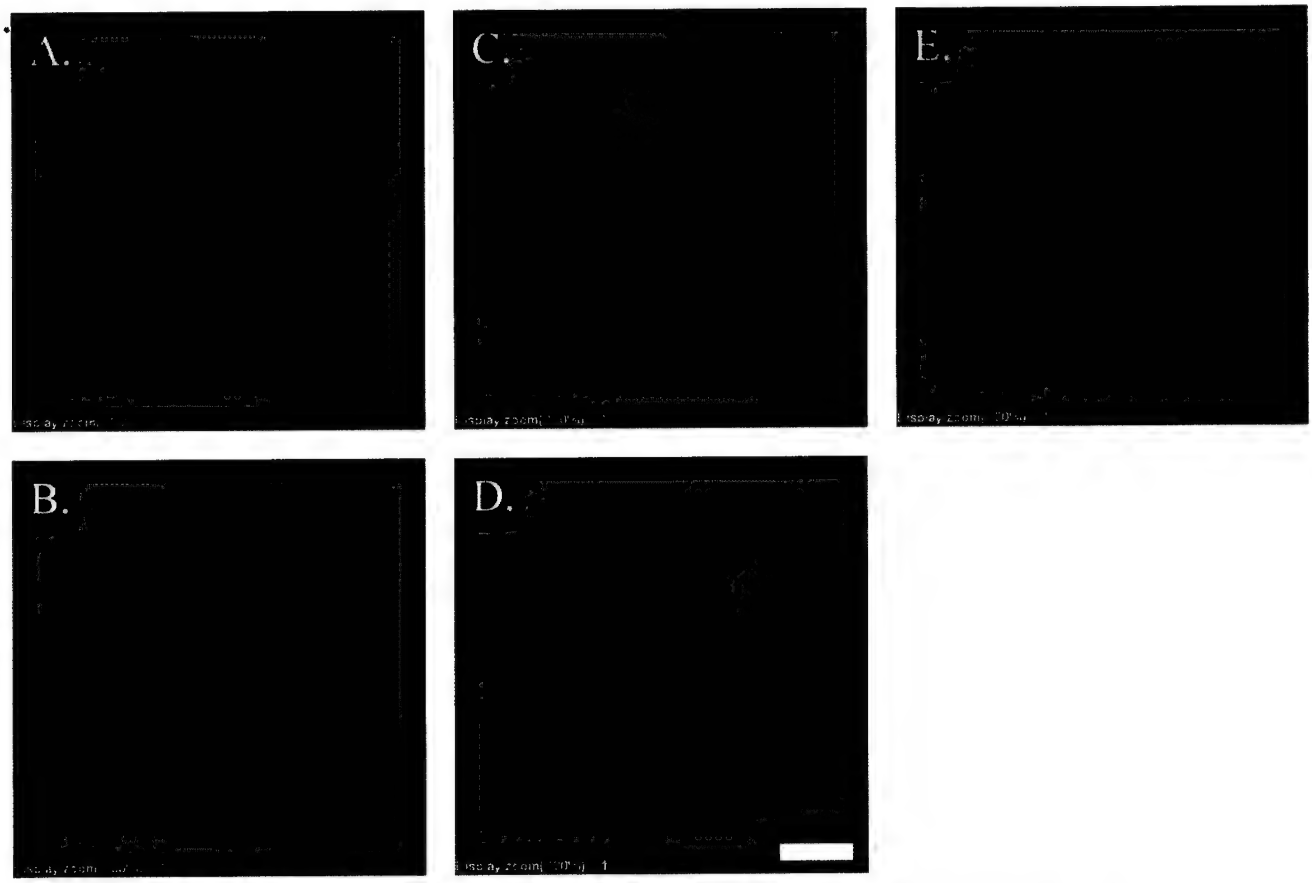

Fig. 2. Localization of tubulin dimer in several carcinoma cells. Cells were stained with 0.1 mg/ml fluorescein-colchicine and visualized by confocal microscopy. **A:** C6 cells; **B:** T98G cells; **C:** MCF-7 cells; **D:** MDA-MB-435 cells; **E:** Hela cells. Bar = 10 μ.

rescein-colchicine. Small bodies apparently corresponding to the nucleoli in the phase contrast pictures were extensively stained, suggesting that tubulin dimers accumulate in the nucleoli of these cells. In order to confirm that β_{II}-tubulin accumulates in the nucleolus, the nuclear matrix of these cells was stained with rhodamine-conjugated β_{II} antibody as well as a monoclonal antibody specific for nucleolin, a nucleolar marker. The fluorescent pattern of β_{II}-tubulin in these cells (Fig. 4A, D, G, J, and M) resembles that of fluorescein-colchicine staining (Fig. 3A, C, E, G, and H). Superimposing the confocal micrographs of β_{II}-tubulin staining (red) and nucleoli staining (green) shows that β_{II}-tubulin colocalizes with nucleolin in the nucleolus (yellow spots), while the rest of the nucleus was stained with a light red color (Fig. 4C, F, I, L, and O). These results confirmed that β_{II}-tubulin localizes in the nuclear matrix and concentrates in the nucleoli of C6, T98G, MCF-7, MDA, and Hela cells.

Effects of Taxol on Nuclear β_{II}-Tubulin in C6 Cells

When C6 cells were treated with taxol at a concentration as low as 20 nM, nuclear β_{II}-tubulin began to rearrange into aggregated forms (Fig. 5*C*), and multiple micronuclei were observed in the same cells (Fig. 5D). Since micronucleation is a marker for apoptosis [Hoshino et al., 2001], our results suggested that these cells were undergoing apoptosis. When C6 cells were treated with 1 μM taxol, nuclear β_{II}-tubulin began to diminish (Fig. 5E), and the cytoplasmic microtubules were strongly bundled, which is one of taxol's known effects [Schiff and Horwitz, 1980; Turner and Margolis,

Fig. 1. Subcellular localizations of tubulin β_I, β_{II}, β_{III}, β_{IV} in several carcinoma cells. Indirect immunofluorescence was performed using monoclonal anti-β_I, anti-β_{II}, anti-β_{III}, and anti-β_{IV} followed by confocal microscopy. **A–D:** C6 cells. **E–H:** T98G cells. **I–L:** MCF-7 cells. **M–P:** MDA-MB-435 cells. **Q-T:** Hela cells. A, E, I, M, and Q: localization of β_I; B, F, J, N, and R: localization of β_{II}; C, G, K, O, and S: localization of β_{III}; D, H, L, P, and T: localization of β_{IV}. Bar = 10 μ.

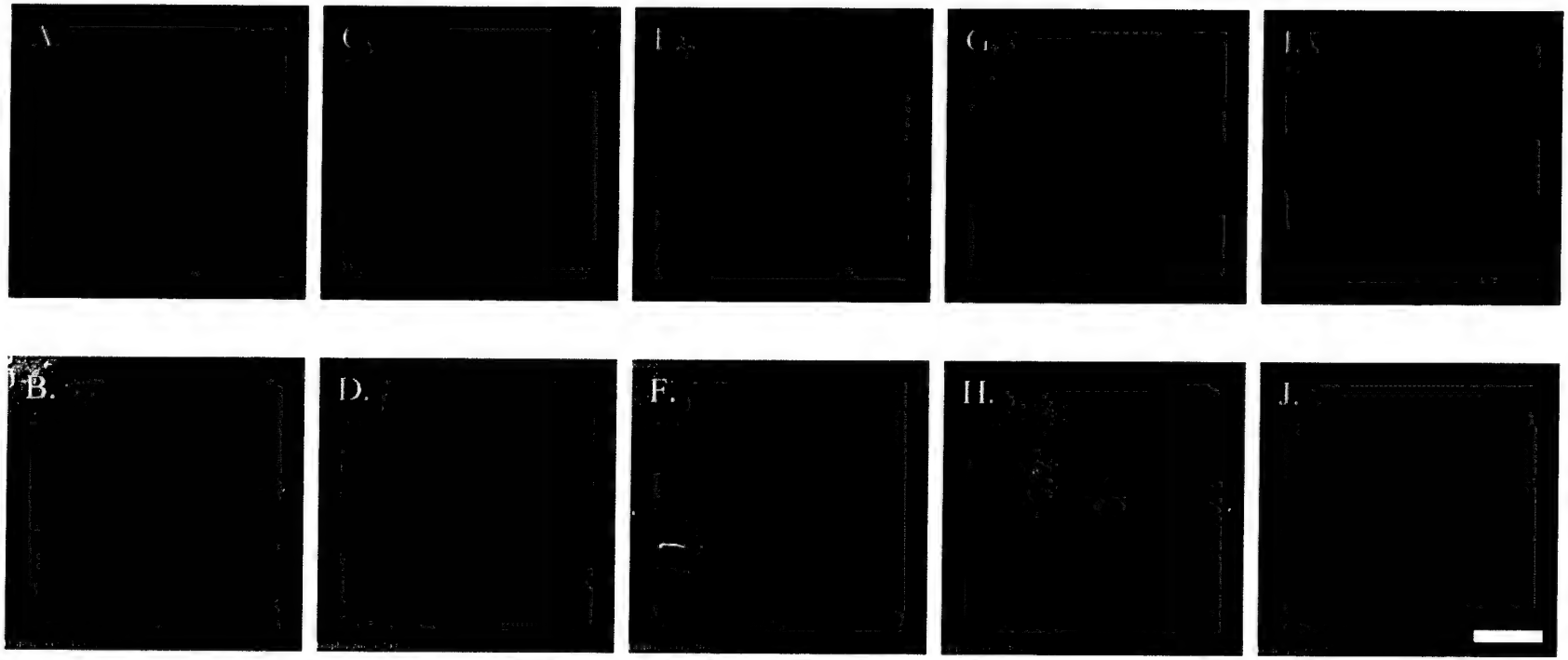

Fig. 3. Localization of tubulin dimer in the nuclear matrix of several carcinoma cells. Cells were grown on glass coverslips, and nuclear matrix was prepared as described in Materials and Methods. The extracted cells were then fixed and incubated with 0.1 mg/ml fluorescein-colchicine. **A,C,E,G,I:** Confocal micrographs showing the localization of tubulin dimer. **B,D,F,H,J:** Phase contrast micrographs showing the nuclei and the nucleoli in the same cells. A and B: C6 cells; C and D: T98G cells; E and F: MCF-7 cells; G and H: MDA-MB-435 cells; I and J: Hela cells. Bar = 10 μ.

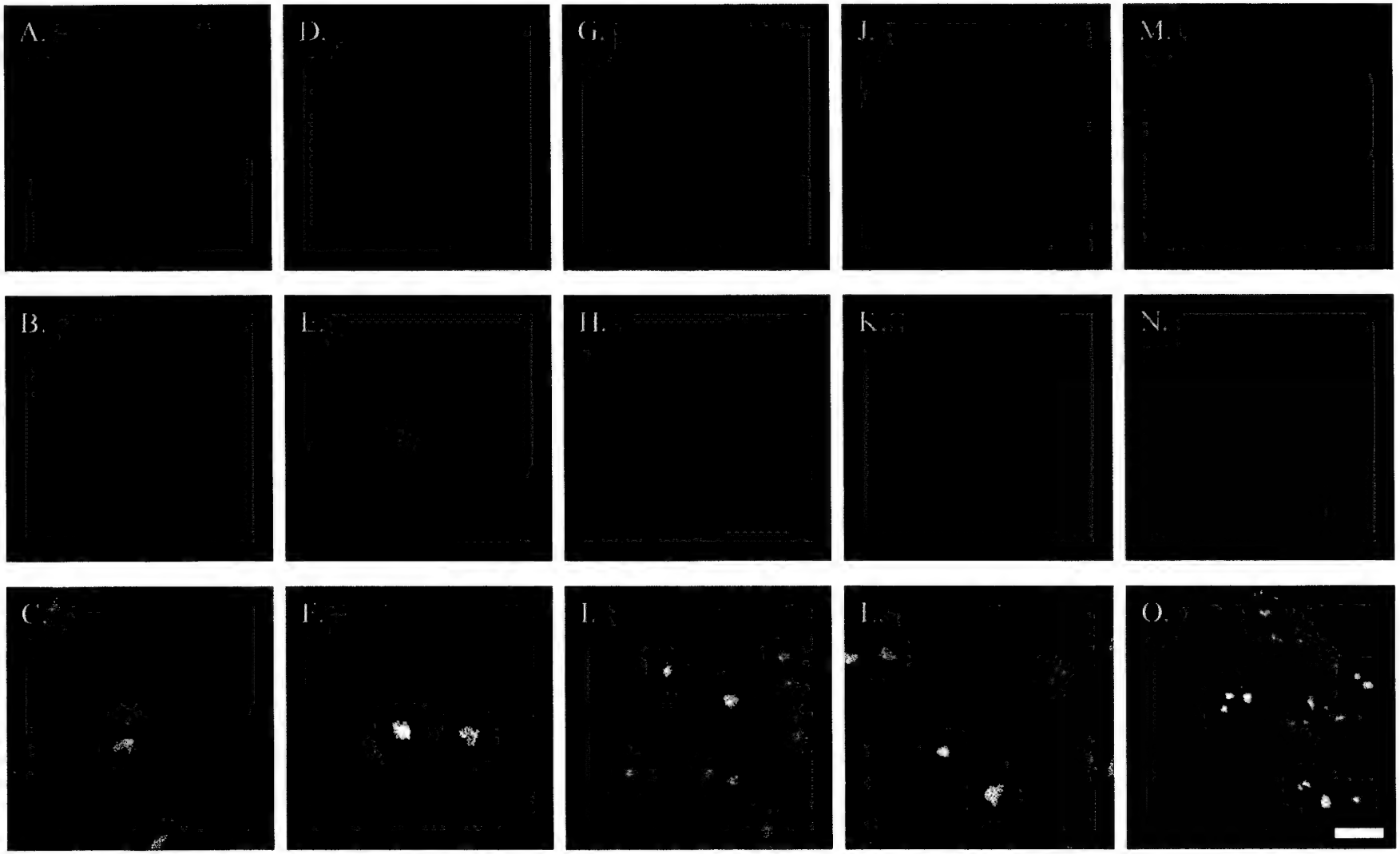

Fig. 4. Accumulation of β_{II}-tubulin in the nucleoli of several carcinoma cells. Cells were extracted as described in Materials and Methods and incubated with the monoclonal anti-nucleolin primary antibody followed by fluorescein-conjugated secondary antibody. The same cells were then incubated with rhodamine-conjugated anti-β_{II} primary antibody. Confocal micrographs showing the localization of β_{II}-tubulin (red) were superimposed on those showing the localization of nucleoli (green) in the same cells. **A, D, G, J, M:** β_{II}-tubulin staining in the nuclear matrix of C6 cells, T98G cells, MCF-7 cells, MDA-MB-435 cells, and Hela cells, respectively. **B, E, H, K, N:** Nucleolin staining in the nuclear matrix of C6 cells, T98G cells, MCF-7 cells, MDA-MB-435 cells, and Hela cells, respectively. **C, F, I, L, O:** Superimposed micrographs of A and B, D and E, G and H, J and K, and M and N, respectively. Bar = 10 μ.

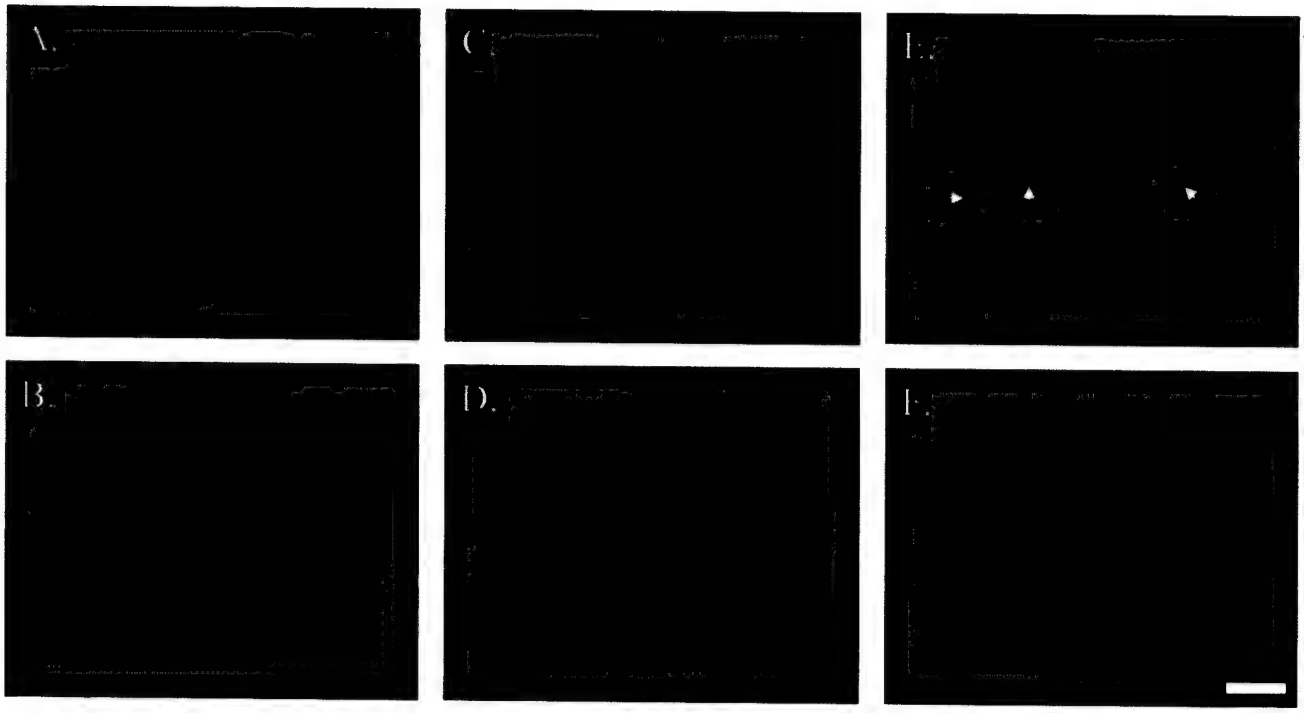

Fig. 5. The effects of taxol on nuclear β_{II}-tubulin in C6 cells. Cells were treated with indicated concentration of taxol for 24 h. **A,C,E:** Cells stained with anti-β_{II}. **B,D,F:** The same cells stained with DAPI. A and B: C6 cells in the absence of taxol. C and D: C6 cells incubated with 20 nM taxol. E and F: C6 cells incubated with 1 μM taxol. *Arrows* point to the cells depleted of nuclear β_{II}-tubulin but clearly containing bundles of microtubules in the cytoplasm. Other cells still retain some nuclear β_{II}. Bar = 10 μ.

1984; Roberts et al., 1989]. Confocal microscopy confirmed the depletion of nuclear β_{II}-tubulin caused by taxol treatment (not shown). Meanwhile, the appearance of the micronuclei in certain cells in Figure 5F suggest that these cells were apoptotic. Though taxol binds specifically and reversibly to the β-tubulin subunit in the microtubules in vitro [Caplow et al., 1994], the uptake of taxol into cells is not easily reversible [Jordan et al., 1993, 1996]. To determine whether the effect of taxol on C6 cells is reversible, we incubated C6 cells with taxol for 24 h; the cells were then washed and kept in normal growth medium for 48 h. It turned out that the rearrangement and depletion of nuclear β_{II}-tubulin were not reversed (data not shown), suggesting an irreversible effect of taxol on C6 cells. Numbers of C6 cells lacking nuclear β_{II} or showing micronuclei treated with or without taxol were counted and plotted against the concentration of taxol. As shown in Figure 6A, nuclear β_{II} was depleted in a concentration-dependent manner in response to taxol treatment. Meanwhile, the percentage of apoptotic cells increased with increasing concentrations of taxol up to 5 μM but remained almost the same with higher concentrations (Fig. 6B), suggesting that mechanism(s) other than nuclear β_{II} depletion are involved in the apoptotic pathway in C6 cells at very high taxol concentrations. The effect of taxol on C6 cell apoptosis was confirmed by DNA fragmentation analysis. A DNA ladder was observed when C6 cells were treated with 5, 20, or 50 μM taxol, while the genomic DNA of the untreated C6 cells was intact, indicated by the single band in the agarose gel.

To visualize the localization of taxol inside cells, 1 μM 7-O-[N-(2,7-difluoro-4′-fluoresceincarbonyl)-L-alanyl]taxol (flutax-2) was used to treat C6 cells at 37°C for 3 h. As shown in Figure 7, flutax-2 stained the cytoplasm, which was probably due to the binding of taxol to the cytoplasmic microtubules since taxol has been found to bind directly to microtubules in cells [Manfredi et al., 1982]. In addition, the nucleoli were stained by flutax-2, suggesting that tubulin binding to flutax-2 was enriched in the nucleoli though taxol binds to soluble tubulin dimers with a reduced affinity [Parness and Horwitz, 1981; Takoudju et al., 1988; Diaz et al., 1993; Sengupta et al., 1995]. This result is consistent with the fluorescein-colchicine staining of the nuclear matrix in C6 cells, in which an accumulation of tubulin dimers in the nucleolus was observed (Fig. 3). As a control, incubation with fluorescein did not show any fluorescence of C6 cells (data not shown). Since taxol has higher specificity for β_{II}-tubulin [Derry et al., 1997] and only β_{II} localizes in

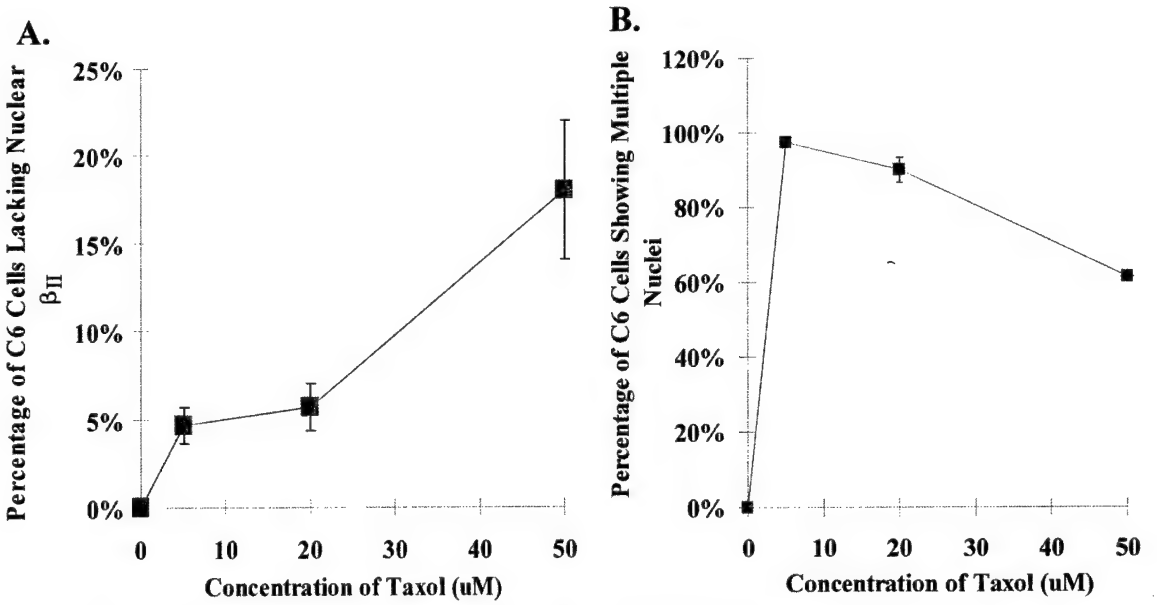

Fig. 6. The effects of taxol on nuclear β_{II}-tubulin depletion and micronucleation in C6 cells. Cells were treated with increasing concentrations of taxol for 24 h followed by immunofluorescence. About 500 cells were counted for each treatment. The percentages of cells lacking nuclear β_{II} (**A**) and showing multiple nuclei (**B**) were determined. Results are presented as mean ± SEM for three separate experiments.

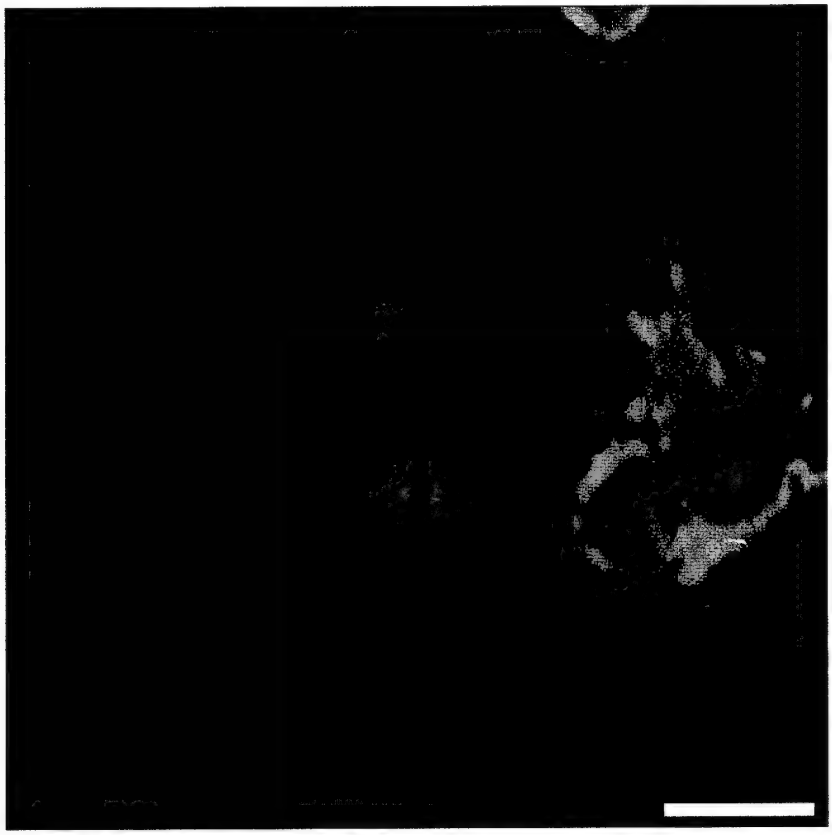

Fig. 7. Flutax-2 stains both the cytoplasm and the nucleoli of C6 cells. A concentration of 1 μM for flutax-2 was chosen for the 3-h incubation with C6 cells. Then cells were fixed by 3.7% paraformaldehyde. The fixed cells were then washed with PBS and mounted on glass slides prior to confocal microscopy. At this concentration, taxol causes considerable diminution of nuclear β_{II}, but even after 24 h of treatment with 1 μM taxol, certain cells still retain some nuclear β_{II} (Fig. 6E). Bar = 10 μ.

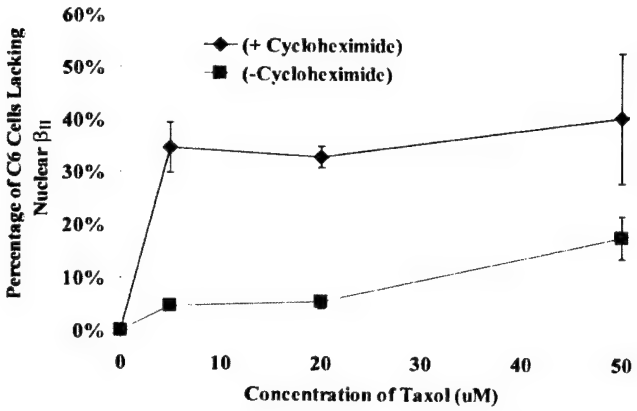

Fig. 8. The effect of cycloheximide on taxol-induced nuclear β_{II} depletion in C6 cells. Cells were incubated with 1 μg/ml cycloheximide for 1 h, followed by treatment with taxol for 24 h. Cells were then stained with β_{II} antibody. About 500 cells were counted for each treatment. Results are presented as mean ± SEM for three separate experiments.

the nucleoli of C6 cells (Figs. 2 and 3), these results support the hypothesis that taxol can indeed bind to nuclear β_{II} in vivo though with low affinity.

As shown in Figure 5, taxol induces disappearance of nuclear β_{II}-tubulin; this is accompanied by the concomitant appearance of β_{II} in what appear to be bundles of microtubules in the cytoplasm. It is natural to hypothesize that taxol induces β_{II} to migrate from the nucleus into the cytoplasm. However, one could imagine a different model, one in which taxol somehow causes the nuclear β_{II} to be degraded or masked and at the same time, more β_{II} is synthesized de novo in the cytoplasm. By this model, there would be no migration of β_{II} from the nucleus into the cytoplasm. In order to test this second hypothesis, we treated C6 cells with cycloheximide, a protein synthesis inhibitor, for 1 h prior to taxol treatment. No nuclear β_{II} depletion was observed when cells were treated only with cycloheximide (Fig. 8). However, the percentage of cells lacking nuclear β_{II}-tubulin pretreated with cycloheximide was higher than that of cells only treated with taxol. These results suggest that ongoing new protein synthesis is not required by taxol to deplete nuclear β_{II}-tubulin. Moreover, inhibition of ongoing protein synthesis potentiates the depletion of nuclear β_{II}-tubulin caused by taxol in C6 cells, yet the depletion is initiated by taxol.

Effects of Other Anti-Tubulin Drugs on Nuclear β_{II}-Tubulin in C6 Cells

C6 cells were treated with different concentrations of colchicine or nocodazole for 24 h. As shown in Figure 9A and C, neither 10 μM colchicine nor 10 μM nocodazole affected nuclear β_{II}-tubulin content while the cytoplasmic microtubule networks were totally disrupted. Moreover, no nuclear β_{II} depletion was observed at colchicine or nocodazole concentrations of 10 nM, 100 nM, 1 μM, and 100 μM (data not shown). Since colchicine [Banerjee et al., 1992] and nocodazole [Xu et al., 2002] have been found to have higher specificity for $\alpha\beta_{IV}$ while taxol has higher specificity for $\alpha\beta_{II}$ than for other tubulins [Derry et al., 1997], these results support the hypothesis that anti-tubulin drugs with lower relative affinity for β_{II}-tubulin are less effective in depleting nuclear β_{II}-tubulin. Multiple nuclei were observed in cells treated with either colchicine or nocodazole (Fig. 9B and D), suggesting that colchicine and nocodazole can cause apoptosis in C6 cells by affecting cytoplasmic microtubules.

DISCUSSION

We investigated the subcellular localization of β_I-, β_{II}-, β_{III}-, and β_{IV}-tubulin in five different tumor cell types, including C6 glioma cells, T98G glioma cells, MCF-7 breast carcinoma cells, MDA-MB-435 breast carcinoma cells, and Hela cervix carcinoma cells. In all these cells, only β_{II}-tubulin was localized in both the nucleus and the cytoplasm, while the other isotypes were only observed in the cytoplasm. Although its function is not yet known, nuclear β_{II}-tubulin has been observed previously. Ranganathan et al. [1997] reported that β_{II}-tubulin was expressed to a greater extent in malignant compared to benign prostate glands, and that some nuclei of the neoplastic prostate glands showed intense β_{II} isotype staining. The existence of nuclear β_{II}-tubulin was also observed in a breast tumor in situ as well as in cultured rat kidney mesangial cells [Walss et al., 1999, 2000; Walss-Bass et al., 2002]. In contrast, biopsy samples of several normal human tissues using immunoperoxidase staining did not show any evidence for the existence of nuclear β_{II} [Roach et al., 1998]. Collectively, the nuclear localization of β_{II}-tubulin seems to be a unique feature of tumor cells. Since it has been observed that β_{II}-tubulin forms part of the spindle and the midbody during mitosis, and re-enters the nucleus at the end of telophase [Walss et al., 1999], it is possible that β_{II}-tubulin is stored in the nucleus during interphase to be readily available for use during mitosis, where it may conceivably play a role in regulating the process. In other words, nuclear tubulin could be a "passenger" protein, a nuclear protein that has no nuclear function per se but whose nuclear location positions it appropriately to perform some function during mitosis. Other proteins have been suggested to be "passenger" proteins; these include mitosin, NuMA and p62 as has been proposed for other proteins [Zhu et al., 1997; Saredi et al., 1996; Warner and Sloboda,

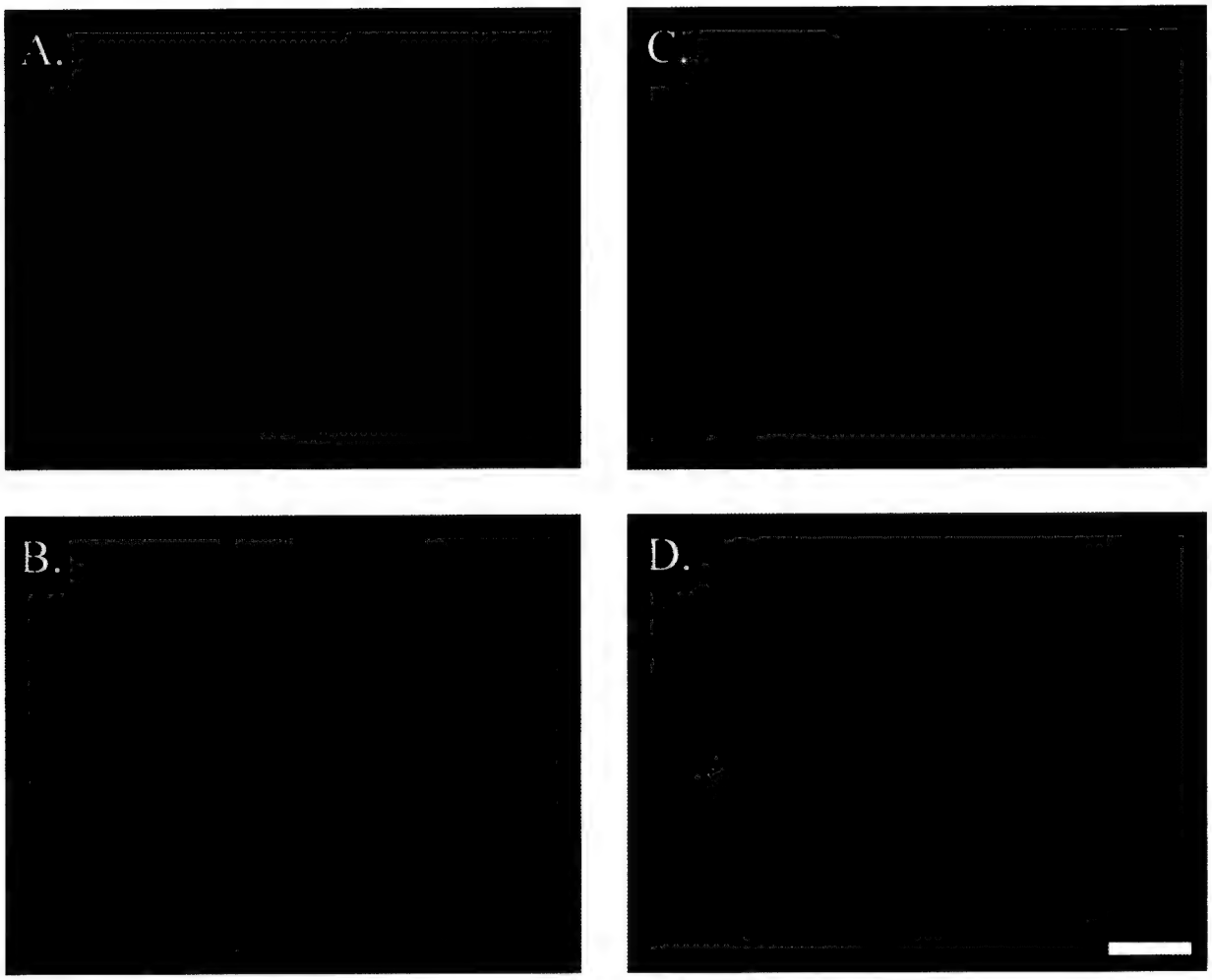

Fig. 9. The effects of colchicine and nocodazole on nuclear β_{II}-tubulin in C6 cells. Cells were treated with colchicine or nocodazole for 24 h followed by immunostaining with β_{II} antibody and DAPI. **A,C:** β_{II} staining. **B,D:** DAPI staining. A and B: cells treated with 10 μM colchicine. C and D: cells treated with 10 μM nocodazole. Bar = 10 μ.

1999]. However, the hypothesis that nuclear tubulin is a passenger protein remains to be tested; it will also be interesting to understand why it is β_{II}, rather than the other isotypes, that occurs in the nuclei of tumor cells.

Nuclear β_{II} did not appear to be in the form of microtubule networks (Fig. 1B, F, J, N, and R), but rather as an $\alpha\beta_{II}$-heterodimer, demonstrated by fluorescein-colchicine staining (Figs. 2 and 3) and double immunostaining of α- and β_{II}-tubulin (not shown). Our results also suggest that the $\alpha\beta_{II}$-heterodimer is a component of the nuclear matrix and accumulates in the nucleoli of C6, T98G, MCF-7, MDA, and Hela cells (Figs. 3 and 4). Nucleolar localization of β_{II}-tubulin was shown by co-localization with the nucleolar marker nucleolin (Fig. 4). We have shown elsewhere that β_{II}-tubulin co-localizes with RNA in the nucleus, also consistent with nucleolar localization [Walss-Bass et al., 2002]. Another cytoskeleton protein, F-actin, has been found in the nuclei of a variety of cell types [Clark and Merriam, 1977; Fukui, 1978; Fukui and Katsumaru, 1979; Clark and Rosenbaum, 1979; Osborn and Weber, 1980; Welch and Suhan, 1985; De Boni, 1994; Yan et al., 1997] and has been suggested to play a role in RNA export or other intranuclear transport phenomena [Pederson, 1998]. The accumulation of $\alpha\beta_{II}$-tubulin in the nucleolus raises the possibility that $\alpha\beta_{II}$-tubulin is involved in certain functions in the nucleolar area, possibly RNA export or transcription. On the other hand, as a component of the nuclear matrix, the skeleton of the nucleus, nuclear $\alpha\beta_{II}$-tubulin may play a role in maintaining nuclear shape.

Being synthesized in the cytoplasm, β_{II}-tubulin does not contain any known nuclear localization signal

(NLS) [Kalderon et al., 1984], suggesting other mechanism(s) may be involved in localizing β_{II}-tubulin in the nucleus. Earnshaw and Bernat [1991] found that the INCENP's and other proteins could enter the nucleus by binding to chromosomes during mitosis. Thus, we hypothesize that β_{II}-tubulin localizes in the nucleus by remaining attached to chromatin after cell division. This hypothesis is supported by the findings that tubulin interacts with chromatin in vitro [Mithieux et al., 1986], and that cell division may be necessary for β_{II}-tubulin to enter the nucleus [Walss-Bass et al., 2001].

Since of the four β isotypes we are able to study, β_{II} is the only one present in the nucleus, we examined the effect on nuclear β_{II}-tubulin of anti-tubulin drugs of known isotype specificity. We first characterized the effect on nuclear β_{II} of taxol, which has higher specificity for the $\alpha\beta_{II}$ dimers than for the other isotypes [Derry et al., 1997]. Our results suggest that, depending on the concentration, taxol has two effects on C6 cells. At nanomolar concentrations, taxol affects the cytoplasmic microtubules and causes the rearrangement of nuclear β_{II}-tubulin as well as cell apoptosis (Fig. 5C and D); at micromolar concentrations, taxol additionally depletes nuclear β_{II}-tubulin (Figs. 5E,F, 7, 8, and 9). As an anti-tumor drug, taxol is known to freeze microtubule dynamics and induce cell apoptosis at low concentrations (<10 nM) [Jordan et al., 1993]. This is probably the mechanism by which nanomolar concentrations of taxol affect the cytoskeleton and apoptosis in C6 cells though other possibilities cannot be excluded. To the best of our knowledge, the depletion of nuclear β_{II}-tubulin caused by micromolar concentrations of taxol is a novel finding. Based on its potential function(s) involved in tumor cell proliferation, nuclear β_{II} may be a novel target for taxol in the anti-tumor process. Multiple nuclei were observed even at 20 nM taxol treatment when nuclear β_{II} was not depleted (Fig. 5D), suggesting that the depletion of nuclear β_{II}-tubulin may not be essential for C6 cell apoptosis. However, this does not exclude the possibility that nuclear β_{II} depletion may lead to apoptosis.

Pretreatment with cycloheximide increased the percentage of nuclear β_{II} depletion in C6 cells (Fig. 8), suggesting that the inhibition of ongoing new protein synthesis can potentiate the depletion of nuclear β_{II}-tubulin caused by taxol. A possible model for the depletion of nuclear β_{II} is that there is an equilibrium between nuclear β_{II} and cytoplasmic β_{II}, and that taxol treatment lowers the concentration of cytoplasmic β_{II} thus driving the equilibrium toward the direction of cytoplasmic β_{II}. Cycloheximide treatment may further lower the concentration of cytoplasmic β_{II}, while taxol seems to be essential to initiate nuclear β_{II} depletion since cycloheximide alone cannot cause this effect (data not shown). The proteins involved in the translocation of β_{II} are still unknown. One of the candidates can be Ran, a small nuclear GTPase, because of its identified roles in both regulating microtubules [Desai and Hyman, 1999] and nuclear protein transport [Melchior and Gerace, 1995; Azuma and Dasso, 2000; Moore, 2001]. However, this possibility remains to be tested.

If the effect of taxol on nuclear β_{II}-tubulin is due to the higher specificity of taxol for $\alpha\beta_{II}$-tubulin, one would expect that the effect would be less with drugs of lower specificity for $\alpha\beta_{II}$. Two anti-tubulin drugs, colchicine [Banerjee and Ludueña, 1992] and nocodazole [Xu et al., 2002], both binding best to $\alpha\beta_{IV}$, were used to treat C6 cells. No nuclear β_{II} depletion was observed in C6 cells treated with either colchicine or nocodazole (Fig. 9A and C). This supports the hypothesis that drugs with lower specificity for $\alpha\beta_{II}$-tubulin are less effective in altering nuclear β_{II}-tubulin content. On the other hand, multiple nuclei were also observed when C6 cells were treated with either colchicine or nocodazole (Fig. 9B and D), which is probably due to the known effect of these drugs on cytoplasmic microtubules.

Our results raise the possibility that nuclear β_{II}-tubulin may be widespread in cancer cells. They also suggest that nuclear β_{II}-tubulin represents a separate population of tubulin with a unique set of properties; such a population may constitute a novel target for anti-tumor drugs.

ACKNOWLEDGMENTS

We thank Dr. Martin Adamo for C6 and T98G cells, Dr. Robert Klebe for MCF-7 cells, Dr. Susan Mooberry for MDA and Hela cells, and Dr. Matthew Suffness for taxol. We appreciate technical instruction in confocal microscopy from Dr. Victoria Centonze Frohlich. We also thank Dr. Asok Banerjee, Dr. Asish Chaudhuri, Veena Prasad, Consuelo Walss-Bass, Patricia Schwarz, and Mohua Banerjee for technical support and helpful advice. We are grateful to Dr. Larry Barnes, Dr. Jean Jiang, and Dr. Jeffrey Kreisberg for helpful discussion and advice. This study was supported by grants to R.F.L. from the NIH (CA26376), US Army BCRP (DAMD 17-98-1-8246 and DAMD 1701-1-0411), and the Welch Foundation (AQ-0726) as well as grant P30 CA54174 from the NIH to the San Antonio Cancer Institute.

REFERENCES

Azuma Y, Dasso M. 2000. The role of Ran in nuclear function. Curr Opin Cell Biol 12:302–307.

Banerjee A, Ludueña RF. 1992. Kinetics of colchicine binding to purified β-tubulin isotypes from bovine brain. J Biol Chem 267:13335–13339.

Banerjee A, Roach MC, Wall KA, Lopata MA, Cleveland DW, Ludueña RF. 1988. A monoclonal antibody against the type II isotype of β-tubulin. Preparation of isotypically altered tubulin. J Biol Chem 263:3029–3034.

Banerjee A, Roach MC, Trcka P, Ludueña RF. 1990. Increased microtubule assembly in bovine brain tubulin lacking the type III isotype of β-tubulin. J Biol Chem 265:1794–1799.

Banerjee A, Roach MC, Trcka P, Ludueña RF. 1992. Preparation of a monoclonal antibody specific for the class IV isotype of β-tubulin. Purification and assembly of $\alpha\beta_{II}$, $\alpha\beta_{III}$, and $\alpha\beta_{IV}$ tubulin dimers from bovine brain. J Biol Chem 267:5625–5630.

Bryan J, Wilson L. 1971. Are cytoplasmic microtubules heteropolymers? Proc Natl Acad Sci USA 68:1762–1766.

Caplow M, Shanks J, Ruhlen R. 1994. How taxol modulates microtubule disassembly. J Biol Chem 269:23399–23402.

Clark TG, Merriam RW. 1977. Diffusible and bound actin nuclei of *Xenopus laevis* oocytes. Cell 12:883–891.

Clark TG, Rosenbaum JL. 1979. An actin filament matrix in hand-isolated nuclei of *X. laevis* oocytes. Cell 18:1101–1108.

De Boni U. 1994. The interphase nucleus as a dynamic structure. Int Rev Cytol 150:149–171.

Derry WB, Wilson L, Khan IA, Ludueña RF, Jordan MA. 1997. Taxol differentially modulates the dynamics of microtubules assembled from unfractionated and purified β-tubulin isotypes. Biochemistry 36:3554–3562.

Desai A, Hyman A. 1999. Microtubule cytoskeleton: no longer an also Ran. Curr Biol 9:704–707.

Diaz JF, Menendez M, Andreu JM. 1993. Thermodynamics of ligand-induced assembly of tubulin. Biochemistry 32: 10067–10077.

Earnshaw WC, Bernat RL. 1991. Chromosomal passengers: toward an integrated view of mitosis. Chromosoma 100:139–146.

Fey EG, Wan KM, Penman S. 1984. Epithelial cytoskeletal framework and nuclear matrix-intermediate filament scaffold: three-dimensional organization and protein composition. J Cell Biol 98: 1973–1984.

Fukui Y. 1978. Intranuclear actin bundles induced by dimethyl sulfoxide in interphase nucleus of Dictyostelium. J Cell Biol 76:146–157.

Fukui Y, Katsumaru H. 1979. Nuclear actin bundles in Amoeba, Dictyostelium and human HeLa cells induced by dimethyl sulfoxide. Exp Cell Res 120:451–455.

Hoshino R, Tanimura S, Watanabe K, Kataoka T, Kohno M. 2001. Blockade of the extracellular signal-regulated kinase pathway induces marked G1 cell cycle arrest and apoptosis in tumor cells in which the pathway is constitutively activated. J Biol Chem 276:2686–2692.

Jordan MA, Toso RJ, Thrower D, Wilson L. 1993. Mechanism of mitotic block and isnhibition of cell proliferation by taxol at low concentrations. Proc Natl Acad Sci USA 90:9552–9556.

Jordan MA, Wendell K, Gardiner S, Derry WB, Copp H, Wilson L. 1996. Mitotic block induced in HeLa cells by low concentrations of paclitaxel (Taxol) results in abnormal mitotic exit and apoptotic cell death. Cancer Res 56:816–825.

Kalderon D, Richardson WD, Markham AF, Smith AE. 1984. Sequence requirements for nuclear location of simian virus 40 large-T antigen. Nature (Lond) 311:33–38.

Ludueña RF. 1998 Multiple forms of tubulin: different gene products and covalent modifications. Int Rev Cytol 178:207–275.

Ludueña RF, Shooter EM, Wilson L. 1977. Structure of the tubulin dimer. J Biol Chem 252:7006–7014.

Manfredi JJ, Parness J, Horwitz SB. 1982. Taxol binds to cell microtubules. J Cell Biol 94:688–696.

Melchior F, Gerace L. 1995. Mechanisms of nuclear protein import. Curr Opin Cell Biol 7:310–318.

Mithieux G, Roux B, Rousset B. 1986. Tubulin-chromatin interactions: evidence for tubulin-binding sites on chromatin and isolated oligonucleosomes. Biochim Biophys Acta 888:49–61.

Moore J. 2001. The Ran-GTPase and cell-cycle control. BioEssays 23:77–85.

Osborn M, Weber K. 1980. Dimethylsulfoxide and the ionophore A23187 affect the arrangement of actin and induce nuclear actin paracrystals in PtK2 cells. Exp Cell Res 129:103–114.

Parness J, Horwitz SB. 1981. Taxol binds to polymerized tubulin in vitro. J Cell Biol 91:479–487.

Pederson T. 1998. Thinking about a nuclear matrix. J Mol Biol 277:147–159.

Ranganathan S, Salazar H, Benetatos CA, Hudes GR. 1997. Immunohistochemical analysis of β-tubulin isotypes in human prostate carcinoma and benign prostatic hypertrophy. Prostate 30:263–268.

Roach MC, Boucher VL, Walss C, Ravdin PM, Ludueña RF. 1998. Preparation of a monoclonal antibody specific for the class I isotype of β-tubulin: the β isotypes of tubulin differ in their cellular distributions within human tissues. Cell Motil Cytoskeleton 39:273–285.

Roberts JR, Rowinsky EK, Donehower RC, Robertson J, Allison DC. 1989. Demonstration of the cell cycle positions of taxol-induced "asters" and "bundles" by sequential measurements of tubulin immunofluorescence, DNA content, and autoradiographic labeling of taxol-sensitive and -resistant cells. J Histochem Cytochem 37:1659–1665.

Sabbatini P, McCormick F. 1999. Phosphoinositide 3-OH kinase (PI3K) and PKB/Akt delay the onset of p53-mediated, transcriptionally dependent apoptosis. J Biol Chem 274:24263–24269.

Saredi A, Howard L, Compton DA. 1996. NuMA assembles into an extensive filamentous structure when expressed in the cell cytoplasm. J Cell Sci 109:619–630.

Schiff PB, Horwitz SB. 1980. Taxol stabilizes microtubules in mouse fibroblast cells. Proc Natl Acad Sci USA 77:1561–1565.

Schiff PB, Horwitz SB. 1981. Taxol assembles tubulin in the absence of exogenous guanosine 5′-triphosphate or microtubule-associated proteins. Biochemistry 20:3247–3252.

Sengupta S, Boge TC, George GI, Himes RH. 1995. Interaction of a fluorescent paclitaxel analogue with tubulin. Biochemistry 34: 11889–11894.

Takoudju M, Wright M, Chenu J, Gueritte-Voegelein F, Guenard D. 1988, Absence of 7-acetyl taxol binding to unassembled brain tubulin. FEBS Lett 227:96–98.

Turner PF, Margolis RL. 1984. Taxol-induced bundling of brain-derived microtubules. J Cell Biol 99:940–946.

Walss C, Kreisberg JI, Ludueña RF. 1999. Presence of the β_{II} isotype of tubulin in the nuclei of cultured mesangial cells from rat kidney. Cell Motil Cytoskeleton 42:274–284.

Walss C, Barbier P, Banerjee M, Bissery MC, Ludueña RF, Fellous A. 2000. Nuclear tubulin as a possible marker for breast cancer cells. Proc Am Assoc Cancer Res 41:553.

Walss-Bass C, Kreisberg JI., Ludueña RF. 2001. Mechanism of localization of β_{II}-tubulin in the nuclei of cultured rat kidney mesangial cells. Cell Motil Cytoskeleton 49:208–217.

Walss-Bass C, Xu K, David S, Fellous A, Ludueña RF. 2002. Occurrence of nuclear β_{II}-tubulin in cultured cells. Cell Tissue Res (in press).

Warner AK, Sloboda RD. 1999. C-terminal domain of the mitotic apparatus protein p62 targets the protein to the nucleolus during interphase. Cell Motil Cytoskeleton 44:68–80.

Welch WJ, Suhan JP. 1985. Morphological study of the mammalian stress response: characterization of changes in cytoplasmic organelles, cytoskeleton, and nucleoli, and appearance of intranuclear actin filaments in rat fibroblasts after heat-shock treatment. J Cell Biol 101:1198–1211.

Wilson L, Jordan MA. 1994. Pharmacological probes in microtubule function. In: Hyams JS, Lloyd CW, editors. Microtubules. New York: Wiley-Liss. p 59–83.

Xu K, Schwarz PM, Ludueña RF. 2002. Interaction of nocodazole with tubulin isotypes. Drug Dev Res 55:91–96.

Yan C, Leibowitz, N, Melese T. 1997. A role for the divergent actin gene, ACT2, in nuclear pore structure and function. EMBO J 16:3572–3586.

Zhu X, Ding L, Pei G. 1997. Carboxyl-terminus of mitosin is sufficient to confer spindle pole localization. J Cell Biochem 66:441–449.

Cell Tissue Res (2002) 309:331–335
DOI 10.1007/s00441-002-0591-2

Appendix 3

SHORT COMMUNICATION

Karen Woo · Heather C. Jensen-Smith
Richard F. Ludueña · Richard Hallworth

Differential synthesis of β-tubulin isotypes in gerbil nasal epithelia

Received: 5 November 2001 / Accepted: 29 April 2002 / Published online: 27 June 2002

Abstract Compartmentalization of β-tubulin isotypes within cells according to function was examined in gerbil olfactory and respiratory epithelia by using specific antibodies to four β-tubulin isotypes (β_I, β_{II}, β_{III}, and β_{IV}). Isotype synthesis was cell-type-specific, but the localization of the isotypes was not compartmentalized. All four isotypes were found in the cilia, dendrites, somata, and axons of olfactory neurons. Only two isotypes (β_I and β_{IV}) were present in the cilia of nasal respiratory epithelial cells. The β_{IV} isotype, thought to be an essential component of cilia, was present in olfactory neurons and respiratory epithelial cells, which are ciliated, but was not found in basal cells (the stem cells of olfactory sensory neurons, which have no cilia). Olfactory neurons therefore do not synthesize β_{IV}-tubulin until they mature, when functioning cilia are also elaborated. The failure to observe compartmentalization of β-tubulin isotypes in olfactory neurons sheds new light on potential functions of the β-tubulin isotypes.

Keywords Tubulin isotypes · β-Tubulin · Cilia · Olfactory neuron · Respiratory epithelium · Gerbil

This work was supported by NIH grant CA26376, US Army grant DAMD17-98-1-8246, and Welch Foundation grant AQ-0726 to R.F.L., and NIH grant DC02053 to R.H. Purchase of the confocal microscope used in this study was made possible by grants from the Taub Foundation and the Nebraska Health Futures Foundation

K. Woo
The Medical School,
University of Texas Health Science Center at San Antonio,
San Antonio, TX 78229-3900, USA

H.C. Jensen-Smith · R. Hallworth (✉)
Department of Biomedical Sciences, Creighton University,
Omaha, NE 68178, USA
e-mail: hallw@creighton.edu
Tel.: +1-402-2803057, Fax: +1-402-2802690

R.F. Ludueña
Department of Biochemistry,
University of Texas Health Science Center at San Antonio,
San Antonio, TX 78229-3900, USA

Introduction

Microtubules perform a variety of functions in the eukaryotic cell, including providing cell form and rigidity and facilitating the transport of organelles. Microtubules consist of heterodimers of α- and β-tubulin. The seven β-tubulin isotypes in mammals (β_I, β_{II}, β_{III}, β_{IVa}, β_{IVb}, β_V, and β_{VI}) are among the most highly conserved proteins known (Ludueña 1998). Nevertheless, the isotype-specific sequence differences are also highly conserved, which suggests that there are important functional differences between the isotypes.

The multi-tubulin hypothesis (Fulton and Simpson 1976) proposes that the isotypes have specific functional roles. Consistent with this idea, different cell types have been found to synthesize different isotypes even within the same tissue (Roach et al. 1998; Hallworth and Ludueña 2000). However, little is known about the functions of the seven isotypes, except that the β_{IV} isotype appears to be associated with axonemal microtubules and with actin stress fibers (Renthal et al. 1993; Lu et al. 1998; Roach et al. 1998; Walss-Bass et al. 2001). If β-tubulin isotypes have specific functional roles, they may be sequestered to different compartments of the same cell according to function.

In olfactory epithelia, microtubules exist in discrete populations (Burton 1992). For example, olfactory neurons have four identifiable microtubule compartments (cilium, dendrite, soma, and axon; Graziadei 1973), each of which may have microtubules with different functions. Olfactory cilia contain the 9+2 arrangement of axonemal microtubules but are not motile. Within the dendrite, microtubules are longitudinally arranged. The dendrite, soma, and axon of the olfactory neuron each represent potentially distinct compartments for microtubules. Bordering the olfactory epithelium is the respiratory epithelium, whose cells bear motile cilia with an entirely different function from that of the olfactory cilia. The varied microtubule populations in olfactory and respiratory epithelia therefore offer an excellent opportunity to test this aspect of the multi-tubulin hypothesis.

Materials and methods

The synthesis of β-tubulin isotypes was examined by using indirect immunofluorescence microscopy in frozen sections of gerbil olfactory and respiratory epithelium. Adult gerbils (22 days old or older) were anesthetized with Nembutal and cardiac-perfused with formaldehyde that had been freshly prepared by dissolving 4% paraformaldehyde in phosphate-buffered saline (PBS). After decapitation, the dorso-posterior nasal epithelium of the gerbil was dissected away from the septum, rinsed in PBS, cut into strips, equilibrated in 30% sucrose in PBS as a cryoprotectant, and quickly frozen in O.C.T. (Tissue-Tek, Miles Laboratories, Elkart, Ind., USA). Transverse sections (10 μm thick) were prepared on a cryostat (Leica Microsystems, Bannockburn, Ill., USA). Sections were blocked and permeabilized in PBS containing 1% bovine serum albumin (BSA), 0.25% Triton-X100, and 5% normal goat serum and then rinsed in PBS plus 0.1% BSA. Sections were labeled with primary mouse monoclonal antibodies specific for each β-tubulin isotype, rinsed, and labeled with secondary antibody, viz., goat anti-mouse IgG coupled to fluorescein isothiocyanate (Sigma, St. Louis, Mo., USA) or to Alexa 488 (Molecular Probes, Eugene, Ore., USA). Sections were sealed under coverslips on glass slides in 50% PBS:50% glycerol containing 1% *n*-propylgallate. All sections were examined on an Axioskop II epifluorescence microscope (Carl Zeiss Jena, Jena, Germany). Images were acquired digitally by using a Spot RT digital camera (Diagnostic Instruments, Sterling Heights, Mich., USA). Confocal images were obtained on a Radiance 2000 confocal microscope (Bio-Rad, Hercules, Calif., USA) or an Eclipse 800 epifluorescence microscope (Nikon Instruments, Kawasaki, Japan).

The isotype-specific antibodies had previously been prepared against an epitope unique to the C-terminus of that isotype (Banerjee et al. 1988, 1990, 1992; Roach et al. 1998). Since the C-termini of β_{IVa} and β_{IVb} are virtually identical, the anti-β_{IV} antibody is unable to discriminate between them. Positive controls were performed by using the same procedures as above but with a non-isotype-specific antibody against β-tubulin (Sigma). Negative controls were performed by omitting the primary antibody.

For immunoblotting, strips of nasal epithelium were removed from anesthetized and decapitated gerbils and homogenized in SDS sample buffer. Approximately 18 μg of protein was loaded onto each lane of a 8% poly-acrylamide TRIS-glycine gel (Gradipore, French's Forest, N.S.W., Australia), and this was run at 150 V for 90 min in SDS electrophoresis buffer. The proteins were then transferred to nitrocellulose sheets soaked in chilled TRIS-glycine/methanol transfer buffer. Lanes were cut into strips for labeling with the β-tubulin isotype antibodies or with a non-isotype-specific antibody against β-tubulin (Sigma). The strips were rinsed in TRIS-buffered saline (TBS) with 0.1% Tween, blocked in 2% powdered milk in TBS, and exposed to one of the five primary antibodies overnight at 4°C. After being rinsed, the strips were incubated in anti-mouse IgG conjugated with biotin-horseradish peroxidase (Cell Signaling Technology, Beverly, Mass., USA) in blocking buffer for 1 h at room temperature. Strips were then rinsed and treated with Luminol reagent (Santa Cruz Biotechnology, Santa Cruz, Calif., USA). After again being rinsed, the protein strips were wrapped in plastic and exposed to XAR5 scientific imaging film (Kodak, Rochester, N.Y., USA).

Preservation of olfactory cilia in frozen sections was achieved only with great difficulty, whereas the more robust cilia of the respiratory epithelium were usually well preserved. Most often, olfactory cilia were seen only in truncated form. As a supplementary approach to identifying the isotypes expressed in sensory cilia, we obtained confocal microscopic images of labeled sections at high magnification. The images obtained demonstrated clear, albeit shortened, processes emanating from dendritic knobs, consistent with olfactory cilia (see below).

Animal care and handling was performed according to approved protocols of the University of Texas Health Science Center at San Antonio and Creighton University School of Medicine Institutional Animal Care and Use Committees.

Results

Western blots of nasal epithelia indicated that labeling for β-tubulin isotypes was restricted to a single band of molecular weight of approximately 50 kDa (Fig. 1), close to the molecular weight of β-tubulin (Ludueña 1998).

The olfactory epithelium consists of a pseudo-stratified layer of round cell bodies. The lowest layer of cell bodies consists of basal cells, which are the stem cells for olfactory neurons. The middle layer consists of the somata of mature olfactory neurons. Each neuron sends a dendritic process to the epithelial surface and an axonal process to the olfactory bulb. Long sensory cilia arise from a small swelling at the apical surface of the dendrite. Above the neuronal somata are the somas of supporting cells, whose processes span the epithelium and intercalate between the neurons. The adjacent respiratory epithelium consists of a thin uniform layer of epithelial cells bearing multiple short cilia.

In the olfactory epithelium, label for β_I-tubulin was found in the olfactory neurons and basal cells (Fig. 2A). The label consisted of a bright irregular strip along the apical surface of the epithelium, apparently representing olfactory cilia. Supporting cell perikarya, the most superficial layer of somata, were unlabeled. Fine strands of label were seen perpendicular to the cilia layer, probably representing the dendrites of olfactory neurons. Deeper in the epithelium, labeling was evident in the perikarya of olfactory neurons and basal cells. Irregularly shaped bundles of bright label, probably representing the axons of olfactory neurons, were present below the epithelium.

In the respiratory epithelium (Fig. 2B), labeling for β_I-tubulin was strongest in the cilia layer. Only background levels of label were seen in the rest of the respiratory epithelium.

On examination under the confocal microscope, labeling for β_I-tubulin could be seen in fine processes emanating from the dendrites of sensory neurons (Fig. 2C, arrow). These appeared to be truncated olfactory cilia, which confirmed the impression obtained from light-microscope observation that cilia were labeled.

In the olfactory epithelium, the labeling pattern for β_{II}- and β_{III}-tubulin was essentially identical to that for β_I-tubulin. Label was seen in olfactory neurons and in basal cells and not in supporting cells. In olfactory neurons, label was found in axons, perikarya, dendrites, and (by confocal inspection) in cilia. However, in the respiratory epithelium, no labeling for β_{II}- or β_{III}-tubulin was detected. Thus, for both β_{II}- and β_{III}-tubulin, there was an abrupt transition from label in the thicker olfactory epithelium to the absence of label in the thinner respiratory epithelium (Fig. 2D, E).

In the respiratory epithelium, label for β_{IV}-tubulin was found strongly in the cilia but not in the perikarya (Fig. 2F) in essentially the same pattern as that for β_I-tubulin. In the olfactory epithelium, however, label for β_{IV}-tubulin was observed in the cilia, perikarya and dendrites of olfactory neurons (Fig. 2G). In the deeper layers

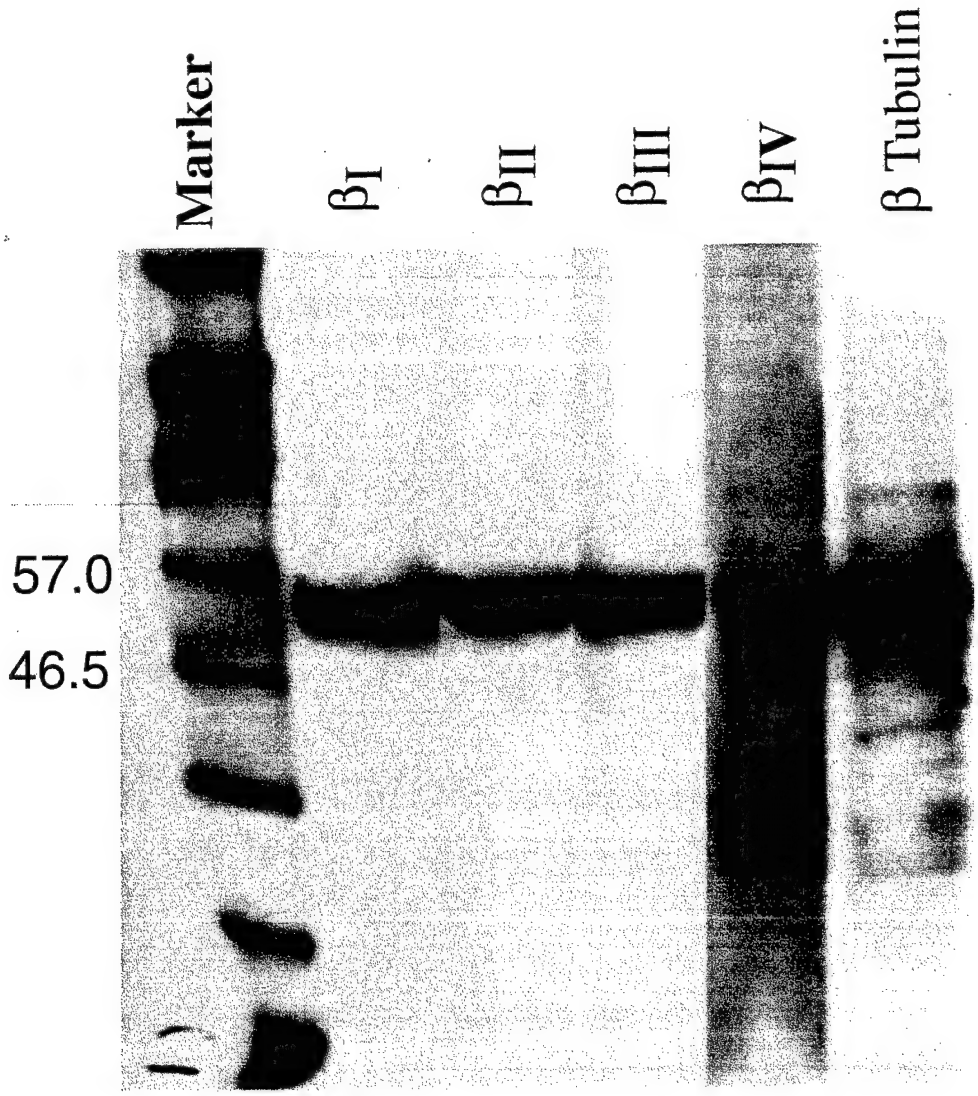

Fig. 1 Western blots showing immunolabeling of gerbil nasal epithelial tissue with an antibody to β-tubulin (*right*) and the isotype-specific β-tubulin antibodies used in this study (*lanes 2–4*). *Marker* Sample of protein standards with molecular weights indicated *left*

of the sensory epithelium, label was strikingly absent from the perikarya of cells in the basal cell layer but was present in the axons. Thus, β_{IV}-tubulin was the only isotype not observed in basal cells.

Discussion

In its original formulation, the multi-tubulin hypothesis (Fulton and Simpson 1976) envisaged specific functions for each isotype. The complexity of the isotype synthesis patterns that have so far been observed, in which even cells of similar function in the same organ express different isotypes (Roach et al. 1998; Hallworth and Ludueña 2000; B. Perry, H. Jensen-Smith, R. F. Ludueña, R. Hallworth, in preparation), seemingly refutes this form of the hypothesis. Here, we have examined whether cells might sequester different isotypes to different pools in the same cell, the olfactory neuron, for functional reasons. However, olfactory neurons were found to express all four studied isotypes (β_I, β_{II}, β_{III}, and β_{IV}-tubulin) in all compartments. In contrast, respiratory epithelial cells selectively synthesize only two of the four β-tubulin isotypes examined, viz., β_I and β_{IV}.

We have not seen label for any β-tubulin isotypes in supporting cells. Undoubtedly, these cells have at least some microtubules, although they may be few in number. The isotypes found in basal cells do not include one found in olfactory neuron somas, viz., β_{IV}-tubulin. Because basal cells develop into olfactory neurons, β_{IV} gene expression in olfactory sensory neurons appears to coincide with the appearance of cilia. β_{IV}-Tubulin is apparently a common feature of cilia. The presence of β_{IV}-tubulin in axonemes is also consistent with the prediction of Raff et al. (1997) who have postulated that, for a β-tubulin isotype to be in an axonemal microtubule, it must have the sequence EGEFEEE near its C-terminus. β_{IV}-Tubulin (both β_{IVa} and β_{IVb}) is the only vertebrate isotype that contains this sequence (Ludueña 1998). In the axoneme of rod outer segments, β_{IV}-tubulin has been found but not β_{II}- or β_{III}-tubulin (β_I-tubulin was not tested; Renthal et al. 1993). In vestibular hair cells, both β_I-

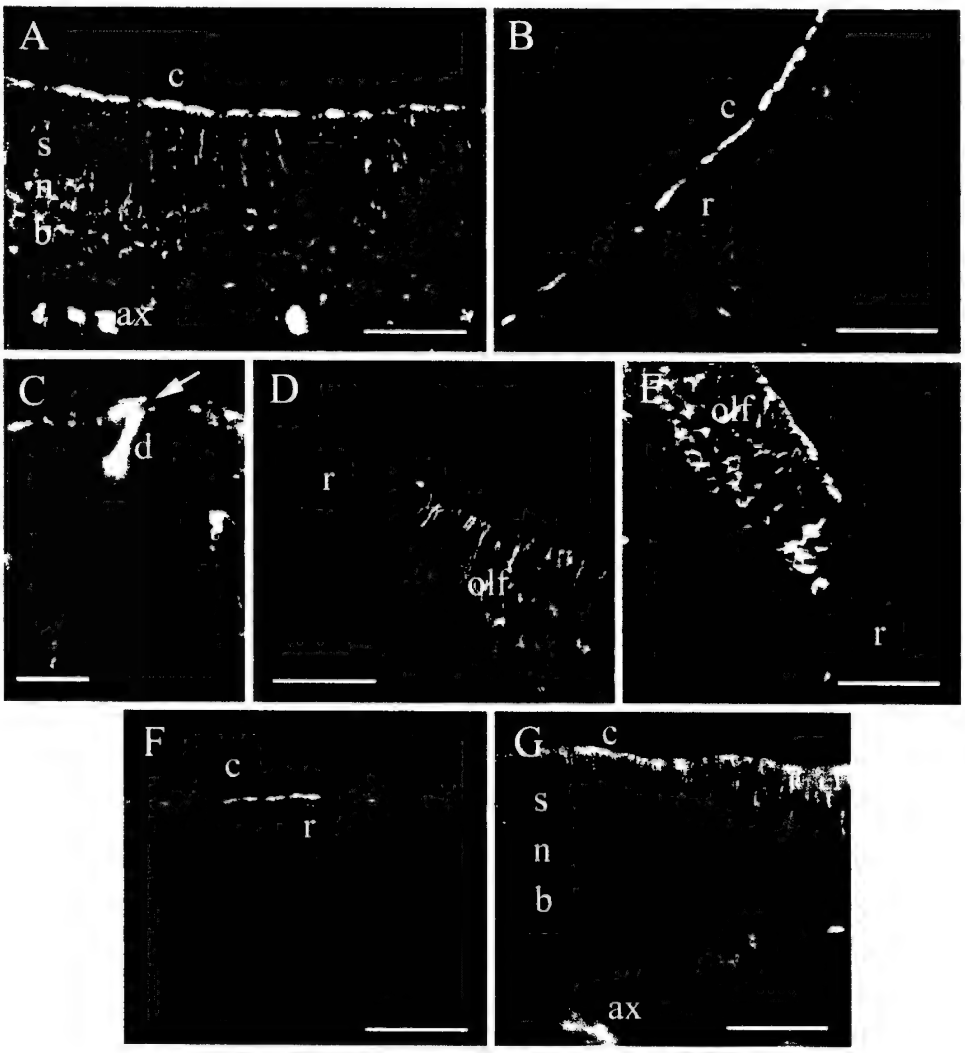

Fig. 2A–G Distribution of β-tubulin isotypes in gerbil nasal epithelia. **A** β_I-Tubulin in a section of olfactory epithelium, showing label in olfactory neurons (*n*), in basal cells (*b*), in the axons of sensory neurons (*ax*), and in cilia (*c*), but not in supporting cells (*s*). **B** β_I-Tubulin in respiratory epithelium (*r*) in which the label is present in the cilia (*c*) only. **C** Confocal view of a section of the olfactory epithelium with β_I-tubulin in cilia (*arrow*) and a dendrite (*d*). **D** β_{II}-Tubulin in a transition region between olfactory (*olf*) and respiratory epithelium (*r*); note the absence of label in the respiratory epithelium. **E** β_{III}-Tubulin in a transition region between olfactory (*olf*) and respiratory epithelium (*r*); again, note the absence of label in the respiratory epithelium. **F** β_{IV}-Tubulin in respiratory epithelium (*r*), showing label in the cilia (*c*). **G** Section of olfactory epithelium stained for β_{IV}-tubulin, with label in olfactory neurons (*n*), in cilia (*c*), and in the axons of sensory neurons (*ax*), but not in basal cells (*b*) or in supporting cells (*s*). *Bars* 50 μm in **A, B, D–G**, 6 μm in **C**

and β_{IV}-tubulin are found in cilia (B. Perry, H. Jensen-Smith, R. F. Ludueña, R. Hallworth, in preparation). β_{IV}-Tubulin has been localized by immuno-electron microscopy to the axonemal microtubules of bovine retinal rod cells and bovine tracheal cilia (Renthal et al. 1993). It is also the only isotype that has been found in oviduct epithelial cilia (Roach et al. 1998) and appears to be the major isotype in mouse sperm flagella (Lu et al. 1998). This isotype, which seems to be essential for cilia and flagella, is apparently synthesized in the olfactory epithelium only when the basal cell matures into a sensory neuron and synthesizes cilia. It is likely that, during the developmental program of the olfactory neuron, β_{IV} synthesis may be initiated only when it is needed for the synthesis of cilia. The presence of the β_{IV} isotype could therefore function as a useful marker for the transition from basal cell to sensory neuron.

Acknowledgements We thank Tom Adrian, Xinquan Li, and Xianzhong Ding for assistance with the Western blots.

References

Banerjee A, Roach MC, Wall KA, Lopata MA, Cleveland DW, Ludueña RF (1988) A monoclonal antibody against the type II isotype of β-tubulin. Preparation of isotypically altered tubulin. J Biol Chem 263:3029–3034

Banerjee A, Roach MC, Trcka P, Ludueña RF (1990) Increased microtubule assembly in bovine brain tubulin lacking the type III isotype of β-tubulin. J Biol Chem 265:1794–1799

Banerjee A, Roach MC, Trcka P, Ludueña RF (1992) Preparation of a monoclonal antibody specific for the class IV isotype of β-tubulin. Purification and assembly of $\alpha\beta_{II}$, $\alpha\beta_{III}$, and $\alpha\beta_{IV}$ tubulin dimers from bovine brain. J Biol Chem 267:5625–5630

Burton PR (1992) Ultrastructural studies of microtubules and microtubule organizing centers of the vertebrate olfactory neuron. Microsc Res Tech 23:142–156

Fulton C, Simpson PA (1976) Selective synthesis and utilization of flagellar tubulin. The multi-tubulin hypothesis. In: Goldman R, Pollard T, Rosenbaum J (eds) Cell motility, vol 3. Cold Spring Harbor Laboratory Press, Cold Spring Harbor, N.Y. pp 987–1005

Graziadei PPC (1973) The ultrastructure of vertebrates olfactory mucosa. In: Friedmann I (ed) The ultrastructure of sensory organs. North Holland, Amsterdam, pp 267–305

Hallworth R, Ludueña RF (2000) Differential expression of β tubulin isotypes in the adult gerbil organ of Corti. Hear Res 148:161–172

Lu Q, Moore GD, Walss C, Ludueña RF (1998) Structural and functional properties of tubulin isotypes. Adv Struct Biol 5:203–227

Ludueña RF (1998) The multiple forms of tubulin: different gene products and covalent modifications. Int Rev Cytol 178:207–275

Raff EC, Fackenthal JD, Hutchens JA, Hoyle HD, Turner FR (1997) Microtubule architecture specified by a β-tubulin isoform. Science 275:70–73

Renthal R, Schneider BG, Miller MA, Ludueña RF (1993) β_{IV} is the major β-tubulin isotype in bovine cilia. Cell Motil Cytoskel 25:19–29

Roach MC, Boucher VL, Walss C, Ravdin PM, Ludueña RF (1998) Preparation of a monoclonal antibody specific for the class I isotype of β-tubulin: the β isotypes of tubulin differ in their cellular distributions within human tissues. Cell Motil Cytoskel 39:273–285

Walss-Bass C, Prasad V, Kreisberg JI, Ludueña RF (2001) Interaction of the β_{IV}-tubulin isotype with actin stress fibers in cultured rat kidney mesangial cells. Cell Motil Cytoskel 49:200–207

Appendix 4

Investigational New Drugs **21:** 3–13, 2003.

Different effects of vinblastine on the polymerization of isotypically purified tubulins from bovine brain

Israr A. Khan* and Richard F. Ludueña
Department of Biochemistry, University of Texas Science Center, San Antonio, TX 78229-3900, USA;
**Present address: Alpha Diagnostics International, 5415 Lost Lane, San Antonio, TX 78238, USA*

Key words: tubulin, tubulin isotypes, microtubules, vinblastine, vinca alkaloids

Summary

Vinblastine, a highly successful antitumor drug, targets the tubulin molecule. Tubulin, the subunit protein of microtubules, consists of an α- and a β-subunit, both of which consist of isotypes encoded by different genes. We have purified three isotypes of bovine brain tubulin, namely, $\alpha\beta_{II}$, $\alpha\beta_{III}$ and $\alpha\beta_{IV}$. Microtubule associated protein-2 (MAP2) and Tau-induced assembly of these isotypes were compared in the presence and absence of vinblastine. MAP2-induced assembly of unfractionated tubulin and all the isotypes except $\alpha\beta_{II}$ tubulin was resistant to 1 μM vinblastine. Vinblastine at low concentrations (<10 μM) progressively inhibited the assembly of all of the isotypes but the vinblastine concentration required for inhibition of MAP2-induced microtubule assembly was minimal for $\alpha\beta_{II}$. The tau-induced assembly of unfractionated tubulin and $\alpha\beta_{III}$ were equally sensitive to 1 μM vinblastine whereas $\alpha\beta_{II}$ and $\alpha\beta_{IV}$ were much more sensitive to vinblastine. The microtubules obtained in the presence of tau from unfractionated tubulin, $\alpha\beta_{II}$ and $\alpha\beta_{IV}$ could be easily aggregated by 20 μM vinblastine whereas such as aggregation of microtubules obtained from $\alpha\beta_{III}$ and tau required approximatedly 40 μM vinblastine. Our results suggest that among the tubulin isotypes, $\alpha\beta_{II}$ is the most sensitive to vinblastine in the presence of MAPs while $\alpha\beta_{III}$ is the most resistant and this intrinsic resistance of $\alpha\beta_{III}$ dimers persists in the polymeric form of $\alpha\beta_{III}$ tubulin as well. These results may be relevant to the therapeutic and toxic actions of vinblastine.

Introduction

Microtubules are long cylindrical organelles playing critical roles in a variety of processes such as mitosis, axonal transport and axonemal motility [1]. The major constituent of microtubules is the 100 kDa protein tubulin, which is a heterodimer consisting of two polypeptide chains designated α and β, both of which exist in several isotypic forms [1–3]. Characterization of these dimers *in vitro* has indicated that properties of microtubules are strongly influenced by the isotypic composition of the constituent β-tubulin. For example, the intrinsic dynamicity of microtubules that is a critical regulator of their function both *in vivo* and *in vitro* [4,5] has been shown to be affected dramatically by the isotypic composition of tubulin [6]. Our previous studies have clearly demonstrated that shortening rates of microtubules composed of purified β-tubulin isotypes are less sensitive to taxol than the microtubules assembled from unfractionated tubulin [7]. The fact that different isotypes assemble into microtubules at different rates [8,9] could be one of the factors affecting the dynamic behavior of microtubules. However, it is not known how the dynamicity and the relative stability of microtubules composed of segregated isotypes are related *in vivo* but the stability of different microtubules is often reflected in their *in vitro* sensitivity to various tubulin/microtubule binding drugs [7,10–13]. Recently [10], we have demonstrated that the antimitotic compound IKP-104 inhibits the assembly of $\alpha\beta_{II}$ dimers more than that of $\alpha\beta_{III}$ and $\alpha\beta_{IV}$ dimers and that high concentrations of IKP-104 induce formation of spiral aggregates from $\alpha\beta_{II}$ and $\alpha\beta_{III}$ but not from $\alpha\beta_{IV}$. On the other hand, the $\alpha\beta_{III}$ dimer interacts much less strongly with colchicine,

and taxol than do the $\alpha\beta_{II}$ and $\alpha\beta_{IV}$ dimers [7,14]. Also, the incorporation of estramustine into the $\alpha\beta_{III}$ isotype of tubulin occurs with a reduced efficiency compared to that of the other isotypes [12].

Among various anti-tubulin agents, vinblastine, a dimeric indole alkaloid derived from *Catharanthus* (*Vinca*) *roseus*, is of special interest because of its widespread use as an antimitotic drug in cancer therapy. It is thought that vinblastine exerts its antimitotic activity by disrupting the functions of microtubules. The vinblastine-induced inhibition of microtubule-function requires a direct interaction of the drug with tubulin and/or the microtubules. At low concentrations (0.2–1 μM), vinblastine acts as a suppressor of microtubule dynamic instability by binding at both ends of microtubules and thus increasing the time spent in the attenuated state [15,16]. At intermediate concentrations, vinblastine acts as an inhibitor of microtubule assembly or promoter of disassembly both *in vitro* and in cells. At concentrations >1 μM it depolymerizes the microtubules by inducing the splaying and peeling of their protofilaments, presumably by interacting with low affinity sites along the microtubule surface [17,18]. At higher concentrations (>5–10 μM) vinblastine induces formation of paracrystals and other aggregates composed of tubulin complexed with vinblastine [19–25]. In previous studies the effect of vinblastine was tested on unfractionated tubulin which is a complex mixture of a number of isotype's. In the present study, we have investigated the interaction of 1–20 μM vinblastine with isotypically pure tubulins, namely $\alpha\beta_{II}$, $\alpha\beta_{III}$ and $\alpha\beta_{IV}$. Furthermore we have used two different microtubule associated proteins (MAPs), namely microtubule associated protein 2 (MAP2) and tau, to dissect the responses of different isotypes to vinblastine in the presence of MAPs. Our results suggest that, of the various tubulin dimers, polymerization of $\alpha\beta_{II}$ is the most sensitive and that of $\alpha\beta_{III}$ the least sensitive to vinblastine.

Materials and methods

Purification of tubulin isotypes

Microtubules, MAP2 and tau were prepared from bovine cerebra and tubulin purified from the microtubules by phosphocellulose chromatography following the procedure of Fellous et al. [26]. The isotypically purified $\alpha\beta_{II}$, $\alpha\beta_{III}$ and $\alpha\beta_{IV}$ tubulin dimers were prepared as described previously [27]. All isotypically purified tubulins were stored at 80 °C until ready for use. The MAP2- or tau-induced assembly and electron microscopy of the polymers obtained were studied using the same batch of tubulin isotypes. The sedimentation and turbidimetric measurements on assembly of isotypically pure tubulins were performed using two different batches of tubulin isotypes. At a fixed tubulin concentration, the net amount of polymers obtained from several different batches of untreated isotypes varied from 0% to 20%.

Tubulin polymerization

Tubulin was thawed on ice water and spun at 18,000 × *g* for 6 min at 4 °C to remove any insoluble tubulin aggregates from the sample. Tubulin present in the supernatant was quantitated by the method of Lowry et al. [28] and mixed with vinblastine and MAP2 or tau in 0.1 M 2-(*N*-morpholino)ethanesulfonic acid, 1 mM GTP, 0.5 nM $MgCl_2$, 0.1 mM ethylenediaminetetraacetic acid, 1 mM ethylene glycol-*bis*(β-aminoethyl ether)-*N*′,*N*′,*N*′,*N*′-tetraacetic acid, 1 mM β-mercaptoethanol, pH 6.4, at 4 °C. Unless otherwise mentioned, the final concentrations of tubulin, MAP2 and tau were 1.5, 0.3 and 0.15 mg/ml, respectively. The temperature of the samples was raised from 4 to 37 °C and the tubulin polymerization was followed by either of the following two methods [27].

(A) *Sedimentation.* Aliquots (100 μl) were withdrawn at various time intervals and centrifuged for 4 min in the Beckman airfuge at 175,000 × *g*. The polymer concentration in the pellets was measured by first solubilizing the pellet in a final volume of 100 μl of 0.05 N NaOH and then quantitating the total protein in the sample by the method of Lowry et al. [28].

(B) *Turbidimetry.* The polymerization of tubulin was followed by measuring the change in turbudity at 37 °C at 350 nm on either a Beckman DU7400 or Gilford 250 spectrophotometer. For each assembly profile presented in this study at least two experiments yielding very similar results were performed under identical conditions.

Electron microscopy

The mixtures of tubulin, MAP2 or tau were incubated for at least 30 min at 37 °C in the presence or absence of the indicated amount of vinblastine sulfate (Sigma

Chemical Co., St. Louis, MO). Aliquots (50 μl) were withdrawn and treated with 1% glutaraldehyde for 30 s, and then layered on 400-mesh carbon over formavar-coated copper grids. After 1 min the grids were washed with 4 drops of water and stained with 1% uranyl acetate for 1 min. Excess stain was removed and, after air-drying, grids were examined in a Phillips 300 electron microscope with an operating voltage of 60 kV [10].

Results

Effect of vinblastine on the polymerization of tubulin isotypes in the presence of MAP2

The turbidimetric measurements on the MAP2-induced assembly of unfractionated tubulin and $\alpha\beta_{II}$ are shown in Figure 1A and B. Compared to unfractionated tubulin, which appeared to be insensitive to 1 μM vinblastine, $\alpha\beta_{II}$ tubulin lost almost one third of its ability to polymerize into microtubules (Table 1). However, the polymerization of $\alpha\beta_{III}$ and $\alpha\beta_{IV}$ was not significantly affected by 1 μM vinblastine. In fact, a slight increase of approximately 3% was observed in the case of unfractionated tubulin and $\alpha\beta_{IV}$ (Figure 1A and D). Treatment of the microtubule samples with 1 μM vinblastine altered their morphology relatively little. Unfractionated tubulin, as well as $\alpha\beta_{III}$ and $\alpha\beta_{IV}$ revealed only microtubules in the presence of the drug, whereas samples of $\alpha\beta_{II}$ contained both microtubules and bundles of protofilaments (not shown).

The addition of 20 μM of vinblastine to the assembly mixture prior to the initiation of assembly caused

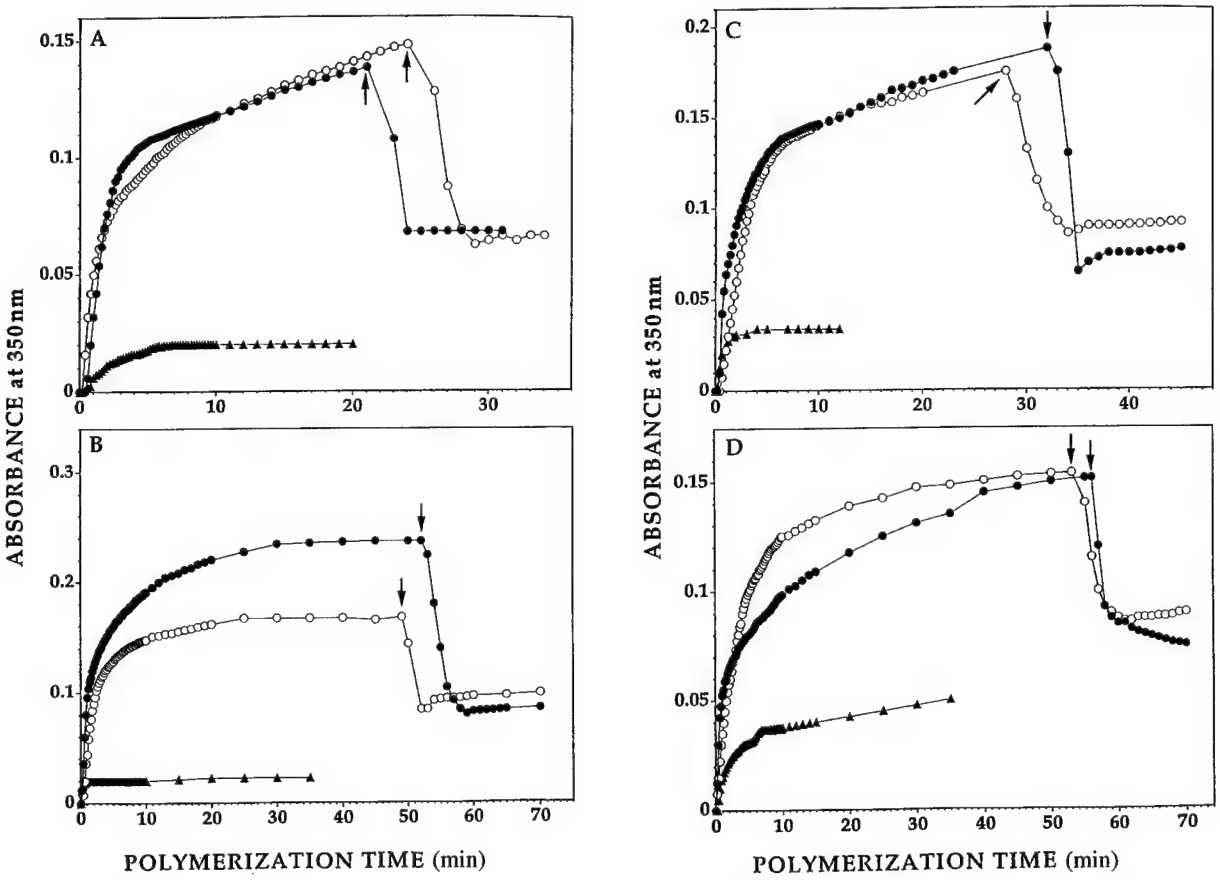

Figure 1. Effect of vinblastine on MAP2-induced assembly of unfractionated and isotypically purified tubulin isotypes. In each sample, tubulin (1.5 mg/ml) was incubated with MAP 2 (0.3 mg/ml) in the absence (●) or in the presence of vinblastine concentrations of either 1 μM (○) or 20 μM (▲). Assembly was followed by turbidimetry. The arrows represent addition of vinblastine (final concentration 20 μM) to the assembly mixture. Conditions were as described in "Materials and methods." Samples were as follows: unfractionated tubulin (A), $\alpha\beta_{II}$ (B), $\alpha\beta_{III}$ (C) and $\alpha\beta_{IV}$ (D).

Table 1. Effect of vinblastine on the assembly of tubulin isotypes

Tubulin	% Inhibition*	
	Tau	MAP2
Unfractionated	31 ± 3 (5)	[1], [3]
$\alpha\beta_{II}$	88 ± 4 (3)	29, 36
$\alpha\beta_{III}$	29 ± 3 (4)	3, 4
$\alpha\beta_{IV}$	65 ± 4 (3)	[3], [5]

*Samples of tubulin (either unfractionated or else isotypically purified $\alpha\beta_{II}$, $\alpha\beta_{III}$ or $\alpha\beta_{IV}$) (1.0 mg/ml) were incubated at 37 °C in the presence of either tau (0.30 mg/ml) or MAP2 (1.5 mg/ml) and in the presence or absence of 1 μM vinblastine. Absorption of each sample at 350 nm was measured at 0, 10, 20 and 40 min (for samples containing tau) or at 0, 15, 30, 45 and 60 min (for samples containing MAP2). The net change in absorbance at 40 min (for tau) or 60 min (for MAP2) due to the presence of vinblastine was used to calculate the drug-induced inhibition of microtubule assembly. Incubations with MAP were done in duplicate, incubations with tau were done either 3, 4 or 5 times. For the duplicate MAP2 samples, both values of the inhibition are given. For the tau samples, the average inhibition is given, together with the standard deviation. Numbers in parentheses indicate the number of incubations. Numbers in brackets indicate enhancement rather than inhibition.

a gradual increase in the turbidity of the sample (Figure 1A–D). Similarly, addition of 20 μM vinblastine to preformed microtubules resulted in the depolymerization of microtubules as reflected in a decrease in absorbance at 350 nm (Figure 1A–D). This greatly exceeded the decrease expected from the 6.7% dilution of the sample. The turbidity obtained in the presence of vinblastine reflected the formation of spirals in the case of unfractionated tubulin and $\alpha\beta_{IV}$ (not shown); for $\alpha\beta_{II}$, addition of vinblastine led to the formation of protofilamentous structure resembling spirals (not shown). In the case of $\alpha\beta_{III}$, bundles of protofilaments were the dominant structures (not shown).

It is evident from the above data that vinblastine at substoichiometric concentrations (1 μM) caused incomplete inhibition of microtubule assembly whereas at high concentrations (20 μM) it caused depolymerization of microtubules and complete inhibition of microtubule assembly. We measured the effect of a series of concentrations of vinblastine on the polymerization of various tubulin dimers and the results of this experiment are shown in Figure 2A–D. The effect of vinblastine on microtubule assembly

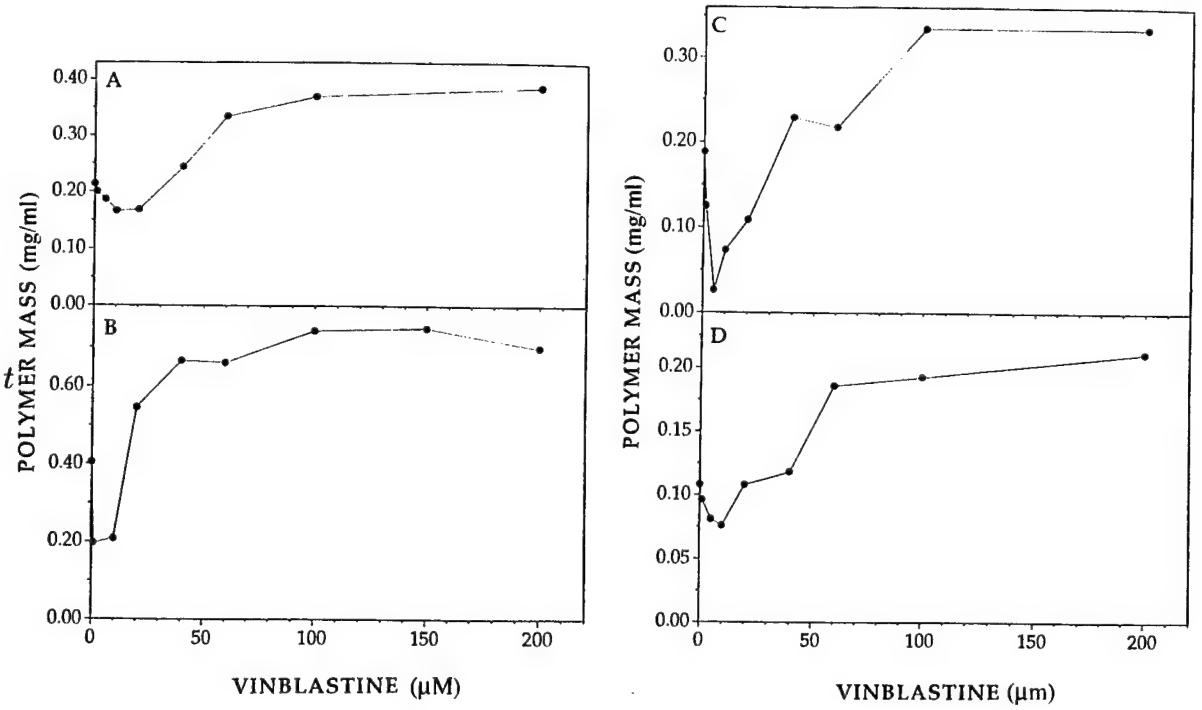

Figure 2. Effect of 0–200 μM vinblastine or MAP2-induced assembly of unfractionated and isotypically pure tubulins. Assembly was followed by sedimentation. Samples were as follows: unfractionated tubulin (A), $\alpha\beta_{II}$ (B), $\alpha\beta_{III}$ (C) and $\alpha\beta_{IV}$ (D) tubulin.

could be dissected into two parts. First, at lower concentrations (<10μM), vinblastine inhibited the MAP-induced formation of microtubules from unfractionated and isotypically pure tubulins. At a concentration of 5 μM, vinblastine caused almost complete inhibition of the polymerization of $\alpha\beta_{III}$ tubulin. Second, at higher concentrations of the drug, depolymerization of microtubules (if any) and the aggregation of tubulin occurred. It should be noted that in the absence of vinblastine and irrespective of the method used to study the polymerization of tubulin, the extent of MAP-induced polymerization of unfractionated tubulin and the isotypes varied from each other. For example, the concentration of polymer mass, as measured by sedimentation, for $\alpha\beta_{II}$, unfractionated tubulin, $\alpha\beta_{III}$ and $\alpha\beta_{IV}$ were 0.41, 0.21, 0.19 and 0.11 mg/ml, respectively (Figure 3A–D). Similarly, the approximate absorbance values, obtained by turbidimetry, for the steady state microtubules obtained from for $\alpha\beta_{II}$, unfractionated tubulin, $\alpha\beta_{III}$ and $\alpha\beta_{IV}$ were 0.23, 0.15, 0.19 and 0.16, respectively (Figure 1A–D). From the above results, it is evident that polymerization of tubulin is more extensive in the case of $\alpha\beta_{II}$ than in either unfractionated tubulin or the other isotypes. It is, therefore, not surprising that in comparison to unfractionated tubulin or the other isotypes, $\alpha\beta_{II}$ is more sensitive to vinblastine. The maximal yield of polymer obtained in the presence of high concentrations of vinblastine varied greatly depending on the isotype composition of the tubulin. $\alpha\beta_{II}$ gave the highest yield (0.74 mg/ml) followed by unfractionated tubulin (0.38 mg/ml), $\alpha\beta_{III}$

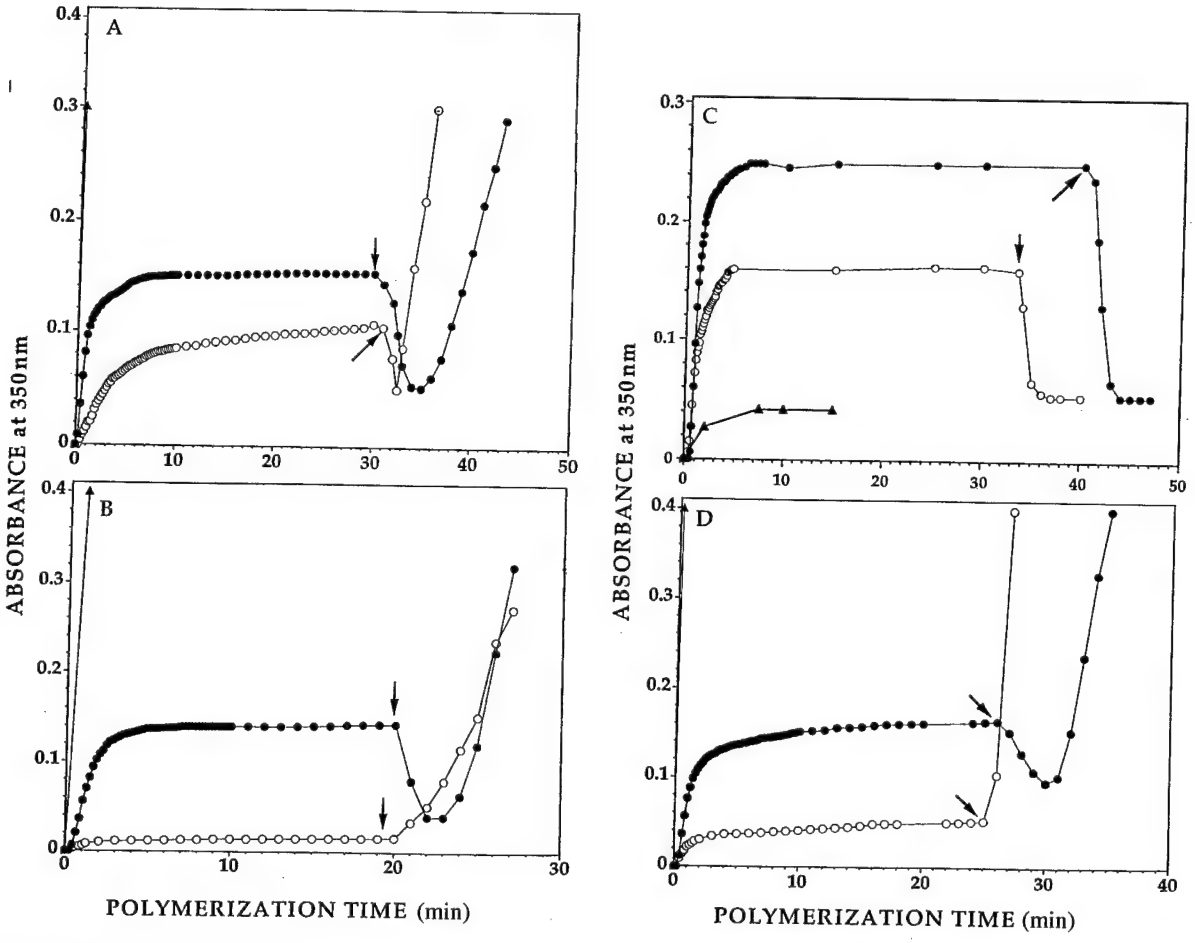

Figure 3. Effect of vinblastine on tau-induced assembly of unfractionated and isotypically purified tubulins. In each sample, tubulin (1.5 mg/ml) was incubated with tau (0.15 mg/ml) in the absence (●) or in the presence of vinblastine concentrations of either 1 μM (○) or 20 μM (▲). Assembly was followed by turbidimetry. The arrows represent addition of vinblastine (final concentration 20 μM) to the assembly mixture. Samples were as follows: unfractionated tubulin (A), $\alpha\beta_{II}$ (B), $\alpha\beta_{III}$ (C) and $\alpha\beta_{IV}$ (D).

(0.33 mg/ml) and $\alpha\beta_{IV}$ (0.22 mg/ml), indicating that the aggregation is more extensive in the case of $\alpha\beta_{II}$ than in unfractionated tubulin or other isotypes. The apparent drug-induced aggregation of tubulin started in the range of vinblastine concentration where the drug caused maximum inhibition of tubulin polymerization (lowest point of the curves shown in Figure 3A–D). This result supports the data of Figure 1 that in comparison to unfractionated tubulin, $\alpha\beta_{III}$ and $\alpha\beta_{IV}$, $\alpha\beta_{II}$ is more sensitive to vinblastine. Analysis of the data in Figure 3 shows that, for unfractionated tubulin, $\alpha\beta_{II}$, $\alpha\beta_{III}$ and $\alpha\beta_{IV}$, half-maximal inhibition of microtubule assembly was obtained at vinblastine concentrations of 3.8, 0.5, 1.8 and 2 μM, respectively, while half-maximal enhancement of aggregation was obtained with vinblastine concentrations of 52, 17, 33 and 48 μM, respectively, suggesting that, in the presence of MAP2, $\alpha\beta_{II}$ is the most sensitive to vinblastine.

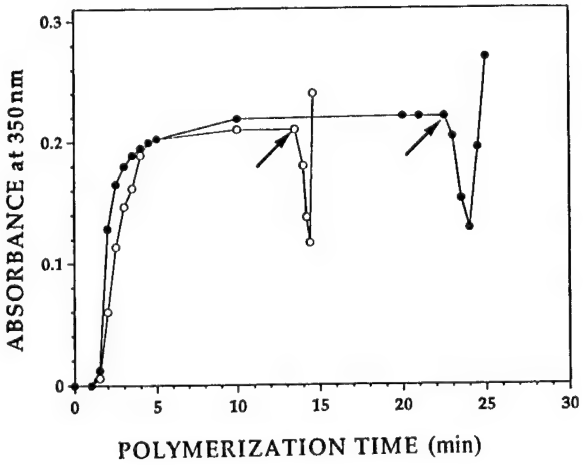

Figure 4. Effect of 40–50 μM vinblastine on the polymerization of $\alpha\beta_{III}$. Assembly was followed by turbidimetry and the depolymerization of microtubules at the steady state was induced by addition of vinblastine to a final concentration of either 40 μM (○) or 50 μM (●) (indicated by the arrows).

Effect of vinblastine on the polymerization of tubulin isotypes in the presence of tau

In contrast to MAP2-induced assembly of unfractionated tubulin, which was resistant to 1 μM vinblastine, tau-induced assembly was inhibited by almost 32% (Figure 3A). The isotypically pure tubulins were more sensitive to 1 μM vinblastine than was unfractionated tubulin, and, among the isotypes, the polymerization of $\alpha\beta_{II}$ tubulin was most sensitive to 1 μM vinblastine (). Addition of 20 μM vinblastine to microtubules preformed from unfractionated tubulin, $\alpha\beta_{II}$ and $\alpha\beta_{IV}$ resulted in depolymerization of microtubules initially; followed by rapid aggregation (Figure 4A, B and D). This phenomenon of rapid aggregation was not observed with either unfractionated or isotypically pure tubulins when the assembly was induced by MAP2 (Figure 2A–D). The most striking difference among the isotypes was that $\alpha\beta_{III}$ did not aggregate even in the presence of 20 μM vinblastine (Figure 4C). However, aggregates of tau-induced microtubules appeared once the vinblastine concentration was raised to 40 μM or above (Figure 5). A tremendous aggregation was observed when 20 μM vinblastine was included in the assembly mixture prior to initiation of the tau-induced polymerization of unfractionated tubulin, $\alpha\beta_{II}$ and $\alpha\beta_{IV}$ (Figure 3A, B and D). Again, in contrast, in the case of $\alpha\beta_{III}$, there was very little aggregation and the amount of aggregates was only 4% of the one produced in the presence of 50 μM vinblastine (Figures 3C and 4). Similar results were obtained when assembly was measured by sedimentation (Figures 6 and 7).

Electron microscopic examination showed that polymers of tubulin obtained in the presence of 1 μM vinblastine included microtubules combined with other protofilamentous structures in the cases of unfractionated tubulin, $\alpha\beta_{II}$ and $\alpha\beta_{IV}$; in contrast, in the case of $\alpha\beta_{III}$ only bundles of protofilaments were observed (not shown). The inclusion of higher amounts of the drug, e.g., 20 μM vinblastine, in the assembly mixture led to formation of only protofilamentous spirals in $\alpha\beta_{IV}$, linear bundles in unfractionated tubulin and $\alpha\beta_{II}$ or other aggregates perhaps resembling spirals in $\alpha\beta_{II}$ and $\alpha\beta_{III}$ (not shown). As shown in Figures 3 and 4, irrespective of the presence of vinblastine in the polymerization mixture, the resultant tau-induced polymers could be depolymerized by 20–40 μM vinblastine.

As seen in Figure 5, the inhibition of tau-induced polymerization of unfractionated and isotypically pure tubulin was observed in the lower concentration range of vinblastine. However, this range of vinblastine concentration for unfractionated tubulin, $\alpha\beta_{II}$ and $\alpha\beta_{IV}$ (1–5 μM vinblastine) was considerably lower than that required for $\alpha\beta_{III}$ (1–20 μM vinblastine). It is also interesting to note that, in the presence of 1 μM vinblastine, unfractionated tubulin, $\alpha\beta_{II}$, $\alpha\beta_{III}$ and $\alpha\beta_{IV}$ lost approximately 50%, 81%, 32% and 67%, respectively, of their ability to polymerize into microtubules (Figure 5A–D). This is consistent with

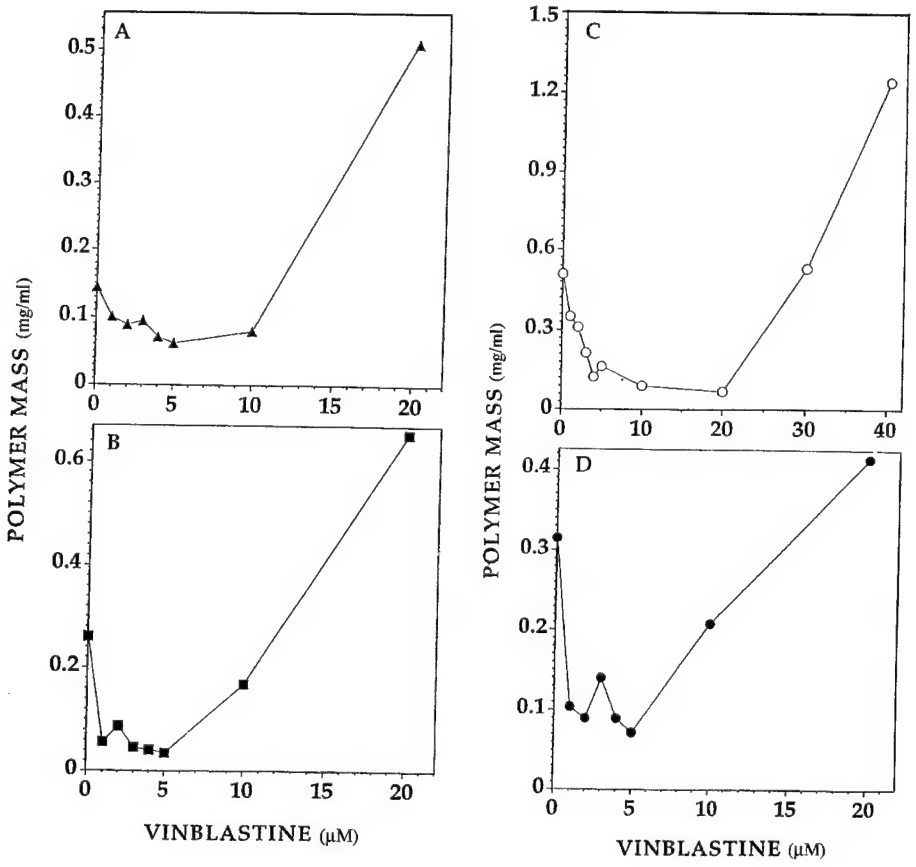

Figure 5. Effect of vinblastine on tau-induced assembly of unfractionated and isotypically purified tubulins. Samples of tubulin (1.5 mg/ml) were incubated at 37 °C in the presence of tau (0.15 mg/ml) with the indicated concentrations of vinblastine. Samples were as follows: unfractionated tubulin (A), $\alpha\beta_{II}$ (B), $\alpha\beta_{III}$ (C) and $\alpha\beta_{IV}$ (D). Assembly was followed by sedimentation.

the pattern of data obtained by turbidimetry (Table 1). Higher concentrations of vinblastine reveal a striking difference between $\alpha\beta_{III}$ on the one hand and $\alpha\beta_{II}$, $\alpha\beta_{IV}$ and unfractionated tubulin on the other hand. For the latter three, the least polymer was obtained at 5 μM vinblastine, whereas for $\alpha\beta_{III}$, this occurred at 20 μM vinblastine. For the latter three, formation of non-microtubule aggregate in the presence of 20 μM vinblastine was much greater than microtubule assembly in the absence of vinblastine. In contrast, for $\alpha\beta_{III}$, this required 40 μM vinblastine. Analysis of the results of Figure 5 suggests that half-maximal inhibition of tau-induced microtubule assembly for unfractionated tubulin, $\alpha\beta_{II}$, $\alpha\beta_{III}$ and $\alpha\beta_{IV}$ was obtained at vinblastine concentrations of 1, 0.6, 2.1 and 0.6 μM, respectively. In conjunction with the fact that MAP2-induced assembly of $\alpha\beta_{II}$ isotype is most sensitive to 1 μM vinblastine (Table 1), the data of Figures 2 and 5 suggest that sensitivity of polymerization of tubulin to vinblastine-induced inhibition is influenced by the type of the tubulin as well as the nature of microtubule associated proteins.

Discussion

Previous studies have shown that vinblastine, at low concentrations, inhibits polymerization of tubulin into microtubules. At higher concentrations, the drug depolymerizes microtubules and induced the formation and aggregation of spirals. We have made the same observations and shown that they may apply to isotypically purified tubulin as well. These observations are in agreement with the consensus on the presence of two types of vinblastine binding sites on tubulin. The first binding site is specific and strong,

involving residues 175–213 on β-tubulin [29] and is probably responsible for the substoichiometric inhibition of microtubule assembly [30]. There are two additional vinblastine-binding sites on tubulin that are weak, nonspecific and responsible for aggregation [29,31]. Since MAPs are present *in vivo*, we considered it important to study the effect of vinblastine on tubulin in the presence of MAPs.

Our results indicate that the type of MAP used to induce tubulin polymerization affected the inhibition of this process by vinblastine. The inhibitory effect of vinblastine on MAP-induced assembly of tubulin may arise from a drug-induced conformational change in either tubulin itself or at the sites where the MAPs bind. Evidence for a structural change induced in tubulin by the drug has come from quenching of tubulin fluorescence, from changes in sulfhydryl reactivity and crosslinking, from altered proteolytic susceptibility, and from immunological reactivity [32–35]. A direct interaction between vinblastine and MAPs has not been documented. Since the sites of interaction of vinblastine and MAP(s) on the tubulin molecule are distinct, it is likely that the drug-induced conformational change in tubulin itself is responsible for the substoichiometric inhibition of assembly [31]. Since the binding of MAPs to the carboxyl terminal of tubulin may influence and regulate both lateral and longitudinal interactions between subunits in tubulin polymers [36,37], the drug-induced conformational change in tubulin can be influenced by the nature of the MAPs present in the assembly mixture. It is not surprising, therefore, that at substoichiometric concentrations of vinblastine, unfractionated tubulin was resistant to the drug when assembly was induced by MAP2. On the contrary, a 30–31% decrease was observed when assembly was induced by tau instead of MAP2 (Table 1 and Figures 1A and 3A). This result is supported by previous findings that, in the presence of vinblastine, tau and MAP2 interact differently with tubulin [38]. This would imply that the regions in the tubulin dimer where the majority of the vinblastine-induced changes occur might alter the subunit–subunit interactions and that the latter is propagated differently to the site(s) within the tubulin molecule where MAP2 and tau bind. By this interpretation, the substoichiometric inhibition of tubulin polymerization by vinblastine should not vary among the isotypes of tubulin, provided the conformations of all the forms of tubulin are identical. As discussed below, however, our results from the experiments with isotypically pure tubulin dimers differ significantly from these expectations.

Vinblastine, at low concentrations, had a very strong inhibitory effect on MAP2-induced assembly of $\alpha\beta_{II}$ whereas the assembly of the other isotypes was affected much less. A possible explanation for our results is that $\alpha\beta_{III}$ binds to vinblastine with lower affinity than do the other two isotypes. This suggests that tubulin isotypes are structurally different from each other and, therefore, that the magnitude and the propagation of vinblastine-induced conformational change differs among the isotypes. If vinblastine binding to microtubules induces a conformational change then one would expect that a tubulin isotype with a relatively rigid conformation would be more resistant to vinblastine-induced inhibition of assembly. This conclusion is also supported by our observation that among the isotypes, $\alpha\beta_{II}$ dimers were found to be most sensitive to vinblastine when assembly was induced by either tau or MAP2. It is worth emphasizing that $\alpha\beta_{III}$, which has a more rigid conformation than those of the other isotypes [39,40] was the least sensitive to low concentrations of vinblastine when assembly was induced by tau.

If the structural rigidity of tubulin isotypes is assumed to be directly related to their relative sensitivity to low concentrations of vinblastine, then polymers formed from a rigid isotype are likely to be most resistant to depolymerization and subsequent aggregation by high concentrations of the drug. As expected, in contrast to unfractionated tubulin, $\alpha\beta_{II}$ and $\alpha\beta_{IV}$, the polymers obtained from $\alpha\beta_{III}$ could not be aggregated by 20 μM vinblastine indicating that $\alpha\beta_{III}$, both in its dimeric and polymeric forms, is most resistant to vinblastine. A much higher concentration of vinblastine (~40–50 μM) was required to induce depolymerization and subsequent aggregation. This further supports our earlier conclusion that conformational stability and thus relative sensitivity of tubulin varies among the isotypes.

Both MAP2 and tau stimulated the vinblastine-induced aggregation of unfractionated, $\alpha\beta_{II}$ and $\alpha\beta_{IV}$ tubulins, but the aggregation was more evident in the case of tau. Similar enhancement of aggregation has been reported after the removal of the carboxyl terminals of tubulin [31]. In the case of $\alpha\beta_{III}$, however, aggregation of tubulin dimers stimulated by tau in the presence of 20 μM vinblastine did not occur. This finding further substantiated our conclusion that among the isotypes, $\alpha\beta_{III}$ is most resistant to vinblastine.

Among all the forms of tubulin tested, only $\alpha\beta_{II}$ exhibited a significant loss in its ability to polymerize into microtubules when the assembly was stimulated by MAP2 in the presence of 1 μM vinblastine. The relatively higher sensitivity of $\alpha\beta_{II}$ was also evident from electron microscopy data. The polymers formed from $\alpha\beta_{II}$ included microtubules as well as a large population of other protofilament-based non-microtubule structures. In contrast, at this concentration of vinblastine, only microtubules were seen with unfractionated tubulin, $\alpha\beta_{III}$ or $\alpha\beta_{IV}$. Similar abnormal structures were obtained in the case of $\alpha\beta_{III}$ but higher (20 μM) vinblastine concentrations were required. At these concentrations, however, other forms of tubulin generated spirals and aggregates. Since the aggregation is induced by binding of vinblastine to weak and nonspecific sites on tubulin, it appears that the affinity of these sites also varies among the isotypes. As described below, our results also provide evidence that isotypically pure tubulins are more sensitive to vinblastine than is unfractionated tubulin but at the same time are less prone to vinblastine-induced aggregation.

From the analysis of the morphology of the tau-induced polymers obtained in the presence of substoichiometric concentration of vinblastine it is clear that in the case of $\alpha\beta_{II}$ and $\alpha\beta_{IV}$, polymers include microtubules and other aggregates as well as spirals. In contrast, polymers obtained from $\alpha\beta_{III}$ include aggregates and bundles of protofilaments but not spirals. In the case of $\alpha\beta_{III}$ a small proportion of polymers included aggregates and spirals, but only at high (20 μM) concentrations of the drug, at which vinblastine interacts nonspecifically with weaker sites on the tubulin molecule.

Our results would appear to contradict those of Lobert et al. [11,41] who found no difference in the binding of vinblastine to the $\alpha\beta_{II}$ or $\alpha\beta_{III}$ dimers. They also observed that vinblastine promoted self-association of $\alpha\beta_{II}$ and $\alpha\beta_{III}$ to the same extent [11]. Interestingly, they also found that vincristine, which is structurally very similar to vinblastine, enhanced self-association of $\alpha\beta_{II}$ better than it did that of $\alpha\beta_{III}$ [11]. A major difference between the experiments of Lobert et al. [11,41] and ours, however, is that the self-association experiments described here were done in the presence of either MAP2 or tau while those of Lobert et al. [11,41] were performed in the absence of MAPs. The tubulin self-association examined by Lobert et al. [11] and previously by Na and Timasheff [42,43] largely involves formation of tubulin oligomers that are to be distinguished from the large filamentous structures seen in the electron microscope, whose formation is facilitated by MAPs. It is quite conceivable that self-association of tubulin is isotype-neutral while MAP-induced aggregation into filamentous structures could be strongly influenced by the nature of the tubulin isotype involved. In other words, one could postulate that the real difference among the isotypes involves only the regions on the tubulin molecule which transduce conformational effects between the vinblastine and the MAP binding sites. We already know that this region is exquisitely sensitive to temperature, as well as to the nature and integrity of the MAP [37,44,45].

In summary, our results indicate that $\alpha\beta_{II}$ is the most sensitive to vinblastine and that $\alpha\beta_{III}$ is the least sensitive. Since vinblastine is a major antitumor drug, our results raise the possibility that sensitivity and resistance of tumors to this drug can be modulated by the tubulin isotype composition of the microtubules in the tumor cell, as was previously postulated by Lobert et al. [11] to be the case for vincristine and as is apparently the case with taxol and estramustine [46–48]. In the case of taxol, we have measured its effect on the dynamic behavior of microtubules formed from isotypically purified tubulin [7]. To choose one parameter, the shortening rate of microtubules made from $\alpha\beta_{III}$ is 4.6–4.7 times more sensitive to taxol than is the case for microtubules made from $\alpha\beta_{III}$ or $\alpha\beta_{IV}$ [7]. Consistent with this finding, tumors treated with taxol often respond by increasing their expression of $\alpha\beta_{III}$ and $\alpha\beta_{IV}$ [46,49]. Future investigation may reveal whether a similar pattern occurs in tumors treated with vinblastine.

Acknowledgments

We are grateful to Drs Asok Banerjee and Asish R. Chaudhuri for their valuable suggestions. We thank Veena Prasad, Mohua Banerjee, Pat Schwarz and Alka Mittal for their help during the preparation of microtubules from bovine cerebra. This research was supported by grants CA26376 and HL07446 from the National Institutes of Health, DAMD17-98-1-8246 and DAMD 17-01-1-0411 from the U.S. Army Medical Research and Materiel Command and AQ-0726 from the Welch Foundation.

References

1. Dustin P: Microtubules, 2nd edn. Springer-Verlag, Berlin, 1984
2. Ludueña RF, Shooter EM, Wilson: Structure of the tubulin dimer. J Biol Chem 252: 7006–7014, 1977
3. Ludueña RF: Multiple forms of tubulin: different gene products and covalent modifications. Int Rev Cytol 178: 207–275, 1998
4. Wilson L, Jordan MA: Pharmacological probes of microtubule function. In: Hyams JS, Lloyd CW (eds) Microtubules. Wiley-Liss, New York, 1994, pp 59–83
5. Wordeman L, Mitchison T: Dynamics of microtubule assembly *in vivo*. In: Hyams JS, Lloyd CW (eds) Microtubules. Wiley-Liss, New York, 1994, pp 287–301
6. Panda D, Miller HP, Banerjee A, Ludueña RF, Wilson L: Microtubule dynamics *in vitro* are regulated by the tubulin isotype composition. Proc Natl Acad Sci USA 91: 11358–11362, 1994
7. Derry WB, Wilson L, Khan IA, Ludueña RF, Jordan MA: Taxol differentially modulates the dynamics of microtubules assembled from unfractionated and purified β-tubulin isotypes. Biochemistry 36: 3554–3562, 1997
8. Banerjee A, Roach MC, Trcka P, Ludueña RF: Increased microtubule assembly in bovine brain tubulin lacking the type III isotype of β-tubulin. J Biol Chem 265: 1794–1799, 1990
9. Banerjee A, Roach MC, Trcka P, Ludueña RF: Preparation of a monoclonal antibody specific for the class IV isotype of β-tubulin. Purification and assembly of $\alpha\beta_{II}$, $\alpha\beta_{III}$, and $\alpha\beta_{IV}$ tubulin dimers from bovine brain. J Biol Chem 267: 5625–5630, 1992
10. Khan IA, Tomita I, Mizuhashi F, Ludueña RF: Differential interaction of tubulin isotypes with the antimitotic compound IKP-104. Biochemistry 39: 9001–9009, 2000
11. Lobert S, Frankfurter A, Correia JJ: Energetics of Vinca alkaloid interactions with tubulin isotypes: implications for drug efficiency. Cell Motil Cytoskeleton 39: 107–121, 1998
12. Laing N, Dahllöf B, Hartley-Asp B, Ranganathan S, Tew KD: Interaction of estramustine with tubulin isotypes. Biochemistry 36: 871–878, 1997
13. Banerjee A, Ludueña RF: Distinct colchicine binding kinetics of bovine brain tubulin lacking the type III isotype of β-tubulin. J Biol Chem 266: 1689–1691, 1991
14. Banerjee A, Ludueña RF: Kinetics of colchicine binding to purified β-tubulin isotypes from bovine brain. J Biol Chem 267: 13335–13339, 1992
15. Toso RJ, Jordan MA, Farrell KW, Matsumoto B, Wilson L: Kinetic stabilization of microtubule dynamic instability *in vitro* by vinblastine. Biochemistry 32: 1285–1293, 1993
16. Dhamodharan P, Jordan MA, Thrower D, Wilson L, Wadsworth P: Vinblastine suppresses dynamics of individual microtubules in living interphase cells. Mol Biol Cell 6: 1215–1229, 1995
17. Jordan MA, Margolis RL, Himes RH, Wilson L: Identification of a distinct class of vinblastine binding sites on microtubules. J Mol Biol 187: 61–73, 1986
18. Singer WD, Jordan MA, Wilson L, Himes RH: Binding of vinblastine to stabilized microtubules. Mol Pharmacol 36: 366–370, 1989
19. Wilson L, Jordan MA, Morse A, Margolis RL: Interaction of vinblastine with steady-state microtubules *in vitro*. J Mol Biol 159: 125–149, 1982
20. Hamel E: Interactions of tubulin with small ligands. In: Avila J (ed.) Microtubule Proteins. CRC Press, Boca Raton, 1990, pp 89–191
21. Bensch KG, Malawista SE: Microtubular crystals in mammalian cells. J Cell Biol 40: 95–107, 1969
22. Warfield RKN, Bouck GB: Microtubule-macrotubule transition: intermediates after exposure to the mitotic inhibitor vinblastine. Science 186: 1219–1220, 1974
23. Himes RH: Interaction of the catharanthus (*Vinca*) alkaloids with tubulin and microtubules. Pharmac Ther 51: 257–267, 1991
24. Schochet SS Jr, Lambert PW, Earle KM: Neuronal changes induced by intrathecal vincristine sulfate. J Neuropathol Exp Neurol 27: 645–658, 1968
25. Wilson L, Morse ANC, Bryan J: Characterization of *acetyl*-^{3}H-labeled vinblastine binding to vinblastine-tubulin crystals. J Mol Biol 121: 255–268, 1978
26. Fellous A, Francon J, Lennon AM, Nunez J: Microtubule assembly *in vitro*. Purification of assembly-promoting factor. Eur J Biochem 78: 167–174, 1977
27. Khan IA, Ludueña RF: Phosphorylation of β_{III}-tubulin. Biochemistry 35: 3704–3711, 1996
28. Lowry OH, Rosebrough NH, Farr AL, Randall RJ: Protein measurement with the Folin phenol reagent. J Biol Chem 193: 265–275, 1951
29. Rai SS, Wolff J: Localization of the vinblastine-binding site on β-tubulin. J Biol Chem 271: 14707–14711, 1996
30. Timasheff SN, Andreu JM, Na GC: Physical and spectroscopic methods for the evaluation of the interaction of antimitotic agents with tubulin. Pharmac Ther 52: 191–210, 1991
31. Correia JJ: Effects of antimitotic agents on tubulin-nucleotide interactions. Pharmac Ther 52: 127–147, 1991
32. Ludueña RF, Roach MC: Tubulin sulfhydryl groups as probes and targets for antimitotic and antimicrotubule agents. Pharmac Ther 49: 13–152, 1991
33. Morgan JL, Spooner BS: Immunological detection of microtubule poison-induced conformational changes in tubulin. J Biol Chem 258: 13127–13133, 1983
34. Prakash V, Timasheff SN: The interaction of vincristine with calf brain tubulin. J Biol Chem 258: 1689–1697, 1983
35. Lee JC, Harrison D, Timasheff SN: Interaction of vinblastine with calf brain microtubule protein. J Biol Chem 250: 9276–9282, 1975
36. Cleveland DW, Hwo SY, Kirschner MW: Physical and chemical properties of purified tau factor and the role of tau in microtubule assembly. J Mol Biol 116: 227–247, 1977
37. Scheele RB, Borisy GG: *In vitro* assembly of microtubules. In: Roberts K, Hyams J (eds) Microtubules. Academic Press, London, 1979, pp 175–254
38. Ludueña RF, Fellous A, McManus L, Jordan MA, Nunez J: Contrasting roles of tau and microtubule-associated protein 2 in the vinblastine-induced aggregation of brain tubulin. J Biol Chem 259: 12890–12898, 1984
39. Schwarz PM, Liggins JR, Ludueña RF: β-Tubulin isotypes purified from bovine brain have different relative stabilities. Biochemistry 37: 4687–4692, 1998
40. Banerjee A, Ludueña RF: Kinetics of colchicine binding to purified β-tubulin isotypes from bovine brain. J Biol Chem 267: 13335–13339, 1992
41. Lobert S, Frankfurter A, Correia JJ: Binding of vinblastine to phosphocellulose-purified and $\alpha\beta$-class III tubulin: the role of nucleotides and β-tubulin isotypes. Biochemistry 34: 8050–8060, 1995

42. Na GC, Timasheff SN: Stoichiometry of the vinblastine-induced self-association of calf brain tubulin. Biochemistry 19: 1347–1354, 1980
43. Na GC, Timasheff SN: Interaction of vinblastine with calf brain tubulin: multiple equilibria. Biochemistry 25: 6214–6222, 1986
44. Prasad V, Jordan MA, Ludueña RF: Temperature sensitivity of vinblastine-induced tubulin polymerization in the presence of microtubule-associated proteins. J Prot Chem 11: 509–515, 1992
45. Fellous A, Prasad V, Ohayon R, Jordan MA, Ludueña RF: Removal of the projection domain of microtubule-associated protein 2 alters its interaction with tubulin. J Prot Chem 13: 381–391, 1994
46. Ranganathan S, Dexter DW, Benetatos CA, Chapman AE, Tew KD, Hudes GR: Increase of β_{III}- and β_{IVa}-tubulin isotypes in human prostate carcinoma cells as a result of estramustine resistance. Cancer Res 56: 2584–2589, 1996
47. Haber M, Burkhart CA, Regl DL, Madafiglio J, Norris MD, Horwitz SB: Altered expression of Mβ2, the class II β-tubulin isotype, in a murine J774.2 cell line with a high level of taxol resistance. J Biol Chem 270: 31269–31275, 1995
48. Dumontet C, Duran GE, Steger KA, Beketic-Oreskovic L, Sikic BI: Resistance mechanisms in human sarcoma mutants derived by single-step exposure to paclitaxel (taxol). Cancer Res 56: 1091–1097, 1996
49. Jaffrézou JP, Dumontet C, Derry WB, Durán G, Chen G, Tsuchiya E. Wilson L, Jordan MA, Sikic BI: Novel mechanism of resistance to paclitaxel (taxol) in human K562 leukemia cells by combined selection with PSC833. Oncol Res 7: 517–527, 1995

Address for offprints: Richard F. Ludueña, Department of Biochemistry, Mail Code 7760, University of Texas Health Science Center, 7703 Floyd Curl Drive, San Antonio, TX 78229-3900, USA; Tel.: (210)567-3732; Fax: (210)567-6595; E-mail: luduena@edu

Appendix 5

Investigational New Drugs **21:** 15–20, 2003.

Effect of the antitumor drug vinblastine on nuclear β_{II}-tubulin in cultured rat kidney mesangial cells

Consuelo Walss-Bass[1,3], Jeffrey I. Kreisberg[2] and Richard F. Ludueña[1]

[1]*Department of Biochemistry and* [2]*Department of Surgery, University of Texas Health Science Center, San Antonio, TX 78229, USA;* [†]*The Research and Development Service, Department of Veteran Affairs, San Antonio, TX 78229, USA;* [3]*Present address: Department of Psychiatry, University of Texas Health Science Center, San Antonio, TX 78229, USA*

Key words: tubulin isotypes, microtubules, vinblastine, nuclear localization, DNA fragmentation

Summary

Tubulin, the main component of microtubules, is a major target for antitumor drugs such as vinblastine. We have recently discovered that the β_{II} isotype of tubulin is present in the nuclei of cultured rat kidney mesangial cells, smooth-muscle-like cells present in the renal glomerular mesangium (Walss C, Kreisberg JI, Ludueña RF: Cell Motil Cytoskeleton 42: 274–284, 1999). Here, we have investigated the effect of vinblastine on nuclear β_{II}-tubulin in these cells. We have found that, at concentrations of 15 nM and higher, vinblastine caused a reversible loss of β_{II}-tubulin from the nucleus. Our results raise the possibility that nuclear β_{II}-tubulin constitutes a population of tubulin that could be a novel target for antitumor drugs such as vinblastine.

Introduction

Because of their crucial role in chromosome segregation during cell division, microtubules have long been a target for antitumor drugs [1]. These drugs inhibit microtubule dynamics by binding to tubulin, the structural subunit of microtubules [2]. Vinblastine, a member of the *Vinca* alkaloid family, is an anti-tubulin drug widely used in chemotherapy [3]. By binding to the β-subunit of tubulin, vinblastine inhibits microtubule dynamics [2]. At high concentrations, vinblastine causes microtubule depolymerization [4] and the formation of tubulin paracrystals [5]. Therefore, this drug is known as a microtubule destabilizing agent. At low, clinically relevant, concentrations, vinblastine is known to arrest cells in mitosis by suppressing the dynamics of spindle microtubules, without significantly changing the amount of polymerized tubulin [6]. The end result of this drug at low concentrations is to impede cell division and ultimately cause cell death.

We have previously reported the presence of a specific isotype of tubulin, β_{II}, in the nuclei of rat kidney mesangial cells [7]. This was demonstrated by immunofluorescence and immunoelectron microscopy and by the fact that both fluorescein-colchicine and micro-injected fluorescently labeled $\alpha\beta_{II}$ tubulin dimer localize to the nucleus in the same pattern as does endogenous β_{II} [7]. Nuclear β_{II}-tubulin exists as an $\alpha\beta_{II}$ tubulin dimer and appears to be in non-microtubule form and, as such, it constitutes a novel population of cellular tubulin. Recently, we have found that β_{II} is present in the nuclei of a variety of human cancer cells, but seems to be absent from the nuclei of many normal human cells [8]. Since tubulin is a major target of certain antitumor drugs, it is of interest to examine the effects of these drugs on nuclear tubulin. Therefore, we have now investigated the effect of vinblastine on nuclear β_{II}-tubulin in rat kidney mesangial cells, smooth-muscle-like cells from the renal mesangium. We have found that, at concentrations higher than what is clinically relevant, these drugs appear to cause β_{II}-tubulin to exit the nucleus. Loss of nuclear tubulin occurs after microtubule depolymerization caused by vinblastine. Removal of the drug allows β_{II} to reenter the nucleus. Treatment of cells with antitumor drugs has been shown to

induce apoptosis. The mechanism by which this occurs remains unclear [9]. Our results raise the possibility that vinblastine may act by binding to nuclear β_{II}-tubulin and preventing it from executing its as yet unknown function.

Materials and methods

Source of cells and antibodies

Rat kidney mesangial cells were obtained as follows. Glomeruli were isolated from 200 g male Sprague–Dawley rats (Harlan Sprague–Dawley, Inc., Indianapolis, IN) using a graded sieve technique and were plated for culture in RPMI 1640 (Gibco BRL, Grand Island, NY) tissue culture medium with 20% FCS plus penicillin, streptomycin, and fungizone (E.R. Squibb and Sons) for explant growth of mesangial cells [10,11]. One hundred percent of the cells were identified as glomerular mesangial cells. Positive identification was obtained by ultrastructural examination, contractile responsiveness to vasopressin and angiotensin II, and shape change in response to cAMP-elevating agents [10–12]. For the experiments described below, cells were used between the 4th and 40th passage. The monoclonal antibodies SAP.4G5 and JDR.3B8 specific for the β_I and β_{II} isotypes of tubulin, were prepared as previously described [13,14].

Immunofluorescence microscopy

Rat kidney mesangial cells were plated on glass coverslips in RPMI 1640 medium (Gibco BRL, Grand Island, NY) containing 20% fetal calf serum (Atlanta Biologicals, Norcross, GA). After 24 h, cells were treated with various concentrations of vinblastine (Sigma Chemical Co., St. Louis, MO) from a 1 mM stock solution prepared fresh in H_2O. After various periods of time, cells were washed twice with PBS (0.15 M NaCl, 0.0027 M KCl, 0.00147 M KH_2PO_4, 0.01 M $NaHPO_4$, pH 7.2), fixed for 15 min with 3.7% paraformaldehyde at room temperature and permeabilized for 1 min with 0.5% Triton X-100 in PBS. Cells were then incubated at 4 °C overnight with the respective isotype-specific monoclonal IgG mouse antibody (anti-β_I, 0.05–0.1 mg/ml; anti-β_{II}), diluted in PBS containing 10% normal goat serum (Jackson Immunoresearch, West Grove, PA). After rinsing in PBS, coverslips were stained with a Cy3-conjugated goat anti-mouse antibody (1 : 100, Jackson Immunoresearch) for 1 h at room temperature. For DNA detection, cells were stained with DAPI (4′,6-diamidino-2-phenylindole, dihydrochloride) (Molecular Probes, Eugene, OR) (2 μl/ml in PBS) during the last wash with PBS after incubation with the secondary antibody. Coverslips were mounted on glass slides and examined with an Olympus epifluorescence photomicroscope using a Plan-Neufluar 100× oil objective. For drug reversibility experiments, cells were incubated with vinblastine at various concentrations for 24 h, after which the drug was removed and cells were incubated in fresh media for 24 h. Cells were then fixed and treated as described above.

Results

Because we were not interested in blocking cells in mitosis, we chose to use vinblastine concentrations higher than those clinically relevant. Therefore, rat kidney mesangial cells were incubated with vinblastine at concentrations of 15–50 nM for 1–6 h. Cells were then fixed and stained with monoclonal antibodies to β_I- and β_{II}-tubulin. The β_{II}-tubulin antibody has been reported previously to detect nuclear β_{II}-tubulin [7]. The β_I-tubulin antibody was used to observe the effect of vinblastine on cytosolic microtubules, since this isotype is present only in the cytosol [7]. Cells treated with anti-β_I in the absence of drug revealed a normal microtubule network in the cytosol (Figure 1A). However, 1 h treatment with 15 nM vinblastine, the lowest drug concentration used, was enough to completely depolymerize the microtubules (Figure 1B). No difference in the cytosolic fluorescence pattern was observed when cells were treated longer or with higher drug concentrations.

Staining of control, drug-free cells, with anti-β_{II} tubulin revealed that all cells contained β_{II}-tubulin in the nucleus, as had been previously reported [7] (Figure 1C). Very little fluorescence was observed in the cytosol. After treatment with 15 nM vinblastine for 1 h, 3 out of 10 cells seemed to have lost their nuclear tubulin, as they contained no nuclear fluorescence (Figure 1D). The nuclei of these cells appeared unaffected, as seen by DAPI staining (Figure 1E). After 3 h of treatment with 15 nM vinblastine, 8 out of 10 cells had lost their nuclear tubulin (Figure 1F) and, as before, DAPI staining revealed that the

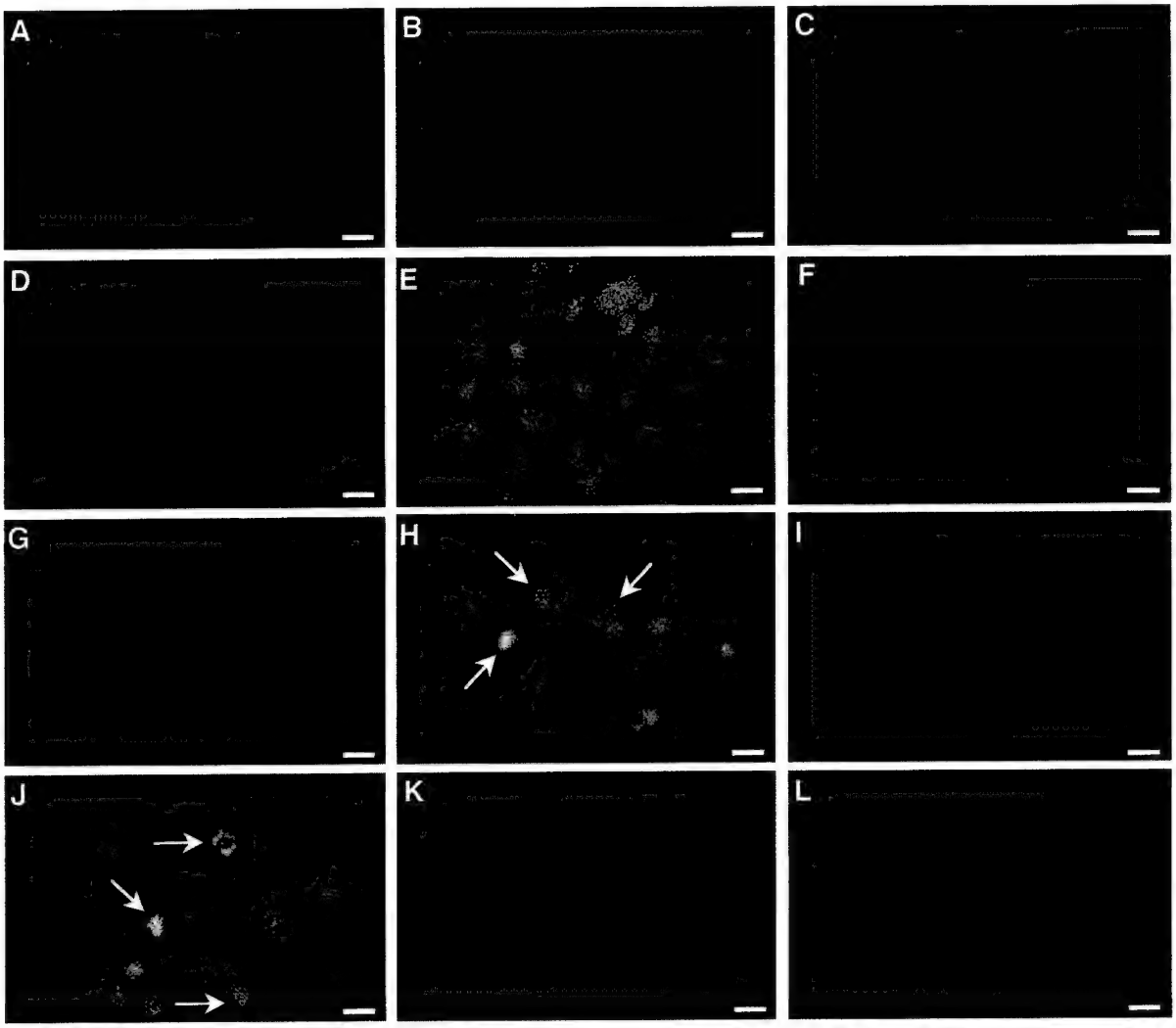

Figure 1. Effect of vinblastine on nuclear tubulin in mesangial cells. (A) Control, drug-free cells, stained with anti-β_I. (B) Cells treated with 15 nM vinblastine for 1 h, stained with anti-β_I. Notice depolymerization of microtubules. (C) Control, drug-free cells stained with anti-β_{II}. Notice the strong nuclear fluorescence. (D) Cells treated with 15 nM vinblastine for 1 h, stained with anti-β_{II}. (E) Same cells as in D, stained with DAPI to reveal the nuclei. (F) Cells treated with 15 nM vinblastine for 3 h, stained with anti-β_{II}. (G) Cells treated with 30 nM vinblastine for 1 h, stained with anti-β_{II}. (H) Same cells as in G, stained with DAPI to reveal the nuclei. (I) Cells treated with 30 nM vinblastine for 3 h, stained with anti-β_{II}. (J) Same cells as in I, stained with DAPI to reveal the nuclei. (K) Cells treated with 50 nM vinblastine for 1 h, stained with anti-β_{II}. (L) Same cells as in K, stained with DAPI, to reveal the nuclei. Arrows indicate micronucleation.

nuclei of these cells appeared intact (not shown). By increasing the vinblastine concentration to 30 nM, 1 h of treatment was enough to cause the loss of nuclear tubulin in 7 out of 10 cells (Figure 1G). At this drug concentration, micronucleation, or DNA fragmentation, was seen by DAPI staining in 3 out of 10 cells, indicating that these cells were probably undergoing apoptosis (Figure 1H). Micronucleation appeared to occur regardless of whether β_{II}-tubulin was present in the nucleus or not. Furthermore, the nuclei of cells that had lost their nuclear tubulin, but had not entered apoptosis, appeared to be normal, as indicated by DAPI staining (Figure 1H). After 3 h of treatment with 30 nM vinblastine, nuclear tubulin was absent in 9 out of 10 cells (Figure 1I and J). Treatment of cells with concentrations of 40–60 nM vinblastine for 1 h caused the total disappearance of nuclear tubulin (Figure 1K and L).

In order to determine if the effect of vinblastine on nuclear tubulin was reversible, cells were incubated with vinblastine at concentrations from 15 to 50 nM for 24 h and then incubated in media without drug for

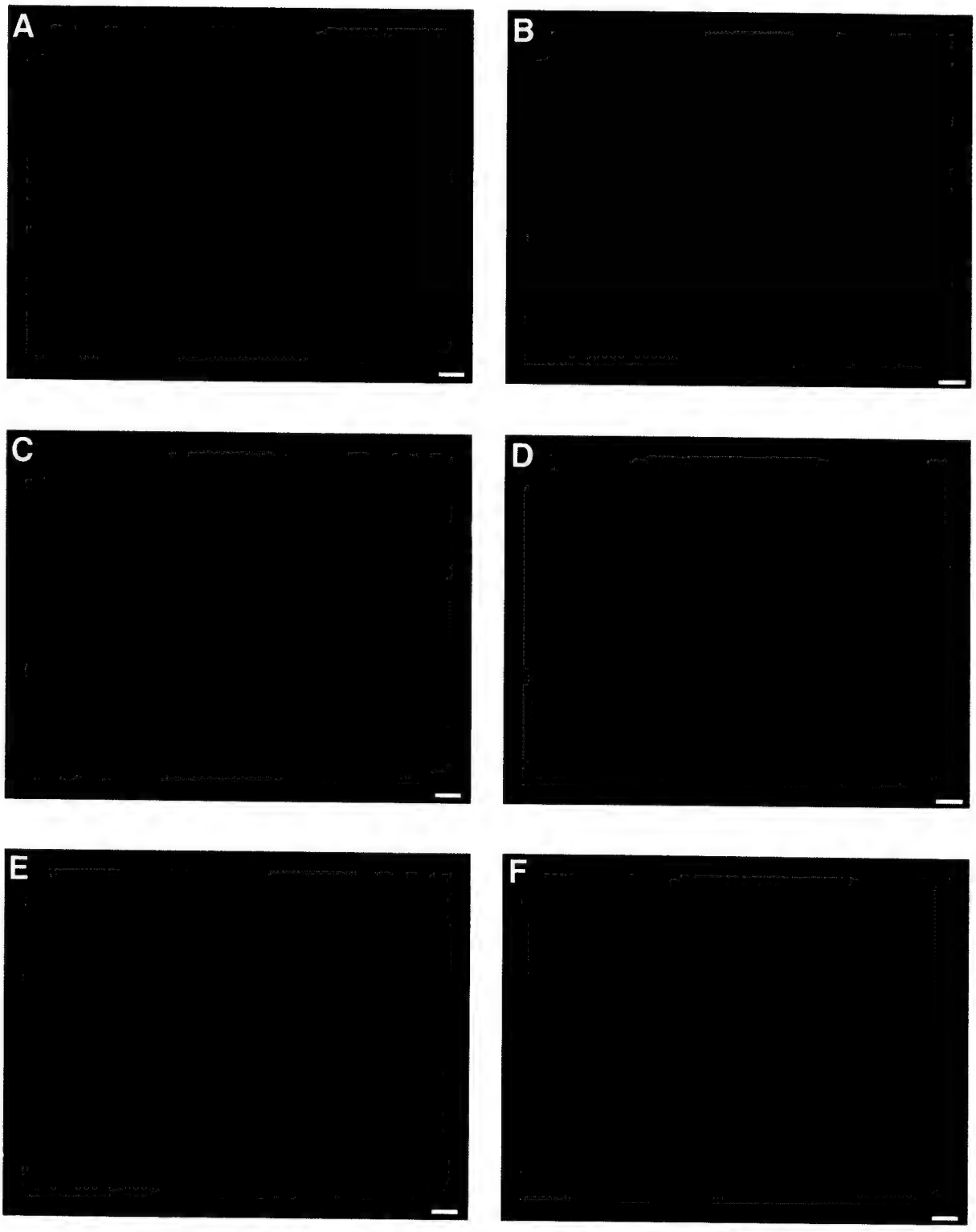

Figure 2. The effect of vinblastine on nuclear tubulin is reversible. (A, C, E) Cells stained with anti-β_{II}. (B, D, F) Cells stained with DAPI. (A, B) Cells treated with 15 nM vinblastine for 6 h, then incubated in media without drug for 24 h. (C, D) Cells treated with 30 nM vinblastine for 6 h, then incubated in media without drug for 24 h. (E, F) Cells treated with 50 nM vinblastine for 6 h, then incubated in media without drug for 24 h.

24 h. Treatment of these cells with anti-β_{II} revealed that cells were able to recover from the effect of the drug, even at the higher concentrations used. Cells appeared nearly confluent, indicating that they were able to proliferate, and very few apoptotic cells were observed. Furthermore, β_{II}-tubulin was able to reenter the nucleus of the cells, as appearance of nuclear fluorescence was seen in nearly all cells examined (Figure 2).

Discussion

The results shown here revealed that the antitumor drug vinblastine, when used at high concentrations, causes β_{II}-tubulin to exit the nucleus. The exit of β_{II}-tubulin from the nucleus may be due to vinblastine binding directly to nuclear tubulin, or, it may be an indirect result of the effect of this drug on cytoplasmic microtubules. It is possible that, in an effort to counteract the effect of vinblastine on microtubules, cells may translocate β_{II}-tubulin into the cytosol, where it may be needed more. However, our studies did not reveal an increase in cytosolic β_{II}-tubulin after treatment with vinblastine. This is most likely due to the fact that vinblastine causes microtubule depolymerization. In fact, vinblastine has been shown to inhibit the assembly of $\alpha\beta_{II}$ microtubules more than it does the assembly of $\alpha\beta_{III}$ and $\alpha\beta_{IV}$ microtubules [15]. It is also possible that vinblastine's effect is nonspecific, that it somehow damages the nuclear membrane or pore complex and thus allows various nuclear proteins to exit the nucleus. Interestingly, however, we have observed that taxol also causes β_{II} to exit from the nucleus [16]; this increases the likelihood that the effects of vinblastine as well as taxol are somehow mediated by interaction with tubulin.

The effect of vinblastine on nuclear tubulin was found to be reversible, since β_{II}-tubulin appeared to reenter the nucleus after the drug was removed and cells were able to recover. This is consistent with the findings by Jordan et al. [17], who reported that vinblastine is effluxed from cells after the drug is removed from the media. The mechanism by which vinblastine and other antitumor drugs trigger apoptosis remains unknown [18]. It is tempting to speculate that the effect of these drugs on nuclear tubulin may somehow be related to activation of the programmed cell death pathway. However, in our present studies, we have found that vinblastine causes cells to enter apoptosis regardless of whether they contain nuclear β_{II}-tubulin or not. This suggests that activation of the apoptotic pathway is independent of the presence of β_{II}-tubulin in the nucleus. The mechanism by which the β_{II} reenters the nucleus after removal of vinblastine is unknown. Our previous work, however, suggests that this requires that the cell go through a cycle of division and that the nucleus reforms around β_{II} rather than β_{II} actually penetrating the nucleus [19]. Other mechanisms for this reentry are certainly possible as well.

Our studies on nuclear tubulin have revealed that β_{II}-tubulin is present in the nuclei of a variety of cultured human cancer cells, while it is absent from the nuclei of some cultured human normal cells [8]. Although the rat kidney mesangial cells used in the present experiments are considered normal, they grow extremely fast in culture [20] and in this sense resemble cancerous cells. These findings have led us to believe that β_{II}-tubulin may be somehow involved in assisting rapid cell proliferation. By blocking microtubule dynamics, the anti-tubulin drug vinblastine inhibits cell proliferation [6]. Therefore, it is possible that the function of β_{II}-tubulin in the nucleus is inhibited by this drug. Vinblastine has been shown to affect cellular processes such as DNA and RNA synthesis [21,22]. The finding of β_{II}-tubulin in the nucleus, and the fact that vinblastine appears to cause this isotype to exit the nucleus, could explain the effect of this drug on these seemingly non-tubulin related functions. Further studies are necessary to determine whether nuclear β_{II}-tubulin is in fact involved in DNA and RNA synthesis.

The concentration of vinblastine used in these studies may be higher than clinically relevant. However, it is certainly possible that some cancer cells concentrate the drug to where the phenomena that we have observed occur in these cells. There is, however, another more subtle possibility. Vinblastine's effect on nuclear tubulin may be analogous to taxol's effect on cytoplasmic microtubules in a certain respect. Previous work has shown that although high concentrations of taxol induce microtubule polymerization and increase a cell's microtubule polymer mass, lower concentrations are sufficient to cause cell death or to arrest mitosis; the latter effects are associated with a more subtle effect of taxol, namely, its ability to inhibit microtubule dynamic instability [23–25]. At low concentrations, taxol can inhibit dynamic instability without affecting microtubule polymer mass [23–25]. Just as taxol has both a gross effect and a more subtle effect, vinblastine may also have

two effects: the gross effect may be the removal of tubulin from the nucleus that we report here; the subtle effect may involve an effect on the still unknown function of nuclear tubulin. It is conceivable that the binding of a small fraction of nuclear tubulin molecules to vinblastine may have a large effect on the properties of this population of tubulin. For example, if nuclear tubulin is a passenger protein whose only function occurs during mitosis, then vinblastine binding to a few of these molecules could "poison" that function.

In conclusion, our present studies on the effect of vinblastine on nuclear β_{II}-tubulin have revealed that anti-tubulin drugs may be useful tools to determine the exact role of β_{II}-tubulin in the nucleus. They also raise the possibility that these drugs may exert their anti-tumor activity through an interaction with nuclear tubulin.

Acknowledgments

This research was supported by grants CA26376 from the National Institutes of Health (RFL), AQ-0726 from the Welch Foundation (RFL), DAMD17-98-1-8246 from the U.S. Army Medical Research Program (RFL), and VA Merit Review to JIK. We are grateful to Phyllis Smith, Asok Banerjee, Pat Schwarz, Asish Chaudhuri, and Veena Prasad for their assistance.

References

1. Dustin P (ed.): Microtubules, 2nd edn. Springer-Verlag, Berlin, 1984
2. Wilson L, Jordan MA: Pharmacological probes of microtubule function. In: Hyams JS, Lloyd CW (eds) Microtubules. Wiley-Liss, New York, 1994, pp 59–83
3. Gerzon K: Dimeric catharanthus alkaloids. In: Cassady JM, Douros JD (eds). Anticancer Agents Based on Natural Product Models. Academic Press, New York, 1980, pp 271–317
4. Owellen RJ, Hartke CA, Dickerson RM, Haines FO: Inhibition of tubulin microtubule polymerization by drugs of the *Vinca* alkaloid class. Cancer Res 36: 3798–3802, 1976
5. Na GC, Timasheff SN: *In vitro* vinblastine-induced tubulin paracrystals. J Biol Chem 257: 10387–10391, 1982
6. Jordan MA, Thrower D, Wilson L: Mechanism of inhibition of cell proliferation by *Vinca* alkaloids. Cancer Res 51: 2212–2222, 1991
7. Walss C, Kreisberg JI, Ludueña RF: Presence of the β_{II} isotype of tubulin in the nuclei of cultured mesangial cells from rat kidney. Cell Motil Cytoskeleton 42: 274–284, 1999
8. Walss-Bass C, Xu K, David S, Fellous A, Ludueña RF: Occurrence of nuclear β_{II}-tubulin in cultured cells. Cell Tiss Res 2002 (in press).
9. Tsukidate K, Yamamoto K, Snyder JW, Farber JL: Microtubule antagonists activate programmed cell death (apoptosis) in cultured rat hepatocytes. Am J Pathol 143: 918–925, 1993
10. Ausiello DA, Kreisberg JI, Roy C, Karnovsky MJ: Contraction of cultured cells of apparent mesangial origin after stimulation with angiotensin II and arginine vasopressin. J Clin Invest 65: 754–760, 1980
11. Kreisberg JI, Venkatachalam MA, Patel PY: Cyclic AMP-associated shape change and its reversal by PGE_2. Kidney Int 25: 874–879, 1984
12. Kreisberg JI, Venkatachalam MA: Vasoactive agents affect mesangial cell adhesion. Am J Physiol 251: C505–C511, 1986
13. Banerjee A, Roach MC, Wall KA, Lopata MA, Cleveland DW, Ludueña RF: A monoclonal antibody against the type II isotype of β-tubulin. Preparation of isotypically altered tubulin. J Biol Chem 263: 3029–3034, 1988
14. Roach MC, Boucher VL, Walss C, Ravdin P, Ludueña RF: Preparation of a monoclonal antibody specific for the class I isotype of β-tubulin: the β isotypes of tubulin differ in their cellular distributions within human tissues. Cell Motil Cytoskeleton 39: 273–285, 1998
15. Khan IA, Ludueña RF: Effect of vinblastine on the assembly of isotypically pure tubulins from bovine brain. Mol Biol Cell 6: 30a, 1995
16. Xu K, Ludueña RF: Characterization of nuclear β_{II}-tubulin in tumor cells: a possible novel target for taxol. Cell Motil Cytoskeleton, 2002 (in press)
17. Jordan MA, Wendell K, Gardiner D, Derry WB, Copp H, Wilson L: Mitotic block induced in HeLa cells by low concentrations of paclitaxel (taxol) results in abnormal mitotic exit and apoptotic cell death. Cancer Res 56: 816–825, 1996
18. Sorger PK, Dobles M, Tournebize R, Hyman AA: Coupling cell division and cell death to microtubule dynamics. Curr Opin Cell Biol 9: 807–814, 1997
19. Walss-Bass C, Kreisberg JI, Ludueña RF: Mechanism of localization of β_{II}-tubulin in the nuclei of cultured rat kidney mesangial cells. Cell Motil Cytoskeleton 49: 208–217, 2001
20. Floege J, Topley N, Hoppe J, Barrett TB, Resch K: Mitogenic effect of platelet-derived growth factor in human glomerular mesangial cells: modulation and/or suppression by inflammatory cytokines. Clin Exp Immunol 86: 334–341, 1991
21. Creasey WA: Modifications in biochemical pathways produced by the Vinca alkaloids. Cancer Chemother Res 52: 501–507, 1968
22. Bernstam VA, Gray RH, Bernstein IA: Effect of microtubule-disrupting drugs on protein and RNA synthesis in *Physarum polycephalum* Amoebae. Arch Microbiol 128: 34–40, 1980
23. Jordan MA, Toso RJ, Thrower D, Wilson L: Mechanism of mitotic block and inhibition of cell proliferation by taxol at low concentrations. Proc Nat Acad Sci USA 90: 9552–9556, 1993
24. Derry WB, Wilson L, Jordan MA: Low potency of taxol at microtubule minus ends: implications for its antimitotic and therapeutic mechanism. Cancer Res 58: 1177–1184, 1998
25. Yvon AM, Wadsworth P, Jordan MA: Taxol suppresses dynamics of individual microtubules in living human tumor cells. Mol Biol Cell 10: 947–959, 1999

Address for offprints: Richard F. Ludueña, Department of Biochemistry, University of Texas Health Science Center, 7703 Floyd Curl Drive, San Antonio, TX 78229-3900, USA; Tel.: 210-5673732; Fax: 210-5676595; E-mail: luduena@uthscsa.edu

peritoneum followed by serial intraperitoneal administration of 0.63 mg/kg, a dose 4-fold lower than the optimal therapeutic dose. (Etievant, C. et al., Cancer Chemother Pharmacol (2001) 48: 62-70). Although, p-glycoprotein was overexpressed in these tumors, the magnitude of resistance to two vinca alkaloids, vinorelbine and vinflunine, was very different. The drug target for antimitotics is tubulin, the major protein of mitotic spindles. Tubulin isotypes levels differ across normal tissues and it has been hypothesized that differences in tubulin isotype levels may contribute to drug resistance. We determined the IC50 values for the P388 parental cells and the vinorelbine-resistant cell line using four antimitotics: vinblastine, vinorelbine, vinflunine and taxol. The IC50 values for resistant cells were 19-and 16-fold higher compared to the parental cells for both vinblastine and vinorelbine. For taxol and vinflunine there were 6- and 4- fold differences in IC50 values compared to parental cells. Because β-tubulin isotype levels may be implicated in antimitotic drug resistance, we used quantitative Western blotting with chemiluminescence to measure the levels of β-tubulin classes I&IV, II and III. We found no differences in tubulin isotype protein levels: β-tubulin classes I&IV 67 % (+/- 1) and 65% (+/- 5) or β-tubulin class II 33% (+/- 1) and 35% (+/- 5) for the parental and resistant cells. β-tubulin class III was less than 1%. In summary, β-tubulin isotype levels do not explain the differential sensitivity of this drug resistant cell line to vinca alkaloids. The mechanisms for drug resistance are yet to be determined. (supported by NIH grant: NR04780, S.L. and J.J.C.)

2605

Acquired β-Tubulin Mutations Affecting Microtubule Stability and Drug Binding

N. Verrills,[1,2] C. Flemming,[1] M. Liu,[1] M. Ivery,[3] M. D. Norris,[1] M. Haber,[1] M. Kavallaris[1] ; [1] Children's Cancer Institute Australia for Medical Research, Sydney, Australia, [2] Australian Proteome Analysis Facility, Sydney, Australia, [3] Dept. Pharmacy, University of Sydney, Sydney, Australia

Antimitotic agents that target tubulin are important in the treatment of a wide range of human cancers. Epothilones were the first novel structural class of compounds to be described since the discovery of paclitaxel, that bind to β-tubulin on the a/β-tubulin dimer and stabilise microtubules (mts). Preclinical evaluation of an epothilone analogue desoxyepothilone B (dEpoB), demonstrated promising *in vivo* antitumour activity over other mt stabilizing agents. To understand the mechanism of action and resistance to this novel anti-mt agent we have selected a series of dEpoB resistant leukaemia sub-lines that display increasing levels of resistance to the selecting drug (21-307-fold). The dEpoB cells are cross-resistant to paclitaxel and hypersensitive to a number of mt destabilizing gagents. Gene and protein sequencing of class I β-tubulin in these cells revealed a novel mutation located in helix 7 in the low-level resistant cells that resides in the drug-binding site on β-tubulin and affects microtubule stability. Despite reduced intrinsic levels of polymerised tubulin in these cells, they still retain the ability to undergo drug-induced tubulin polymerisation. The dEpoB cells selected for resistance to higher levels of drug acquired a second mutation situated in the M-loop of β-tubulin in a region involved in lateral contacts of tubulin protofilaments and hence is likely to also influence mt stability. Indeed, these cells have decreased levels of polymerised tubulin but unlike the low-level dEpoB resistant cells, the mts in these cells fail to undergo drug induced tubulin polymerisation. This is the first report of dEpoB-resistant cells with mutations in β-tubulin associated with decreased mt stability and reduced drug-binding. β-tubulin mutations identified in the resistant cell lines provide novel insights into mt dynamics and drug-target interactions.

2606

Are Earlier Predicted Sites Of Different Plant Tubulins Involved In Interaction With Dinitroanilines?

Y. B. Blume,[1] A. Y. Nyporko,[1] A. I. Yemets,[1] W. V. Baird[2] ; [1] Department of Cell Biology and Biotechnology, Institute of Cell Biology and Genetic Engineering, Kiev, Ukraine, [2] Department of Horticulture, Clemson University, Clemson, SC

The resistance of goosegrass (*Eleusine indica*) to dinitroanilines (DNH) is a result of missense mutation at position 239 (Thr→Ile) of α1-tubulin sequence (Antony et al., 1998; Cronin et al., 1993; Yamamoto et al., 1998). The presence of positively charged cavern on α-tubulin surface from sensitive biotype of *E. indica* was found earlier (Nyporko et al., 2000). This cavern is localized on interdimeric contact area close to mutation site to be involved in interaction with nitrogroups of DNHs and phosphoroamidates. The computer modelling established the absence of this cavity in mutated α-tubulin (Blume at al., 2002). It was postulated that respective substitutions in homologous positions of β- and γ-tubulin sequences (Thr-237 and Thr-240 respectively) can lead also to DNH-resistance (Cronin et al., 1993). To verify this consclusion the comparative analysis of the 3-D models for plant β- (*E. indica*) and γ-(*Arabidopsis thaliana*) tubulins was carried out. The results show clearly that the caverns of assumed interaction on the surfaces of β- and γ-tubulins are absent, when threonine residues was placed in the positions 237 or 240, respectively (in contrary to non-mutated α-tubulin). Thr→Ile substitution at these positions do not change the molecular surface of both tubulins, and it has no functional significance as a consequence. Thus, the phenomenon of plant α-tubulin resistance to DNH can not extrapolate directly onto another tubulins by the finding of respective conservative homologous amino acid motifs. Specific spatial contacts of amino acid residues from different regions of tubulin sequences exposed closely one to other can play more important role in this phenomenon. Therefore, earlier predicted sites of plant β- and γ-tubulin molecules to be involved in interaction with DNHs actually can not be considered as specific targets for these compounds.

2607

Tubulin - Cryptophycin-1 Complexes Are Very Stable, Homogeneous Rings of 8 Tubulin Dimers, Each with Two Unequal Points of Curvature

H. Boukari,[1] N. R. Watts,[2] P. Schuck,[3] R. Nossal,[1] D. L. Sackett[1] ; [1] Limb / nichd, NIH, Bethesda, MD, [2] Niams, NIH, Bethesda, MD, [3] OD, NIH, Bethesda, MD

Cryptophycin-1 (Cr1) is a highly cytotoxic cyclic depsipeptide whose antimitotic action is due to binding at the vinca domain, of one Cr1 per tubulin heterodimer. The IC_{50} in cell culture is in the low picomolar range, indicating tight binding. The tubulin-Cr1 complex is a ring of about 800 kDa by several methods. The rings are highly uniform by sedimentation velocity. Cryoelectron microscopy reveals the rings to have a diameter of 24 nm, and to be composed of 8 dimers, with a 13° intra-dimer bend and a 32° inter-dimer bend. Fluorescence correlation spectroscopy (FCS) of rhodamine-labeled tubulin-Cr1 rings confirms the ring size and demonstrates that the rings do not interact in static solution. FCS also shows that the rings are very stable, and do not dissociate even when diluted to 1 nM tubulin, or when stored for >24 hr at room temperature or 4°C. Other antimitotic peptides exhibit lesser stabilities to dilution by FCS. The stable tight binding of Cr1 to tubulin demonstrated by the ring properties may provide a partial explanation for its potent cytotoxicity.

2608

Generation of A Monoclonal Antibody to the β_V Isotype of Tubulin

A. Banerjee,[1] P. Joe,[1] A. Lazzell,[2] V. Prasad,[1] R. F. Luduena[1] ; [1] Department of Biochemistry, University of Texas Health Science Center at San Antonio, San Antonio, TX, [2] Department of Microbiology, University of Texas Health Science Center at San Antonio, San Antonio, TX

Tubulin, the major constituent of microtubules, exists as various isotypes whose functions *in vivo* are not very clear. In mammalian cells, both α– and β–tubulin occur as 7-8 different genetic variants. We have previously created monoclonal antibodies (MAbs) specific for the β_I, β_{II}, β_{III}, and β_{IV} isotypes and used these as tools and probes for isotype purification and distribution. We have found clear differences among the isotypes in drug-binding, assembly, and conformation as well as in the dynamics of microtubules formed by individual isotypes. One vertebrate β–tubulin isotype, β_V, has a unique C-terminal sequence (EEEINE) and is expressed in low amounts in various tissues. β_V shares with β_{III} a unique configuration of cysteine residues, lacking the highly reactive C239 found in β_I, β_{II} and β_{IV}, and instead containing the unusual C124. In an effort to understand the function of β_V tubulin *in vivo* we have raised a MAb by immunizing mice with the C-terminal peptide CEEINE. One MAb, SHM.12G11, was found to bind specifically to the C-terminal peptide EEEINE; it does not interact with the C-terminal peptides of β_I, β_{II}, β_{III}, or β_{IV}. Immunofluorescence studies are under way to localize this tubulin isotype in cultured cells. In another approach to understand the functions of the β_V and β_{III} isotypes, we are preparing the C124S and S239C mutants of β_{III}. (Supported by grants from the Welch Foundation (AQ-0726) and the US Army Breast Cancer Research Program IDEA Awards DAMD17-01-10411 to RFL and DAMD17-98-1-8244 to AB).

2609

Mutations in α- and β-tubulin genes affect spindle orientation in the *C. elegans* zygote

J. B. Phillips,[1] G. Ellis,[1] R. Lyczak,[2] B. Bowerman[1] ; [1] Institute of Molecular Biology, University of Oregon, Eugene, OR, [2] Department of Biology, Ursinus College, Collegeville, PA

We have isolated two embryonic lethal mutants, *or346ts* and *or362ts*, in which microtubule (MT) dependent events in early embryonic cells are defective. Abnormal orientation of the first mitotic spindle in these mutants leads to mispositioned cleavage furrows and a subsequent disruption of A-P polarity. Both mutants are 100% embryonic lethal at the restrictive temperature. The *or346ts* mutation is dominant, as embryos from heterozygous and homozygous parents exhibit nearly identical spindle defects and embryonic lethality. We identified *or346ts* as an allele of the α-tubulin *tba-1*, and *or362ts* as an allele of the β-tubulin *tbb-2*. Both mutant alleles contain missense mutations. To more thoroughly examine the spindle phenotype in these mutant embryos, we obtained data using immunofluorescence and GFP lines, which revealed well organized and functional spindles, aside from their abnormal orientation. Immunofluorescence and Western Blot analysis with an antibody raised against TBB-2 shows that the protein is present but reduced in *tbb-2(or362ts)*. We also obtained a deletion allele, *tbb-2(gk129)*, from the *C. elegans* gene knockout consortium. TBB-2 protein is undetectable in the mitotic spindle of *tbb-2(gk129)* embryos, and although *tbb-2(gk129)* exhibits temperature dependent embryonic lethality and spindle stability defects, this allele exhibits normal spindle orientation as compared to the missense mutation, and is homozygous viable at all temperatures. Moreover, we observe that using RNA-mediated interference to specifically disrupt *tba-1* in *tba-1(or346ts)* worms results in normal spindle orientation and rescue of the embryonic lethality. We conclude that partially

redundant isotypes of α- and β-tubulin are expressed in the early embryo, and that expression of aberrant tubulins is more deleterious than total absence of the proteins. We are currently examining astral MT contact with the cell cortex in mutant and wild-type embryos to further assay MT stability.

2610

Generation of beta tubulin cDNA Constructs for Mammalian expression: Overexpression of beta III Increases Resistance to Colchicine and Paclitaxel

A. Banerjee,[1] S. Mukherjee,[1] R. F. Luduena,[1] G. G. Choudhury[2] ; [1] Department of Biochemistry, the University of Texas Health Science Center at San Antonio, San Antonio, TX, [2] Division of Nephrology, Department of Medicine, the University of Texas Health Science Center at San Antonio, San Antonio, TX

Tubulin, the dimeric protein of microtubules, occurs as multiple isoforms which have functional differences. Tubulin isoforms have been found to differ in the assembly properties, conformation, stability as well as their interaction with antitumor drugs. Analysis of tubulin expression in paclitaxel resistant cells showed that β_{III} and β_{IVb} are overexpressed in the drug-resistant cells. In an effort to study whether the expression of a specific tubulin isoform alters the drug sensitivity we have generated full length cDNA constructs for β_{I}, β_{II}, β_{III} and β_{IVb} in pcDNA3.1 V5-His topo vector. Transient transfection of human breast and ovarian cancer cells showed that overexpression of β_{III} but not β_{I}, β_{II} or β_{IVb} increases resistance to paclitaxel. Random mutagenesis of β_{III} are under way to identify the binding domains for various antimtotic drugs. (Supported by grants from the Welch Foundation (AQ-0726) and the US Army Breast Cancer Research Program IDEA Awards DAMD17-01-10411 to RFL and DAMD17-98-1-8244 to AB).

2611

Interaction of vaccinia virus F12L protein with components of microtubules

B. J. Murphy, D.C. J. Carpentier, G. L. Smith; Department of Virology, Wright-Fleming Institute, Imperial College, London , UK

Vaccinia virus (VV) is a large, complex, DNA virus that replicates in the cytoplasm. During morphogenesis VV produces four types of virion: intracellular mature virus (IMV), intracellular enveloped virus (IEV), cell associated enveloped virus (CEV) and extracellular enveloped virus (EEV). Genes A33R, A34R, A56R, B5R and F13L encode CEV/EEV-specific proteins, while A36R and F12L are IEV-specific proteins. Microtubules are used (i) to transport IMV away from the virus factories to the site of wrapping by intracellular membranes to form IEV and (ii) to transport IEV from the site of wrapping to the cell surface[1]. Actin tails drive CEV particles away from the cell.the role of the VV F12L protein in IEV transport is being investigated. This protein is conserved in chordopoxviruses but shows no other match against public databases. A virus deletion mutant (vΔF12L) lacking F12L was highly attenuated *in vivo*[2]. In infected cells virus morphogenesis was blocked after IEV formation, such that the production of CEV and EEV were reduced and actin tails were not formed. Confocal microscopy showed that F12L co-localises with IEV particles and microtubules[3]. In addition, during infection the heavy and light-chains of kinesin become redistributed to the cell periphery and co-localise with F12L. Co-immunoprecipitation experiments showed an association of F12L with α- and β-tubulin. The roles of specific domains of the F12L protein are being investigated by expression of mutated forms of F12L within cells infected with vΔF12L.**Refs**[1]Hollinshead et al. (2001). J. Cell Biol. **154**, 389-402.[2]Zhang et al. (2000). J. Virol. **74**, 11663-11670.[3]van Eijl et al. (2002). J. Gen. Virol. **83,** 195-207.

2612

Noscapine derivatives as potent microtubule-interfering agents that perturb mitosis and induce apoptosis

J. Zhou,[1,2] K. Gupta,[3] S. Aggarwal,[4] R. Aneja,[5] R. Chandra,[4] D. Panda,[3] H. C. Joshi[1] ; [1] Department of Cell Biology, Emory University School of Medicine, Atlanta, GA, [2] Graduate Program in Biochem., Cell &Dev. Biol., Graduate Division of Biol. & Biomed. Sci., Emory University, Atlanta, GA, [3] Bhupat and Jyoti Mehta School of Biosciences and Bioengineering, Indian Institute of Technology, Mumbai, India, [4] Dr. B. R. Ambedkar Center for Biomedical Research, University of Delhi, Delhi, India, [5] Department of Chemistry, University of Delhi, Delhi, India

Noscapine has recently been identified as a microtubule interacting agent that binds to tubulin, alters microtubule dynamics, and arrests mitosis. In addition, it causes apoptosis in many mammalian cell types and exhibits potent antitumor activity. We have now selectively designed and synthesized a series of derivatives of noscapine and evaluated their biological properties. These noscapine derivatives exhibit strikingly different tubulin binding activity and affect tubulin polymerization to different degrees. Two of them arrest mitosis and cause apoptosis with much higher efficiency than noscapine in a wide spectrum of human cancer cells. These findings thus indicate a great potential for the use of these two noscapine derivatives as chemotherapeutic agents for the treatment of human cancers.

2613

Association of Brain Gamma-tubulins with Tubulin Dimers

P. Draber,[1] V. Sulimenko,[1] T. Sulimenko,[1] L. Macurek,[1] E. Unger,[2] E. Draberova[1] ; [1] Institute of Molecular Genetics, Academy of Sciences of the Czech Republic, Prague 4, Czech Republic, [2] Institute of Molecular Biotechnology, Jena, Germany

γ-Tubulin is necessary for nucleation and polar orientation of microtubules *in vivo*. The molecular mechanism of microtubule nucleation by γ-tubulin and the regulation of this process are not fully understood. Here we show that there are two γ-tubulin forms in brain that are present in complexes of various sizes. Large complexes tend to dissociate in the presence of high-salt concentration. Both γ-tubulins copolymerized with tubulin dimers and multiple γ-tubulin bands were identified in microtubule protein preparations under conditions of non-denaturing electrophoresis. Immunoprecipitation experiments with monoclonal antibodies against γ-tubulin and α-tubulin revealed interactions of both γ-tubulin forms with tubulin dimers irrespective of the size of complexes. We suggest that besides small and large γ-tubulin complexes, other molecular γ-tubulin form(s) exist in brain extracts. Two-dimensional electrophoresis revealed multiple charge variants of γ-tubulin both in brain extracts and in microtubule protein preparations. Post-translational modification(s) of γ-tubulins might therefore play an important role in the regulation of microtubule nucleation in neuronal cells. Supported by MSMT CR project LN00A026 and GA AVCR grant A5052004.

2614

γ-Tubulin Forms Complex with Gβγ in Centrosomes, Nuclear Fraction, and Assembling Microtubules in PC12 Cells

S. Roychowdhury,[1] L. Martinez,[1] J. Popova,[2] M. M. Rasenick[2] ; [1] Biological Sciences, University of Texas at El Paso, El Paso, TX, [2] Physiology & Biophysics, University of Illinois at Chicago, Chicago, IL

γ-tubulin, a member of tubulin superfamily, is an integral centrosome protein that plays a central role in cell division through its ability to nucleate and organize microtubules in mitotic spindles. Recent results demonstrate that γ-tubulin is also present in the cytoplasm and undergoes dynamic exchange with centrosome-associated γ-tubulin. Previously, we have shown that βγ subunit of G proteins (Gβγ) and γ-tubulin form complexes and colocalize in centrosomes of NIH3T3 and PC12 cells. Although heterotrimeric G proteins are known to transduce signals across the membrane, they also show nuclear localization and associate with the cytoskeleton. Thus, heterotrimeric G proteins may also play a role in cell growth and differentiation. Furthermore, both Gα and Gβγ have been shown to regulate microtubule assembly *in vitro*. This study suggests that the association between γ-tubulin and Gβγ is significantly higher (~10 fold) in nuclear than cytoskeletal, membrane, or soluble fraction of PC12 cells. αβ-tubulin also appears to be a component of this γ-tubulin/Gβγ complex. To confirm the association between γ-tubulin and Gβγ in centrosomes, PC12 cells were fractionated and centrosomes were isolated by sucrose gradient centrifugation. Immunoblotting with anti-Gβ, anti-γ-tubulin, and anti-β-tubulin antibodies revealed co-sedimentation of Gβ with centrosome-associated γ-tubulin and β-tubulin. Microtubule stabilization with taxol increased γ-tubulin and Gβγ association with the cytoskeletal fraction. This suggested possible involvement of γ-tubulin/Gβγ complexes in microtubule assembly. The preferential association of γ-tubulin, Gβγ, and tubulin in centrosomes as well as nuclear fractions of PC12 cells suggests that formation of such complexes may be important for their translocation to centrosomes and subsequent spindle formation during cell division.

2615

Characterization of the human γ-tubulin complex

U. K. Patel, S. M. Murphy, A. M. Preble, T. Stearns; Biological Sciences, Stanford University, Stanford, CA

γ-Tubulin plays a key role in microtubule nucleation and organization in all eukaryotic cells. In animal cells, γ-tubulin is part of a large multi-protein complex that is required for microtubule nucleation at the centrosome. To identify the components of this complex and investigate the mechanism by which it nucleates microtubule polymerization, we purified and characterized the human γ-tubulin complex, and identified its subunits. The human γ-tubulin complex is a ring of approximately 25 nm, has a subunit structure similar to that reported for γ-tubulin complexes from other species, and is able to nucleate microtubule polymerization *in vitro*. Mass spectrometry analysis of the human γ-tubulin complex components confirmed the presence of four previously identified components: γ-tubulin, GCP2, GCP3, and GCP4 and led to the identification of two new components, GCP5 and GCP6. GCP5 and GCP6, like other components of the γ-tubulin complex, localize to the centrosome and associate with microtubules, suggesting that the entire γ-tubulin complex takes part in both of these interactions. Stoichiometry experiments revealed that there is a single copy of GCP5 and multiple copies of γ-tubulin, GCP2, GCP3 and GCP4 within the γ-tubulin complex. Recently we have begun to investigate the role of post-translational modification in regulating the two main activities of the γ-tubulin complex: localization to the centrosome and nucleation of microtubule polymerization. Two-dimensional gel electrophoresis of cytoplasmic γ-tubulin reveals multiple species, and preliminary results show that this profile is altered upon treatment with phosphatase. γ-Tubulin immunoprecipitated from cells reacts with anti-phosphotyrosine antibodies indicating that mammalian γ-tubulin is tyrosine – phosphorylated, as it is in *S. cerevisiae* (Vogel *et al.*, 2001). Phosphorylation may play an important role in both the structure and the function of the γ-tubulin complex.

APPENDIX 7

Fig 1 Effect of Rhizoxin on Cellular microtubules

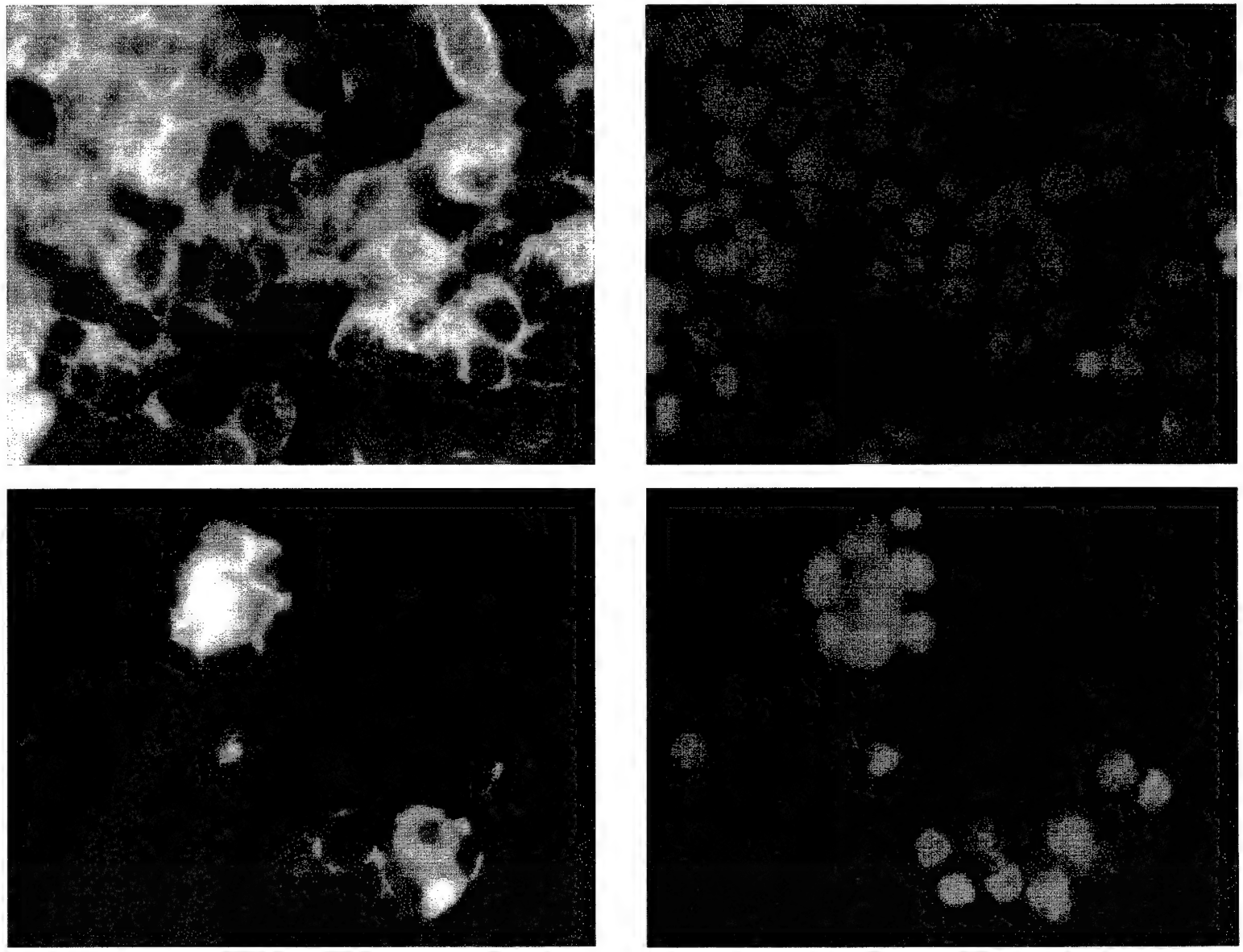

Fig 2 Effect of Rhizoxin on Apoptosis by DNA Fragmentation

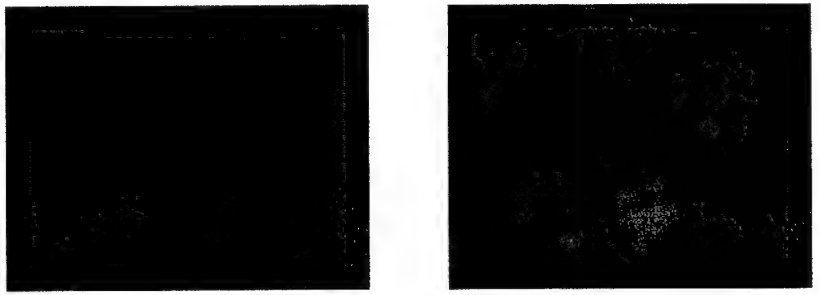

0 nM Rhizoxin

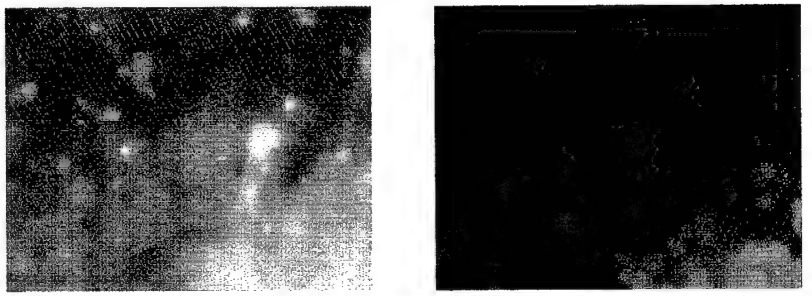

20 nM Rhizoxin

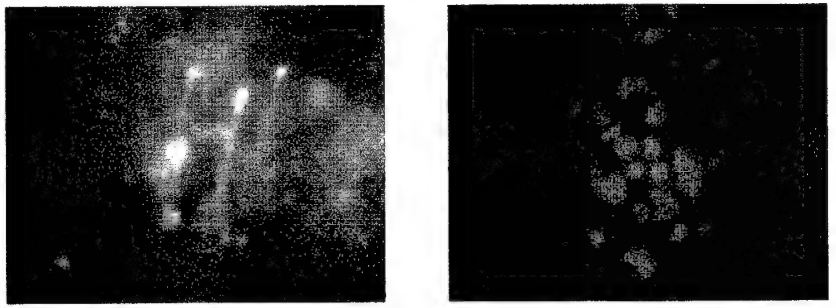

5nMRhizoxin

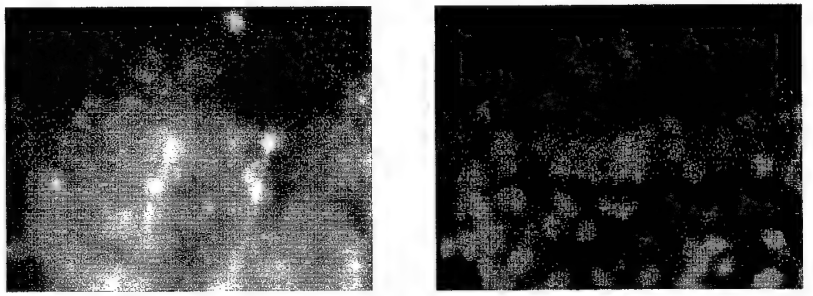

50 nM Rhizoxin

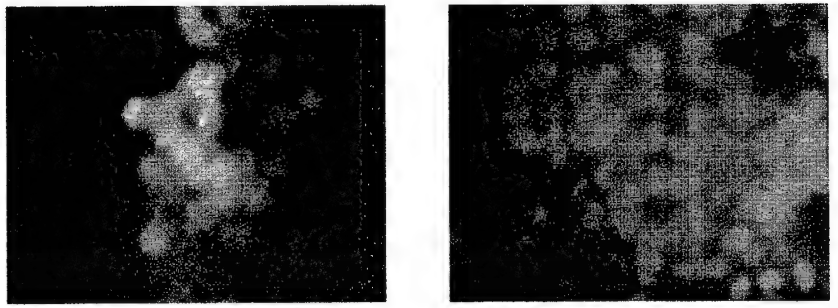

10 nMRhizoxin

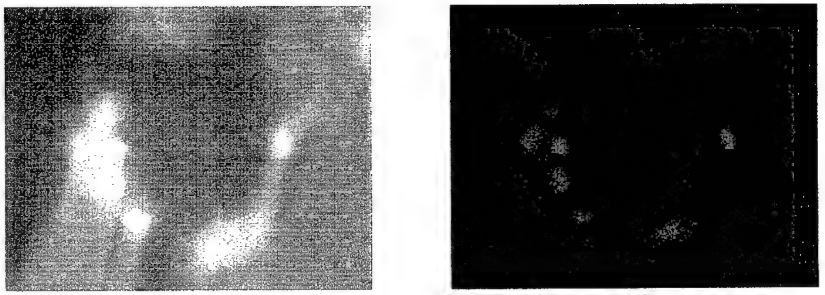

100 nM Rhizoxin

Fragmented DNA DAPI

Fragmented DNA DAPI

Fig 3 Effect of Rhizoxin on Apoptosis Caspase-3 Release

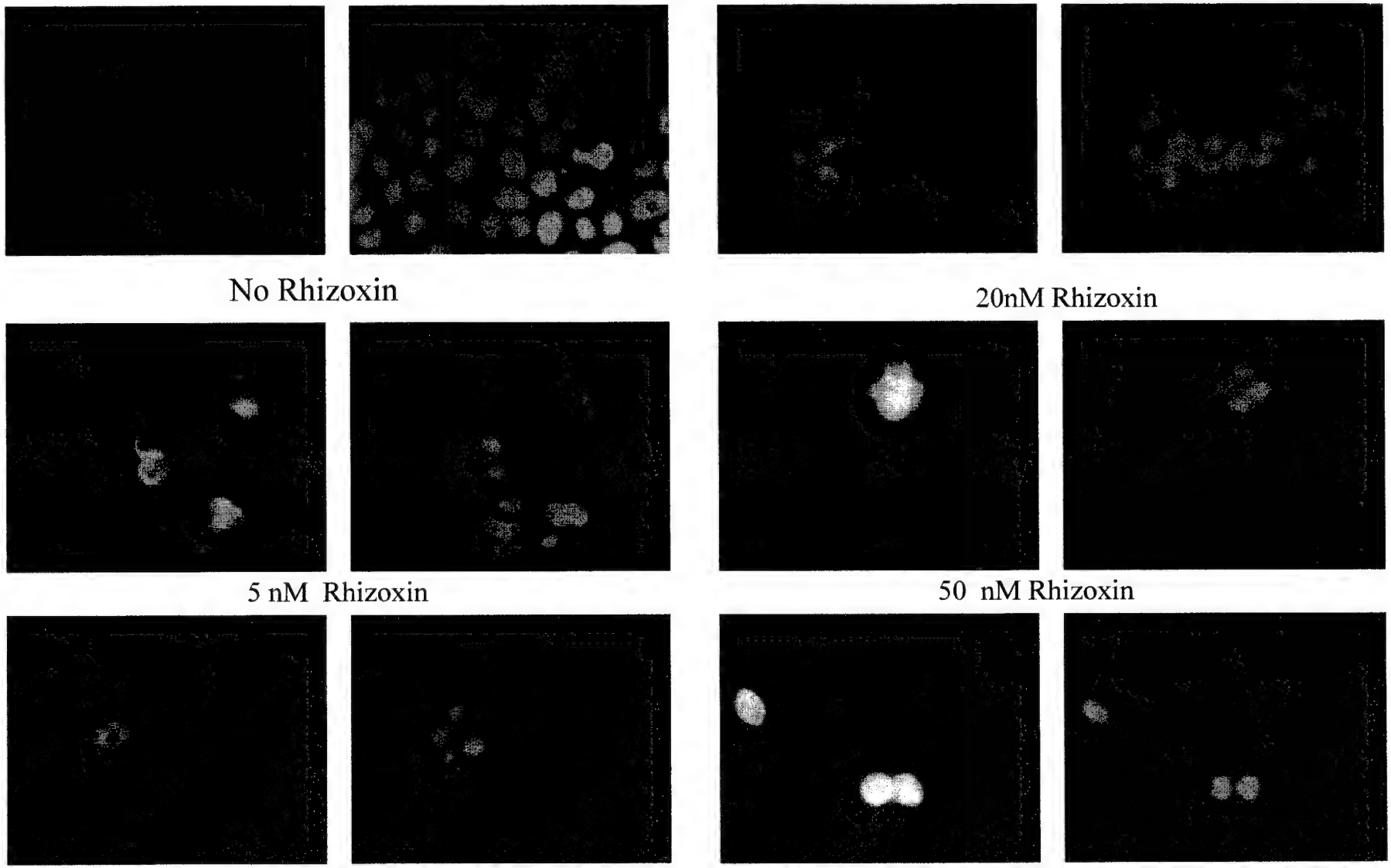

Figure 4

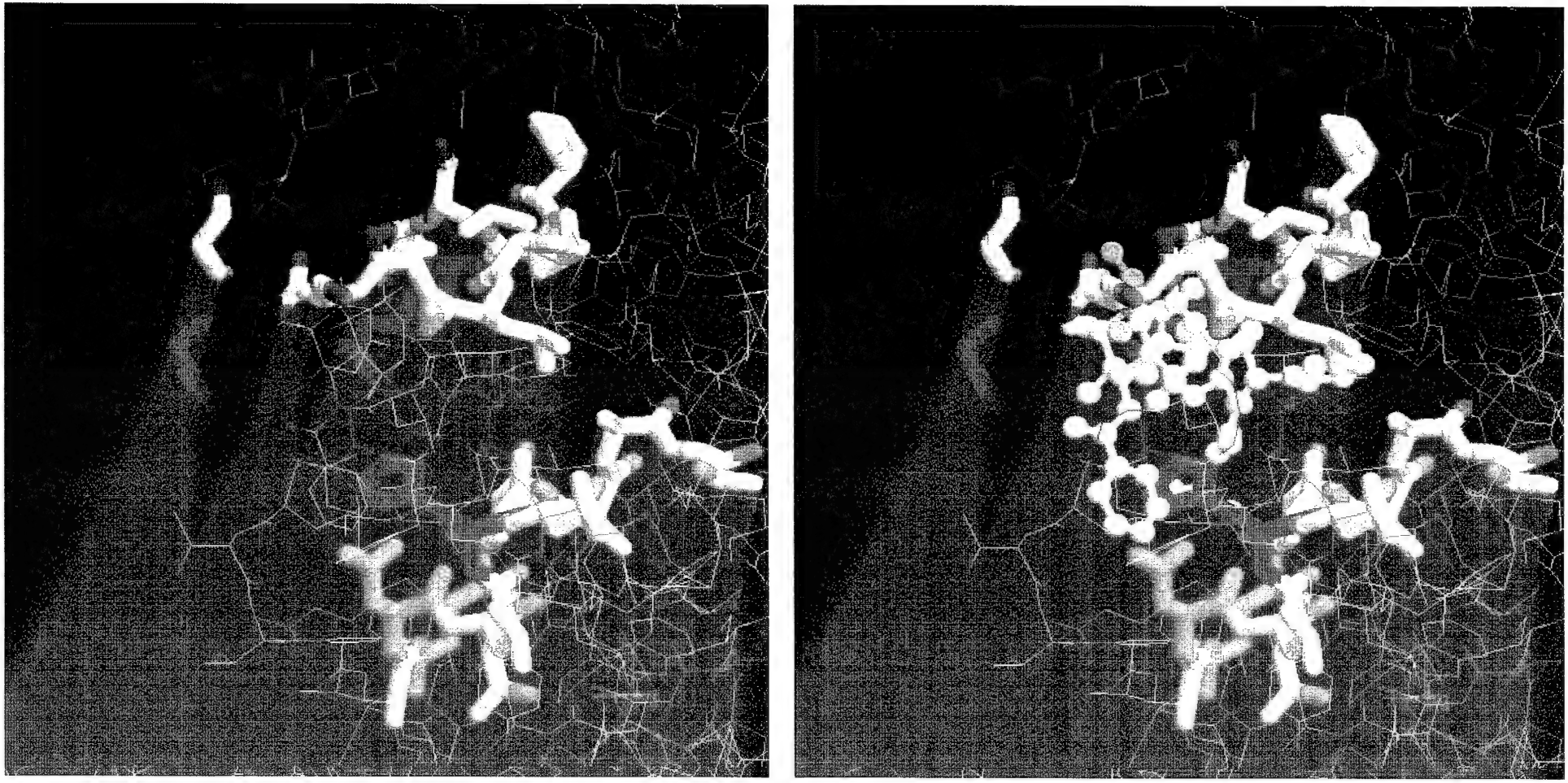

Taxol Binding Site in Bovine Brain Tubulin
with (right) and without taxol (left)
Acidic residues (red); basic residues (blue);taxol (green)

Figure 5

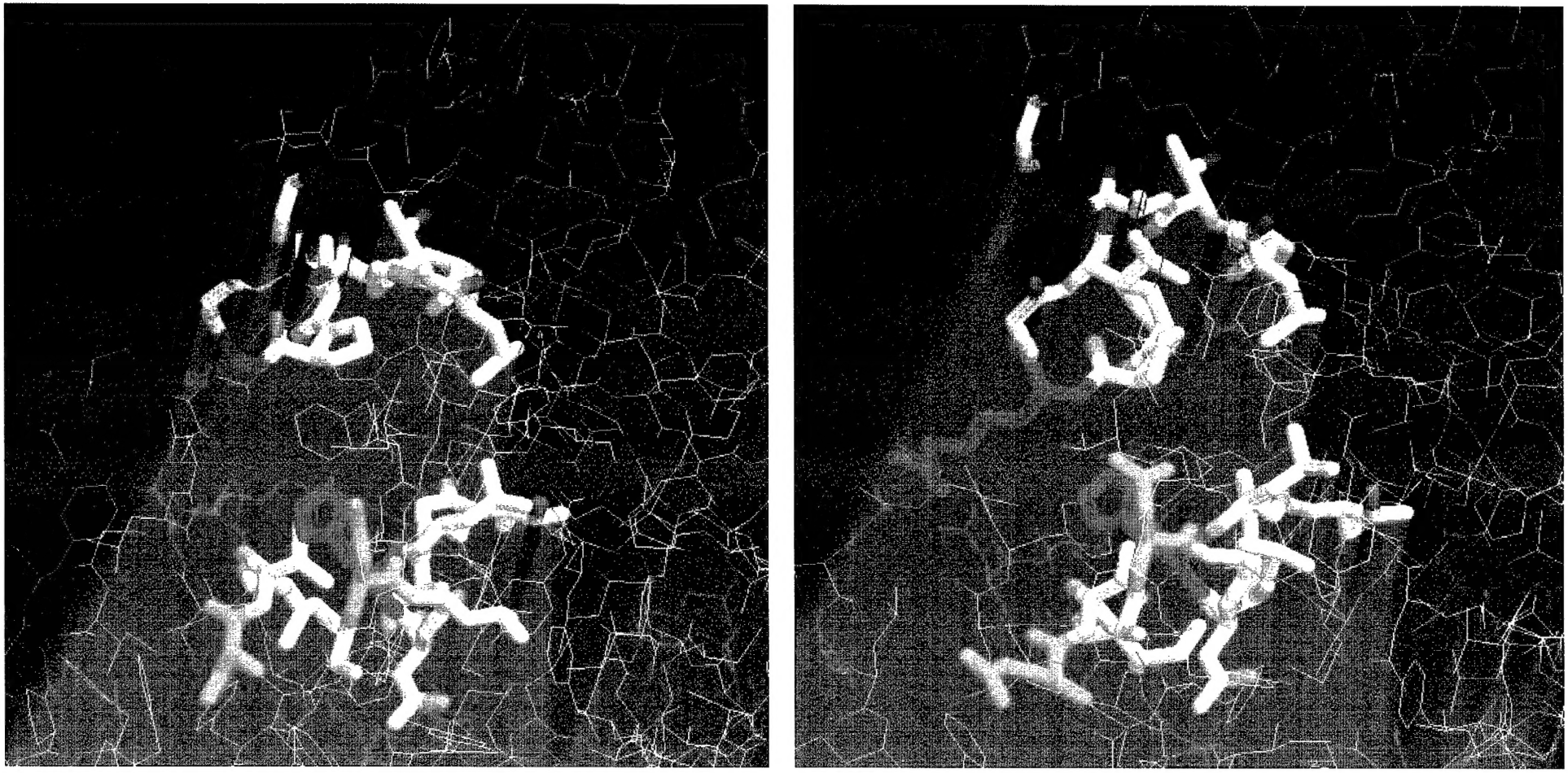

βI βIII

Taxol Binding Site

Acidic residues (red); basic residues (blue)

Figure 6

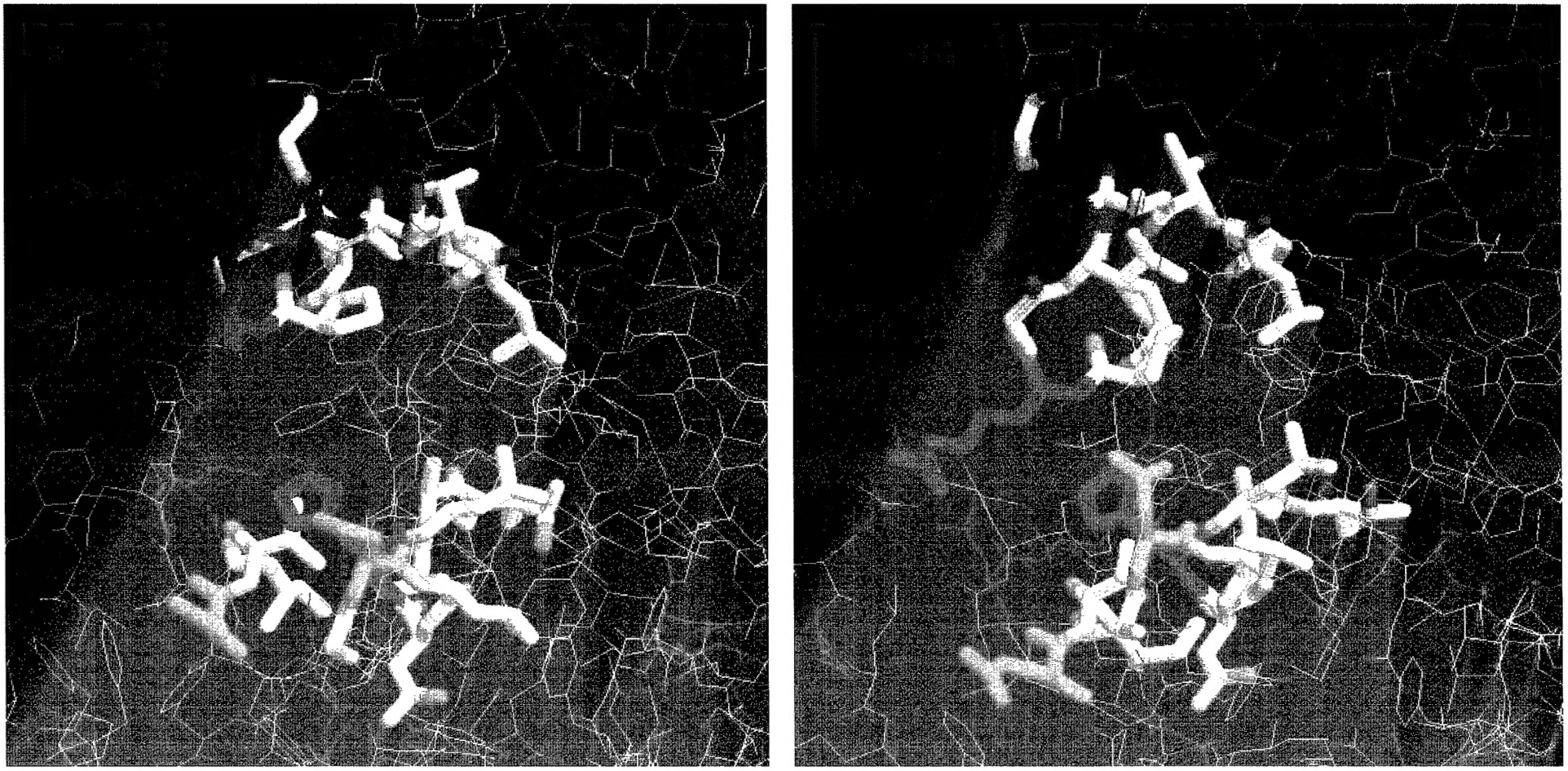

βIVb βIII

Taxol Binding Site

Acidic residues (red); basic residues (blue)

Figure 7

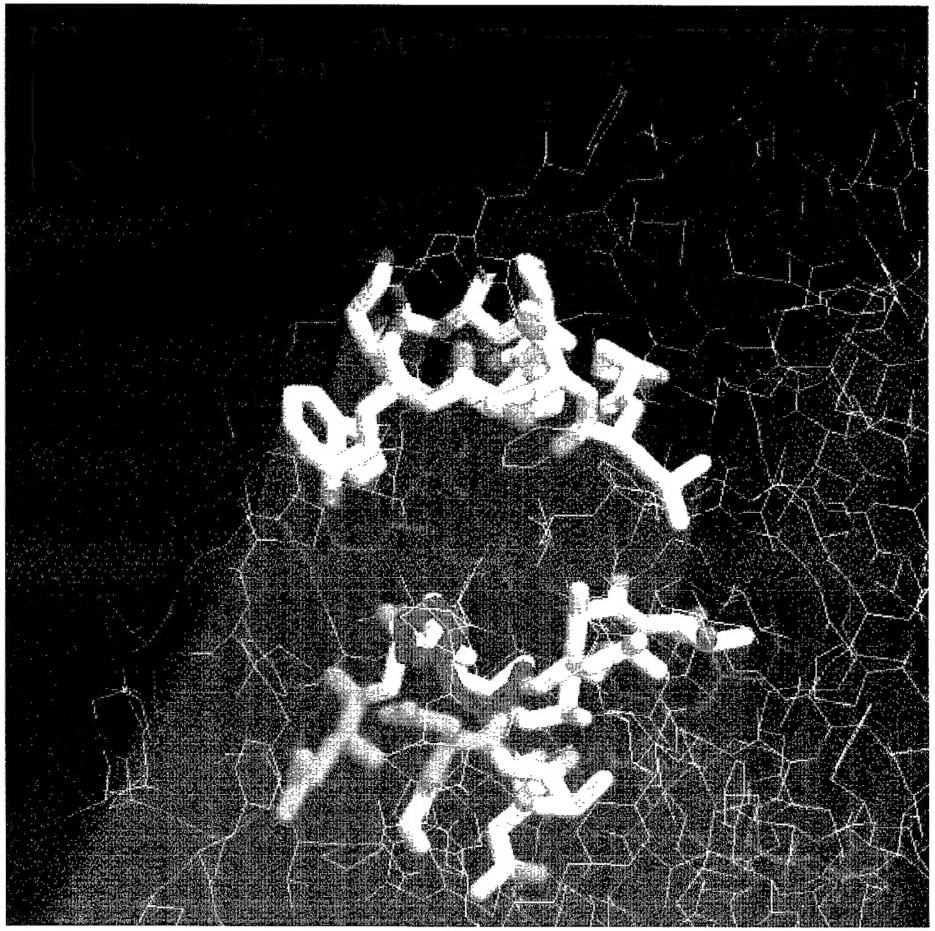

βVII

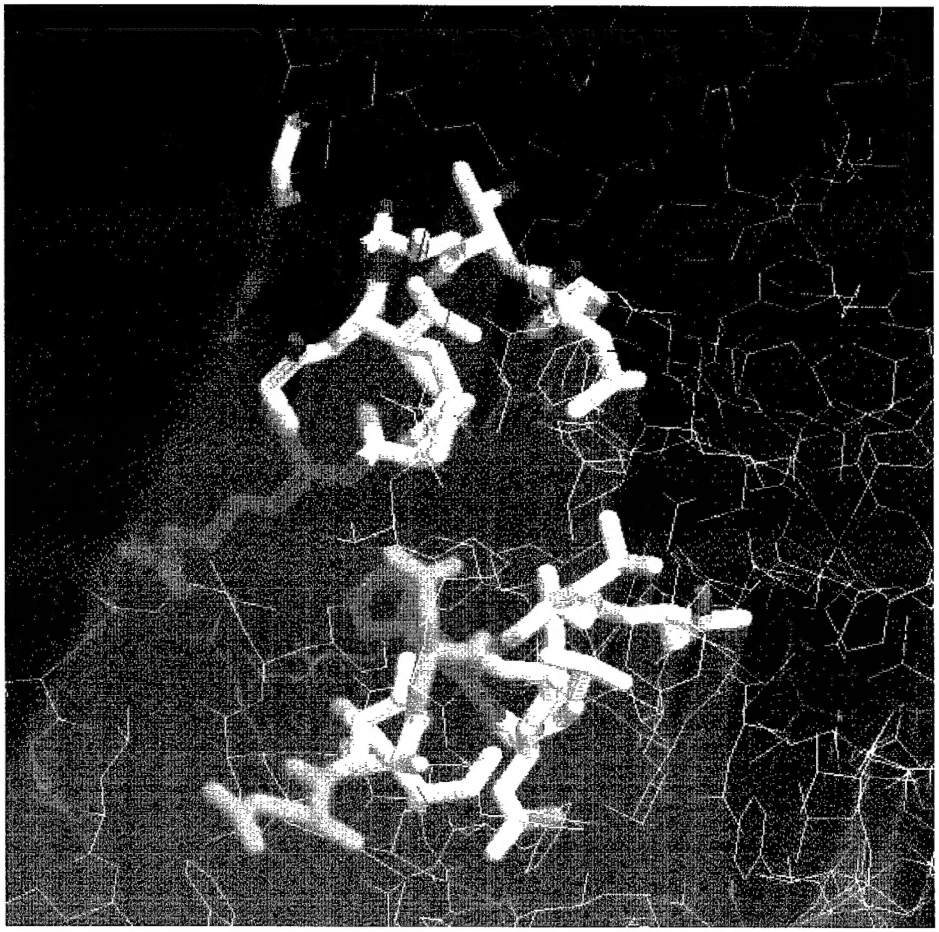

βIII

Taxol Binding Site

Acidic residues (red); basic residues (blue)

Figure 8

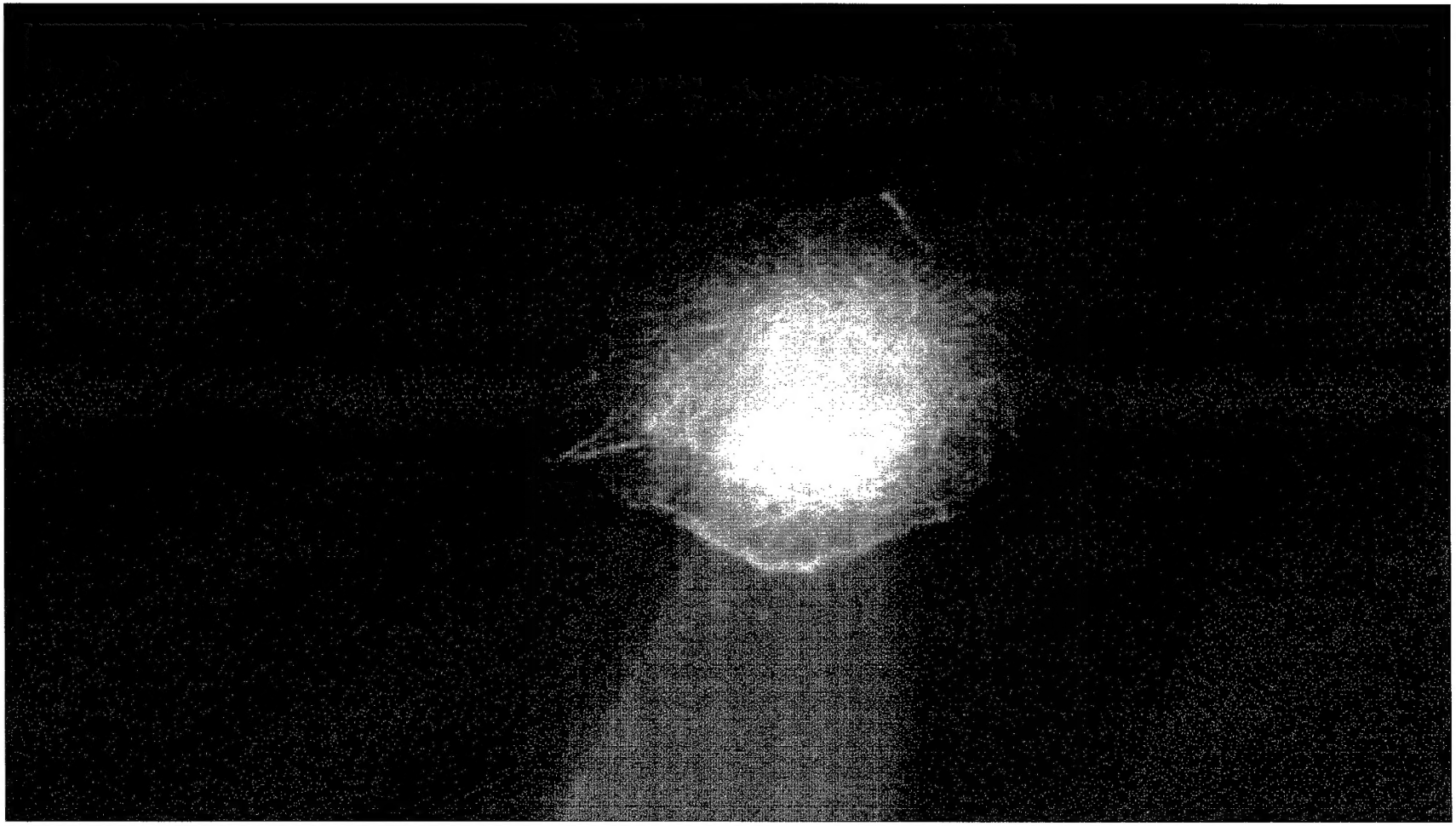

βV in MCF-7 Cells